SESSION III

SYSTEM PROTECTION FROM FIRE, EXPLOSION, AND NATURAL DISASTERS

Monday, August 2, 1976
CHAIRMAN: B. P. Brown

PRELIMINARY RESULTS OF HEPA-FILTER SMOKE PLUGGING TESTS USING THE LLL FULL-SCALE FIRE TEST FACILITY*

J. R. Gaskill, N. J. Alvares, D. G. Beason, and H. W. Ford, Jr.
University of California, Lawrence Livermore Laboratory
Livermore, California 94550

Abstract

As reported in previous Air Cleaning Conferences, hot fire gases can impair the integrity of HEPA filters, and smoke particulates can plug them. This pressurizes the room of fire origin and can lead to the spread of radioactive or other toxic contamination. The heat-damaging effect has been overcome using water sprays in the duct. Previous studies on smoke plugging have been inadequate, however, in determining realistic pyrolysis/combustion rates and in evaluating the effects of fuel arrangements, room geometry, and aging of smoke particulates.

To overcome these deficiencies, Lawrence Livermore Laboratory has constructed a full-size fire-test compartment, equipped it with an exhaust-ventilation system, and provided it with a suitable instrumentation- and data-acquisition system. From a survey of ERDA-contractor facilities, a matrix of fuel loadings (kg/m^2 of combustibles) versus dirty-to-clean ratios (relative yield of particulates) has been prepared. From this, a selected series of fuel arrays is being used to determine the life of HEPA filters during test fires. The effects of high- versus low-exhaust takeoff points, as well as the use or nonuse of sprinklers, are also being investigated.

The fire test facility is described, and the preliminary results obtained to date are reported.

I. Introduction

At the two previous Air Cleaning Conferences, my colleagues and I reported on what we had done to try to ameliorate the effects of unwanted fires on exhaust ventilation systems in facilities where radioactive materials are handled[1],[2]. In 1972, we reported on the successful use of water sprays to overcome the adverse effect of hot fire gases on exhaust ductwork and HEPA filters. In 1974, we reported on an improved method for abating this heat effect, and pointed out some of the difficulties in solving the filter smoke-plugging problem. At that time we indicated that Lawrence Livermore Laboratory was going to build a full-scale fire test facility so that more realistic tests could be conducted. The report today covers a description of the facility and the results of some preliminary fire tests conducted to date.

*Work performed under the auspices of the U. S. Energy Research and Development Administration under contract No. W-7405-Eng-48.

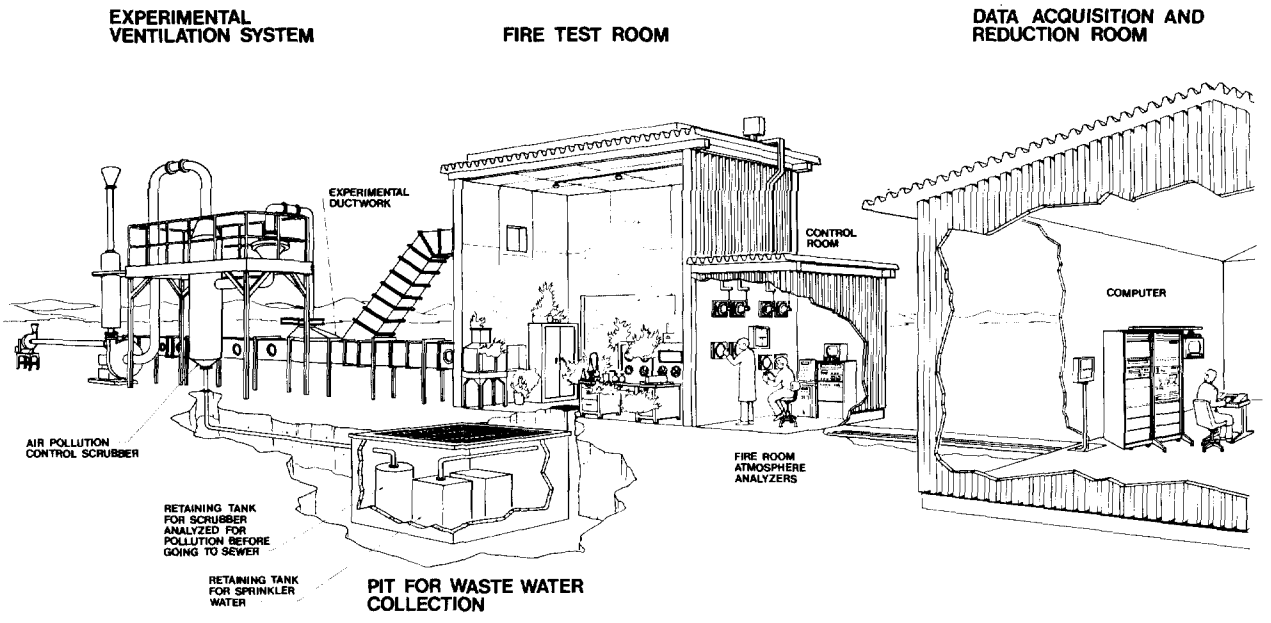

Figure 1 Full-scale fire test facility.

II. Description of Test Facility

As shown in Fig. 1, the full-scale fire facility consists of several elements as follows:

- A fire test room 100 m^3 in volume and an associated small control room containing view-ports into the test cell, gas sampling and analytical equipment; a control valve and meter for the sprinkling system; and a cathode-ray display tube capable of showing data obtained from the various centers on a 30-s update arrangement.
- High- and low-takeoff exhaust ductwork leading through a damper to the experimental duct system.
- A bypass air pollution control system (APC).
- A pit for waste water collection and monitoring.
- A computerized data acquisition system.

The fire test cell consists of a rectangular, square-cross-section, columnar steel framework onto which a steel skin with a Q-deck exterior is welded. Some 1600 stainless forks are welded to the inside of the steel skin walls and ceiling for holding the insulation. This insulation consists of 38 mm of Kastolite* SK-7 with a 985°C rating, followed by 100 mm of Kastolite KS-4V with a 1400°C rating. Kastolite is an alumina-silica mixture containing a small amount of lime. The floor of the cell, which is sloped to sprinkler drains, consists of a sand bed overlayed with fire brick, and finally overcast with Kastolite. The finished interior dimensions of the cell are 5.9 m long × 4.0 m wide × 4.2 m high.

*Reference to a company or product name does not imply approval or recommendation of the product by the University of California or the U.S. Energy Research & Development Administration to the exclusion of others that may be suitable.

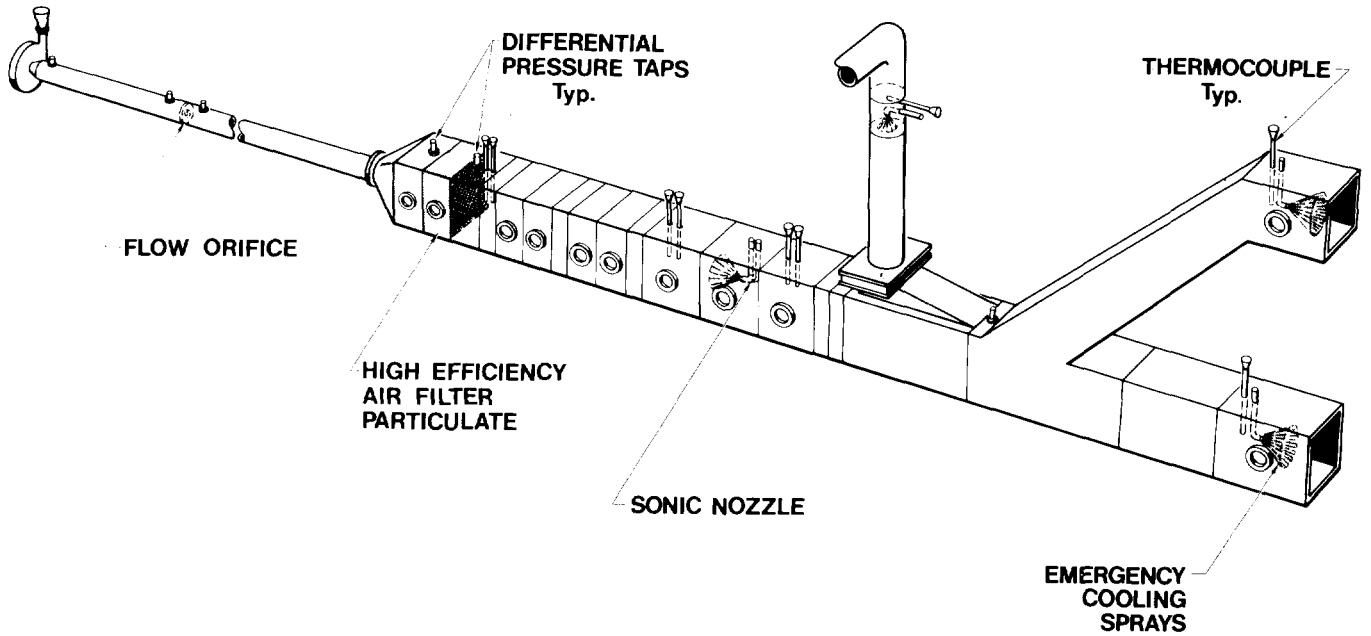

Figure 2 Experimental ductwork for fire test facility.

Figure 2 shows some of the details of the ductwork of which the left-hand section is the experimental modularized portion.

Figure 3 is a photograph of the cell showing one of the two intake air dampers, the exhaust ductwork, the experimental section, and the bypass to the high-pressure-drop venturi scrubber. This latter unit is used when the test is completed and we wish to clear

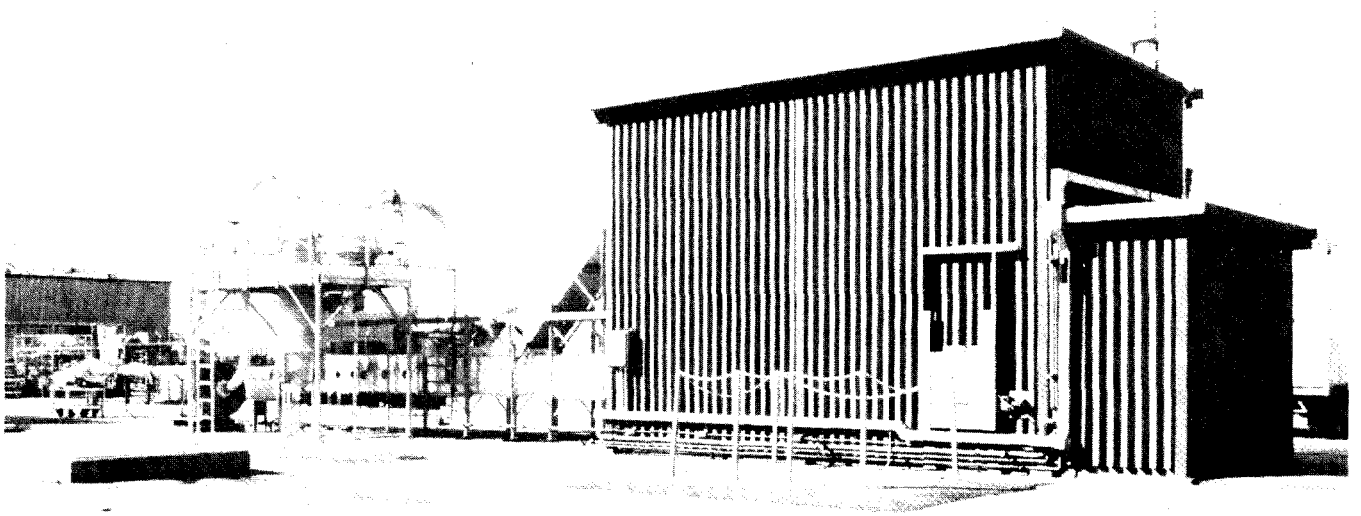

Figure 3 Fire test cell.

the room of smoke particulates and any toxic gases. In the foreground are shown the guard chains around the waste pit, and the exterior of the control room is to the right. Also shown are two secondary patch panels which lead to pluggable holes in the roof and along the lower sides of the test cell for the introduction of the various sensors. Two other subpanels are located respectively along the experimental ductwork and on the opposite side of the test cell.

Figure 4 is a northeast view of the test cell showing the other intake damper, the doors for taking equipment in and out, and another view of the roof patch panel and instrument wire way.

Figure 5 shows a somewhat detailed view of the air pollution control (APC) system consisting of a high-pressure-drop venturi scrubber, a tank, a high-volume high-pressure blower, and a muffler system. Recently this has been enclosed in a sound-deadening wooden structure.

Figure 6 shows the interior of the test cell looking toward the control room, and shows the viewing ports, light ports, one of the intake dampers, the lower instrumentation ports, and one floor drain.

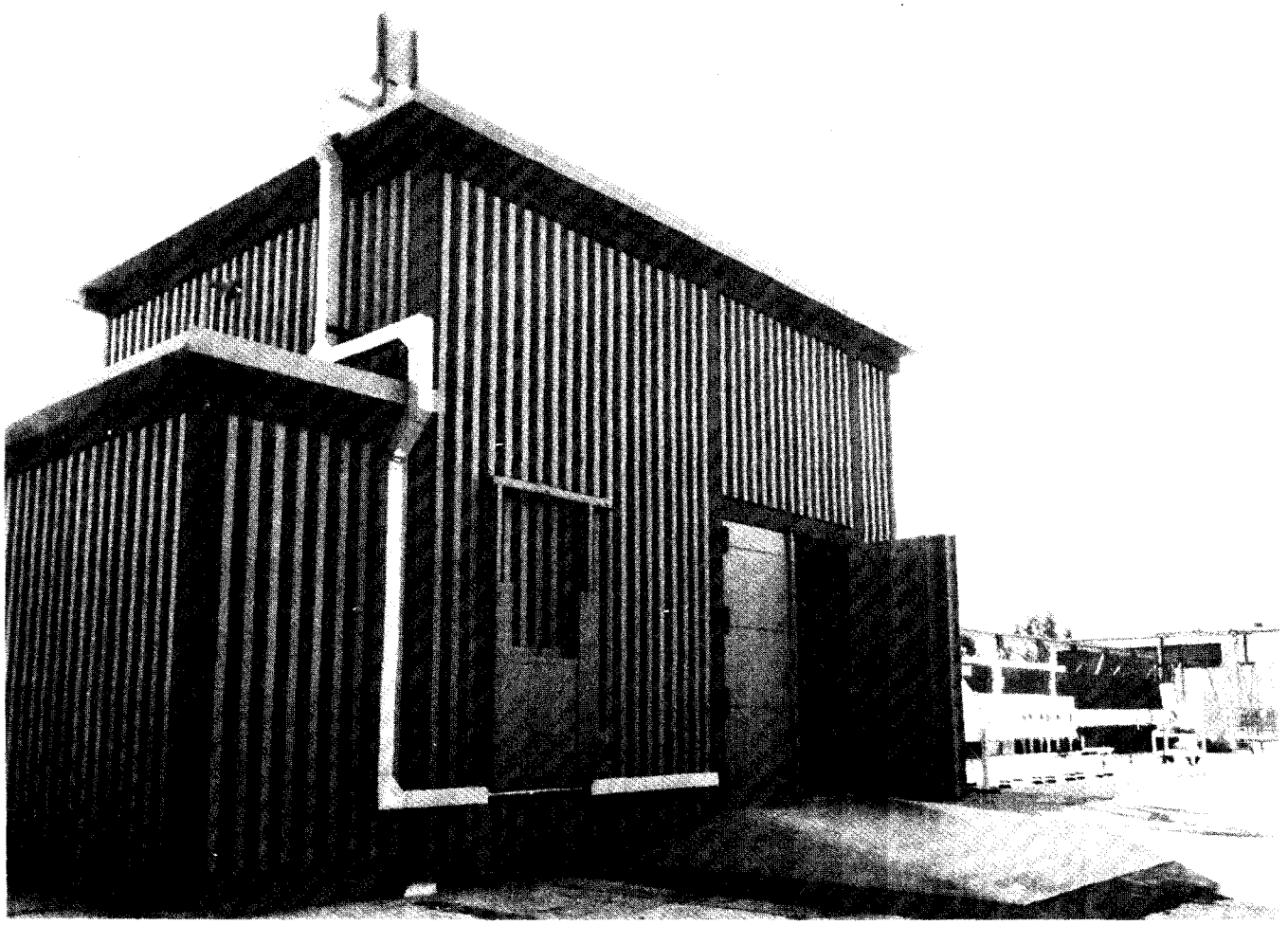

Figure 4 Northeast view of test cell.

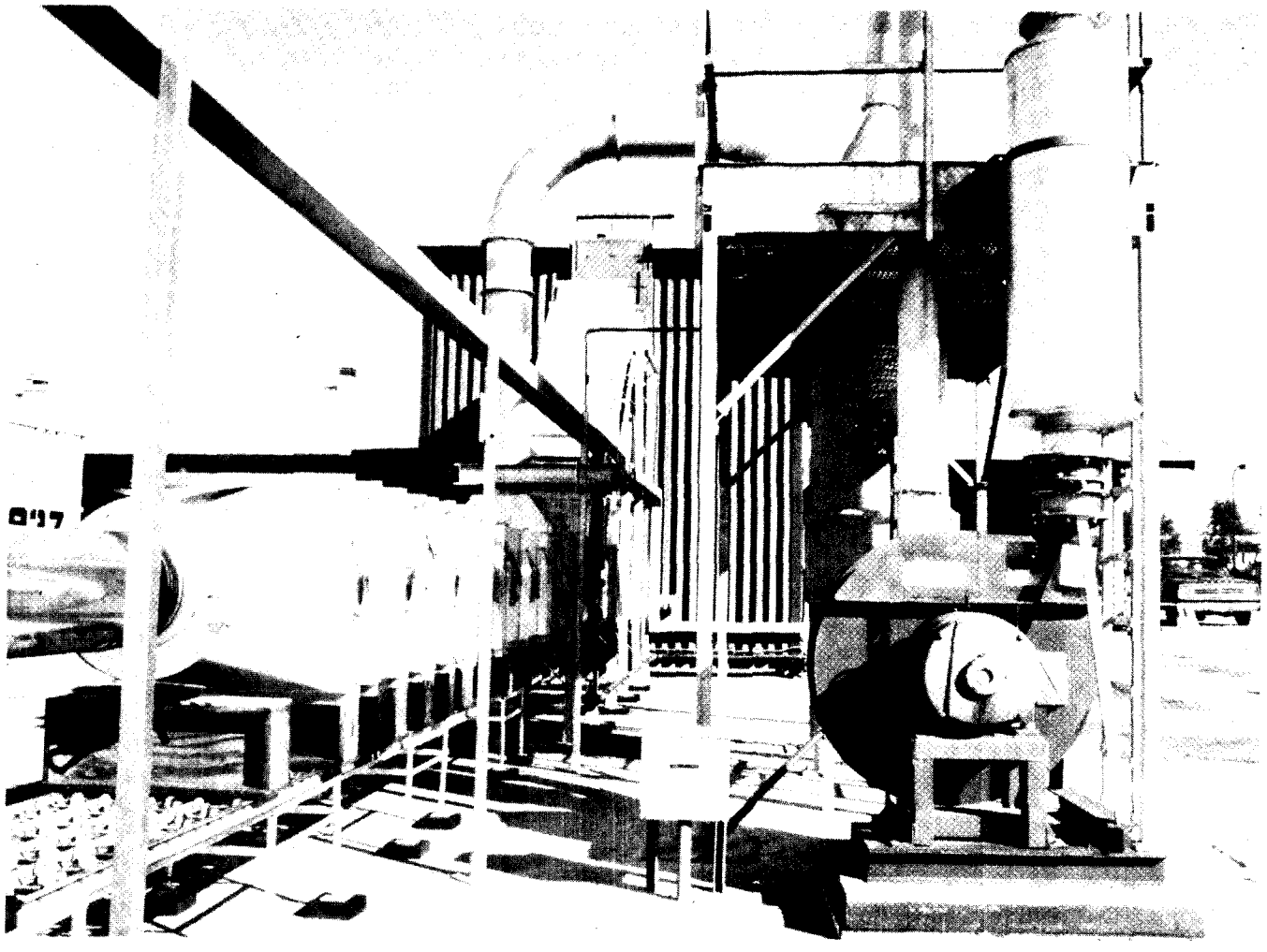

Figure 5 Air pollution control system.

Figure 7 shows the data acquisition/reduction system in the computer room. This consists of the scanner, a magnetic tape storage system, a computer, a CRT display, a display plotter, and a copier.

Figure 8 is an interior view of the control room showing the gas analysis instrument rack. Figure 9 is a view of one of the optical cell systems for determining the light obscuration of the smoke particulates in this test cell. Figure 10 shows a sample intake (currently located in upper exhaust duct) for sampling gases. An external sample port is currently used for taking timed samples for cascade impactor analysis used in determining sizes of smoke-particulates.

Figures 11(a) and (b) illustrate a map of the temperature-measuring sensors, the location of the smoke-density and radiometer sensors, and the pressure-measuring sensors. Figure 12 is a block diagram of the data acquisition system.

Construction of the facility was finished during the summer of 1975. The next several months were spent in installing the ductwork,

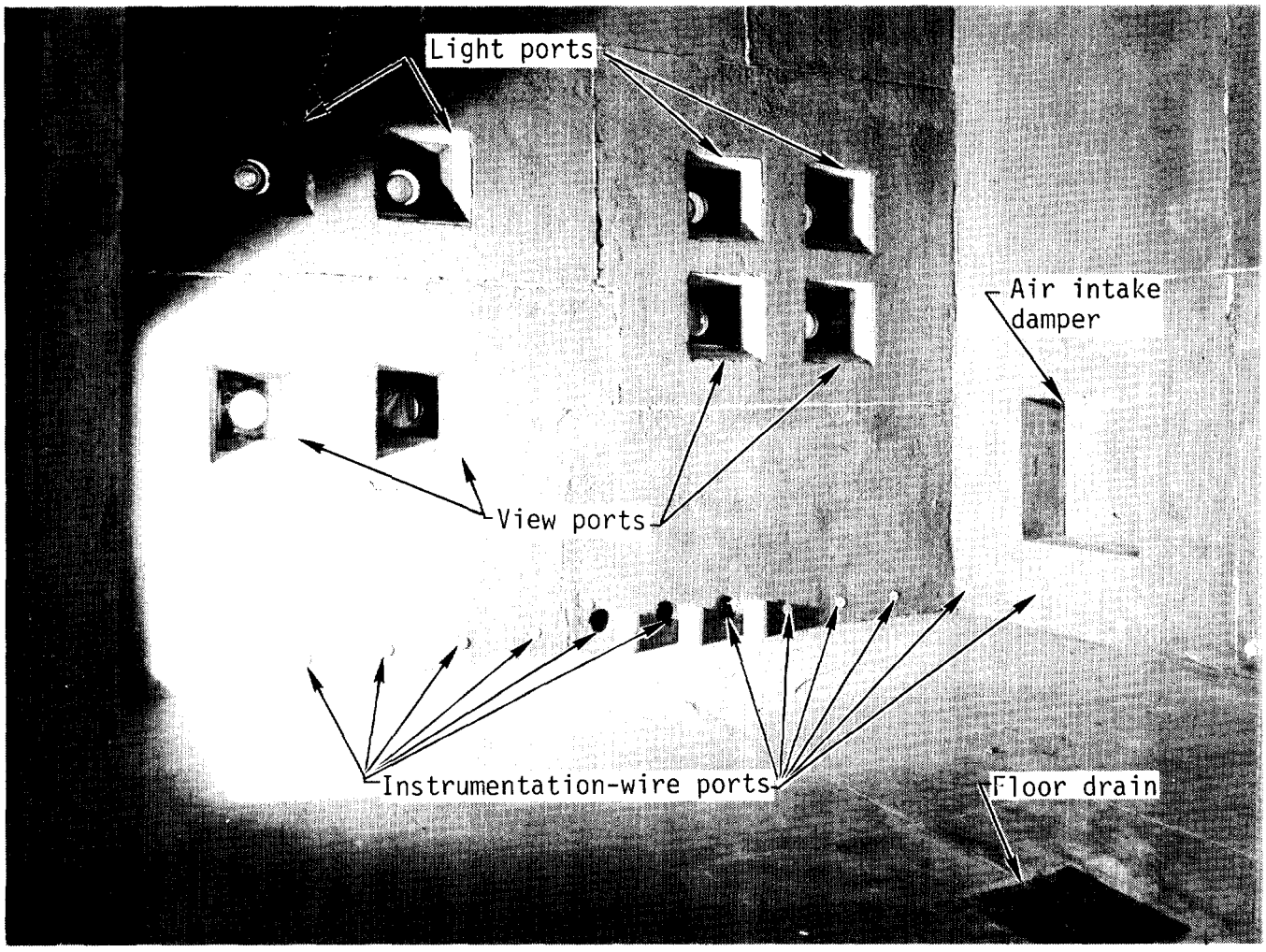

Figure 6 Test cell interior.

APC system, waste drain tanks, and data acquisition system[3]. Following this, some time was spent in installing and connecting the sensors, followed by a period of debugging. We have added more instrumentation during the testing program so that additional data are available from the later burns.

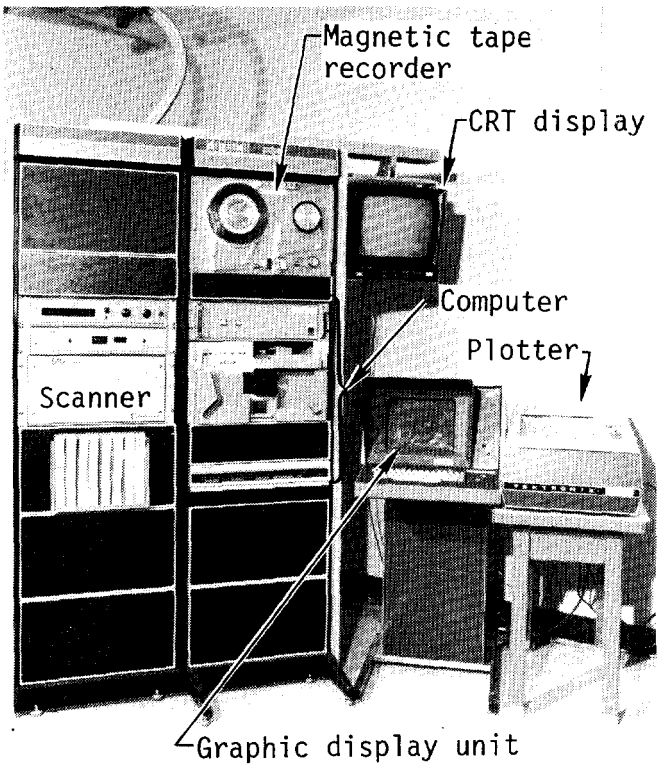

Figure 7 Data acquisition/ reduction system.

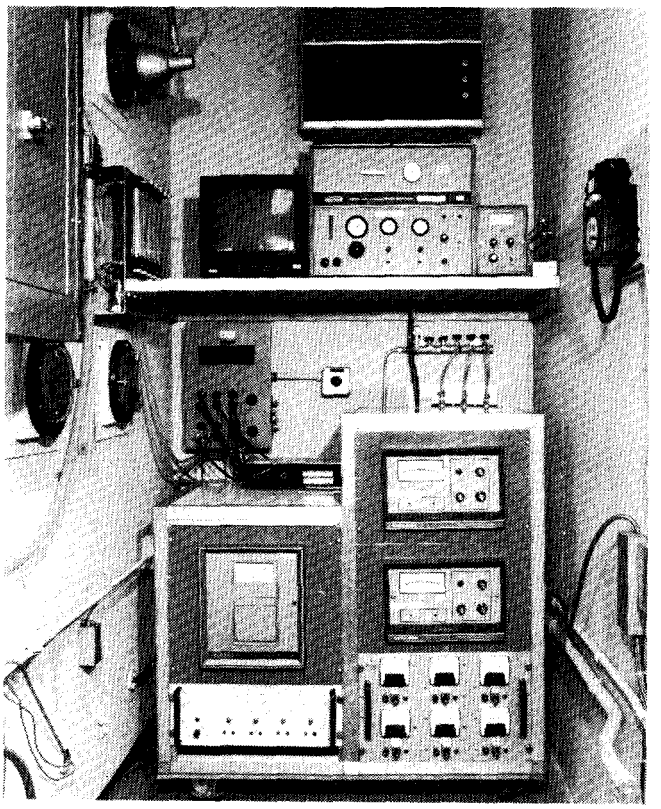

Figure 8 Gas analysis instrument rack.

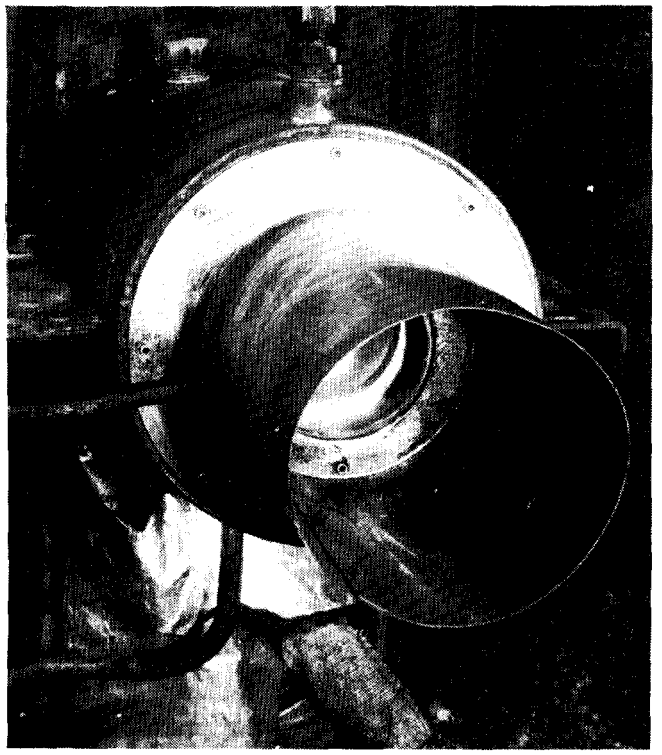

Figure 9 One unit of optical cell for measuring smoke opacity.

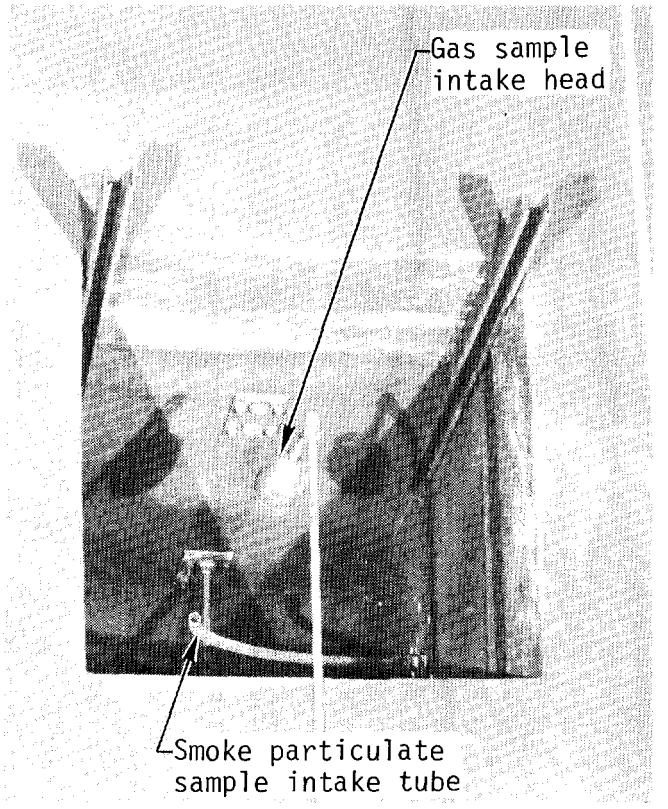

Figure 10 Upper exhaust duct showing gas sample intake tube.

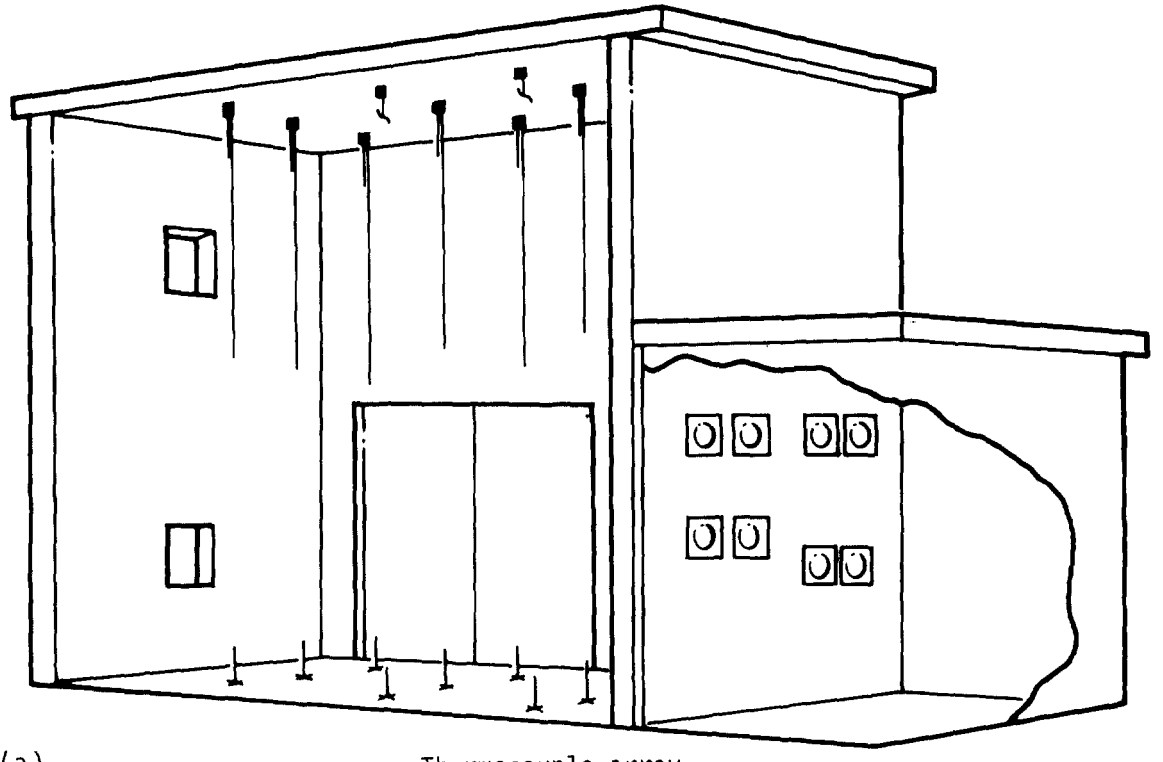

(a) Thermocouple array

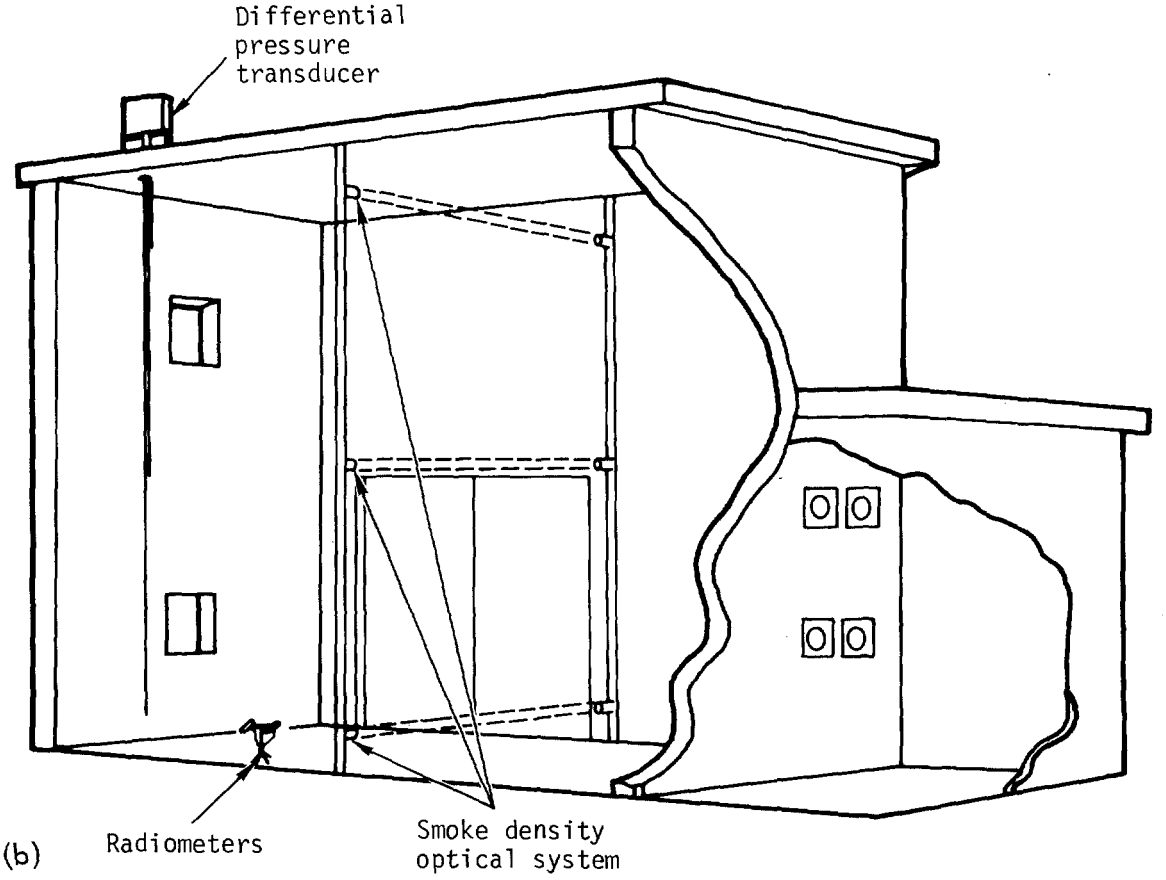

(b)

Figure 11 (a) Map of temperature sensors in test cell; (b) locations of optical-density, pressure, and radiant heat sensors.

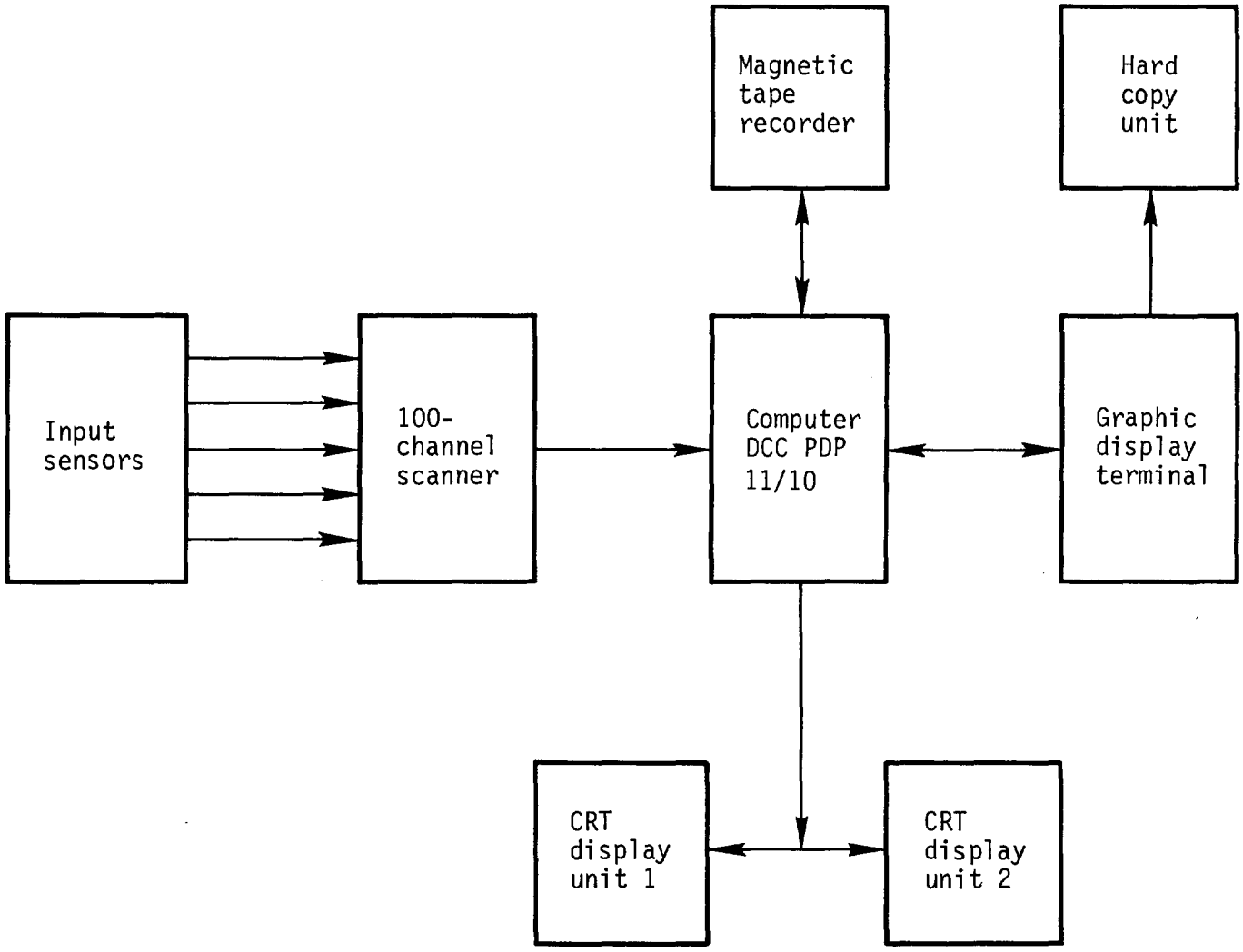

Figure 12 Fire test center data acquisition system.

III. Program Outline

As indicated in our report two years ago[2], our program is divided into two phases: the first is an evaluation of the heat- and smoke-plugging insults delivered to the HEPA filter by various likely fire scenarios; and the second is the development and evaluation of countermeasures. The fire scenarios were divided into four sets of parameters as follows:

- Effects of various fuel and smoke loadings (high versus low; dirty versus clean)
- Effects of high versus low exhaust takeoff
- Effects of the use versus nonuse of sprinklers
- Effects of a fire in the room external to any enclosure versus internal to the enclosure.

Information as to actual fuel loadings was kindly supplied by a number of ERDA contractors in the form of lists and weights of materials and photographs. From these data, we prepared tabulations

expressed as kilograms of combustibles per square meter of floor area in a compartment; we then categorized the various items as "clean" or "dirty" burners. A clean burner is defined as a material or product which when involved in a well-ventilated fire will produce relatively few smoke particulates; a dirty burner is the opposite. Simply expressed, nonfire-retarded cellulosic materials and certain plastic materials are clean burners, whereas fire-retarded materials and a number of plastics are classified as dirty burners.

From these data and categories, a dirty-to-clean (weight) ratio (D/C) for items likely to be found in a laboratory were plotted against the fuel loading (kg/m^2 of floor area). The results are shown in Fig. 13. Using hand calculation methods, we examined the various concentrations of points and settled on four parameters, which are also shown on the chart. These are D/C ratios of 5 and 0.5 and combustible loadings of 2 and 8 kg/m^2.

The test parameters were discussed at a meeting of the project committee in the summer of 1975, and it was concluded that priority should be given to: (1) high-combustible loadings (e.g., 20 and 10 kg/m^2); (2) an evaluation of sprinkler usage or nonusage; (3) an evaluation of D/C ratios of 3 versus 0.5; and (4) ignition sources external to the enclosures. This then, is the program we have initiated since the facility was first activated.

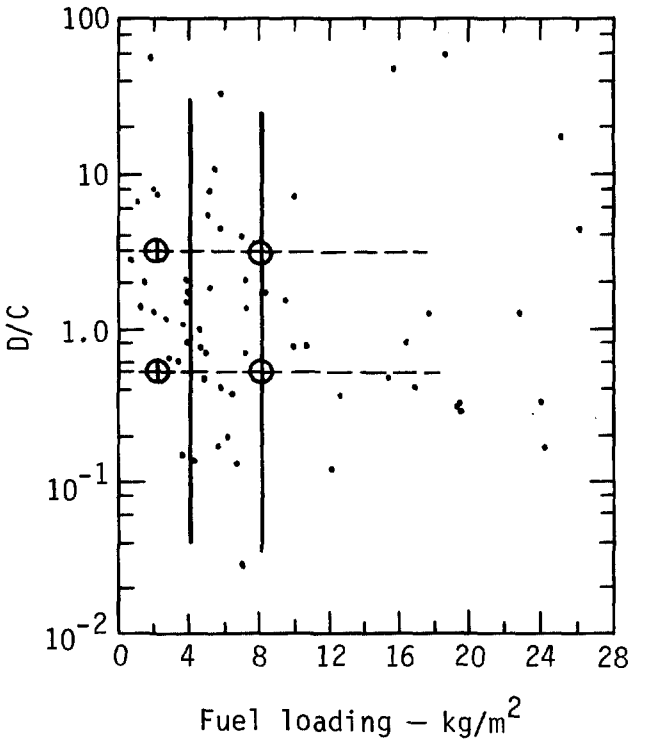

Figure 13 Smoke- versus fuel-loading test parameters.

IV. Preliminary Burns and Results

To date we have conducted eight burns, all classified as preliminary since during this time, we have been doing further debugging of the system and adding instrumentation. The tests are summarized below, and salient details together with results are included in the Appendix. Test No. 3 was a liquid fuel fire conducted to test the operation of the APC system. The system worked, and no data were obtained.

Test No. 1

The first test, conducted to evaluate the operational and safety characteristics of the test cell and components, involved surplus laboratory furnishings at a moderately heavy but dirty fuel loading. Fire was started by igniting 2 ℓ of isopropanol in pans under the fuel array. The test was categorized by moderate ceiling temperatures, an almost immediate obscuration of light caused by dense smoke generation, and an overpressurization of the cell in about 2 min. Analysis of the smoke particulates taken from the exhaust duct revealed: (1) very heavy accumulation (e.g., 3800 mg/m^3), and (2) a particle size distribution which indicated that about half of the weight of the smoke particulates was of 2 μm in size or larger.

Test No. 2

This burn was conducted to determine the effects of a clean, moderately heavy fuel load, and to ascertain whether we could mitigate the overpressurization phenomenon observed in the first test. The ignition source in this case was a plastic waste basket containing milk cartons and paper, the latter soaked with acetone. The results indicate that the fire was clean until the polyester hood ignited, at which time it became very sooty. Efforts to depressurize the room by increasing the exhaust ventilation were unsuccessful because the filter plugged that much sooner. Smoke particulate concentration in the duct was quite heavy – over 3000 mg/m^3 mg per cubic meter. The particle size analysis shows that over 75% of the weight exceeded 3 μm in size.

Test No. 4

In this test, we looked at the effects of a free-burning diesel fuel floated on water in a pan. This fuel was allowed to burn for 20 min and then was extinguished using light water (aqueous film-forming foam). Smoke was dense, moderately heavy (about 1000 mg/m^3), and rather fine in particulate size (50% by weight less than 1 μm in size). The ventilation uniformly decreased, and the filter plugged at about the time we extinguished the fire.

Test No. 5

In this burn, the loading was moderate but dirty (D/C ratio = 5.1). Included in the furnishings was a table-mounted clear plastic hood. The ignition source was 3 ℓ of acetone poured into pans distributed on the floor and ignited remotely. The fire flared-up

immediately, but soon started to decay as indicated by the temperature records, probably because the cell pressurized and air could not be drawn into the enclosure. In spite of the dense smoke which obscured vision in 1.5 min, we could occasionally see flames inside the hood. When the hood burned through (about 11 min into the test), the temperatures in the cell started to rise briefly and then to decay again. Shortly thereafter, the ventilation was switched to the APC system which caused the fire to flare up again. The fire was then extinguished, using the overhead deluge system. During the entire test, the gas temperature just upstream of the HEPA filter did not exceed 100°C. Fuel loss in this test was 9% overall and 10% of the dirty items.

Test No. 6

This was a two-stage burn involving an oversized filter* using two 14-kg portions of diesel fuel floated on a pan of water and ignited using a half litre of gasoline which was in turn lit remotely. In the first stage the fire burned well, and the fuel was exhausted in the 19 min. During this time the ventilation decreased from 250 to 180 ℓ/s, and the pressure drop across the HEPA filter changed from 30 to 1800 Pa, indicating an approach to plugging. After refueling, the ventilation was readjusted by opening the exhaust damper to 250 ℓ/s. The second fire burned for a little over 3 min at which time the pressure drop across the HEPA filter increased to such an extent that the filter ruptured. At that time, the flow had decreased to 210 ℓ/s. Smoke concentration in the duct and particulate sizes were about the same as in test No. 4. Significant concentrations of carbon monoxide and unburned hydrocarbons, accompanied by a considerable decrease in oxygen concentrations, were noted in the exhaust duct leading from the cell.

Test No. 7

This was conducted to determine the effect on filter plugging of a well-ventilated, clean-burning fuel. For this purpose, a wood crib (Douglas fir) was constructed so the fuel loading was 8.2 kg/m^2 and the D/C ratio was zero. An oversized filter was installed in the duct (500 ℓ/s) and the ventilation was adjusted to the filter rating (e.g., equivalent to 18 air changes per hour). A gas burner was installed under the crib and ignited remotely. Gas feed to the burner was 100 ℓ/min throughout the test. The fire burned well for about 16 min at which time it was extinguished. There was little evidence of filter plugging, but much higher temperatures than usual were noted. Half-way through the test a smoke sample taken from the exhaust duct showed a particulate concentration of 1000 mg/m^3, 80% of which by weight was of particles larger than 3 μm.

*In all other tests described in this report a filter rated at 250 ℓ/s was used, and the ventilation rate was set initially at 250 ℓ/s. In test No. 6, a filter rated at 500 ℓ/s was used and the flow was adjusted to 250 ℓ/s initially.

Test No. 8

Test 8 was a repeat of Test 7, except that the initial ventilation rate was halved, i.e., to 250 ℓ/s (9 air changes/hr). The fire burned well for 5 min, decayed to a lower steady state for 14 min, and flared up briefly as the APC system was switched over. It was extinguished at 20 min. The cell pressurized at 3-4 min and a dense, acrid, liquid-particulate smoke emanated from the intake ports. During the latter part of the test, liquid tars started to condense downstream of the HEPA filter. Smoke-particulate concentration and size increased during the test. At 16 min the concentration was 12 g/m^3; 70% of this weight consisted of particles 2 μm or larger.

V. Discussion and Future Work

Whereas the tests conducted to date have been somewhat preliminary in nature and have not been replicated, we can make some tentative observations and conclusions of a general nature.

First, in all the tests so far where normal ventilation was used and no attempt was made to increase the exhaust ventilation in the event of fire, an almost immediate overpressurization of the compartment has been evident.

Secondly, in the one or two cases where we have increased exhaust ventilation and the fire was dirty, i.e., generating large quantities of smoke particulates, the filter plugged faster and the room finally pressurized as the exhaust ventilation was decreased because of this filter plugging.

Thirdly, one of the "clean" fires became dirty when a significantly large dirty-burning item became involved.

Fourth, the smoke particulate concentration in the exhaust ductwork is, in our opinion, quite high when a heterogeneous mixture of furnishings catches fire and the ventilation is insufficient to cause the fire to burn cleanly if this is at all possible.

Fifth, there are two reasons to hope that the smoke particulates generated in the kinds of fires we have been using can be reduced by scrubbing. The first, is that the particle size distribution in our full-scale fire test compartment seems to be tending toward the larger sizes, which means that they may be able to be targeted by fine water sprays with or without wetting agents or with certain chemicals which can cause then to precipitate. Secondly, our air pollution control system has worked quite satisfactorily. However, this is not a very effective method from the installation-, standby-, and operating-cost per unit volume of gas scrubbed.

During the next several months after we run (and check) a few more test fires, we plan to evaluate a number of smoke-abatement counter-measures. These will include the use of single and sequential water sprays with or without additives, and with or without the use of various prefiltering techniques. By our next meeting, we hope to report on cost-effective methods which we can all use.

References

1. J. R. Gaskill and J. L. Murrow, "Fire Protection of HEPA Filters by Using Water Sprays," Proceedings of the Twelfth Air Cleaning Conference, Vol. 1 (1972), pp. 103-122.

2. J. R. Gaskill and M. W. Magee, "The HEPA-Filter Smoke Plugging Problem," Proceedings of the Thirteenth Air Cleaning Conference, Vol. 1 (1974), pp. 584-607.

3. J. R. Gaskill, D. G. Beason, and H. W. Ford, Jr., "HEPA-Filter Fire Protection," Hazards Control Progress Report No. 50, UCRL-50007-75-1 (Jan-June 1975), pp. 20-23.

APPENDIX - TEST RESULTS AND DATA

PRELIMINARY BURN NO. 1 DATE Jan. 23, 1976

PURPOSE To evaluate operational and safety characteristics of Test Cell and components; to determine fire- and filter-plugging effects of dirty, moderately heavy fuel load

FUEL Surplus Laboratory furnishings and equipment

LOADING 9.7 kg/m^2 D/C RATIO 2.66

INITIAL VENTILATION 250 ℓ/s (9 changes/hr) EXHAUST high

IGNITION 2-ℓ isopropanol in pans under fuel ignited by lighting solvent-soaked train of paper tissue.

RESULTS

SUMMARY Immediate flaming; viewports sooted up/2 min; at 10 min APC (Air Pollution Control) system turned on; cell temps climbed again. At 12-13 min deluge system extinguished fire - fuel loss: 30% total; 38% clean; 27% dirty.

DETAILS

Maximum Temperatures (°C)

In Cell >500/2 min in flame In Cell at ceiling 395

In Cell at exhaust — In Duct at HEPA 115

Cell Pressure Overpressured at ∿2 min

Optical Density Not measured

Exhaust Ventilation Flow Not measured

P HEPA (Pa) Not measured

Smoke Particulates-Concentration(mg/m^3) 3800 at 4 min.

"Size" (μm) >3/25%; ∿2/25%; ∿1/28% %

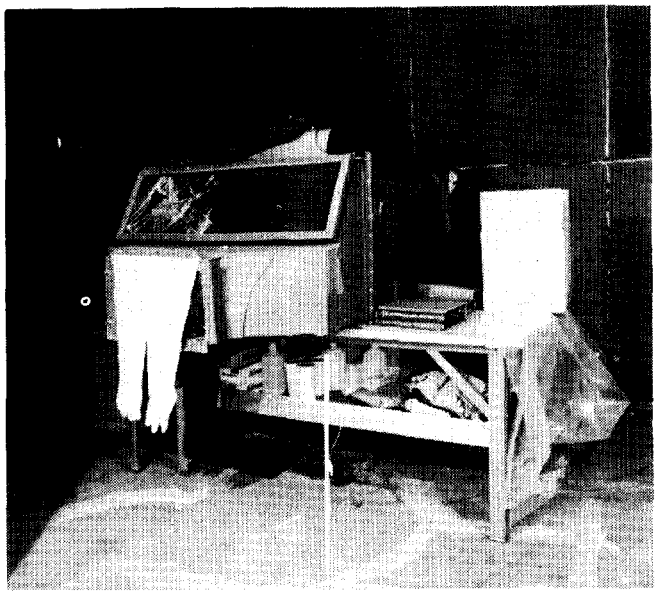

(a)

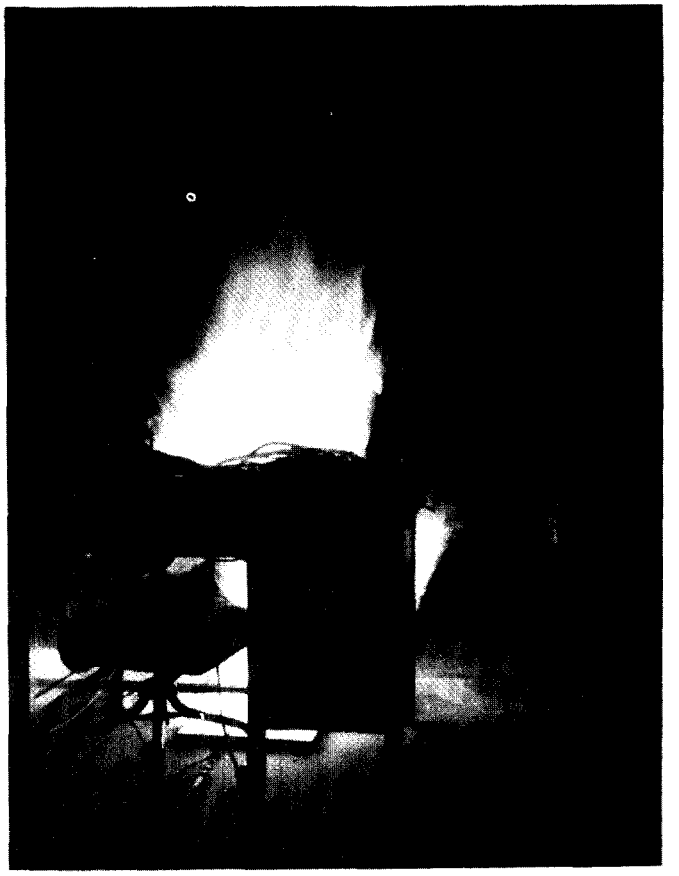

(b)

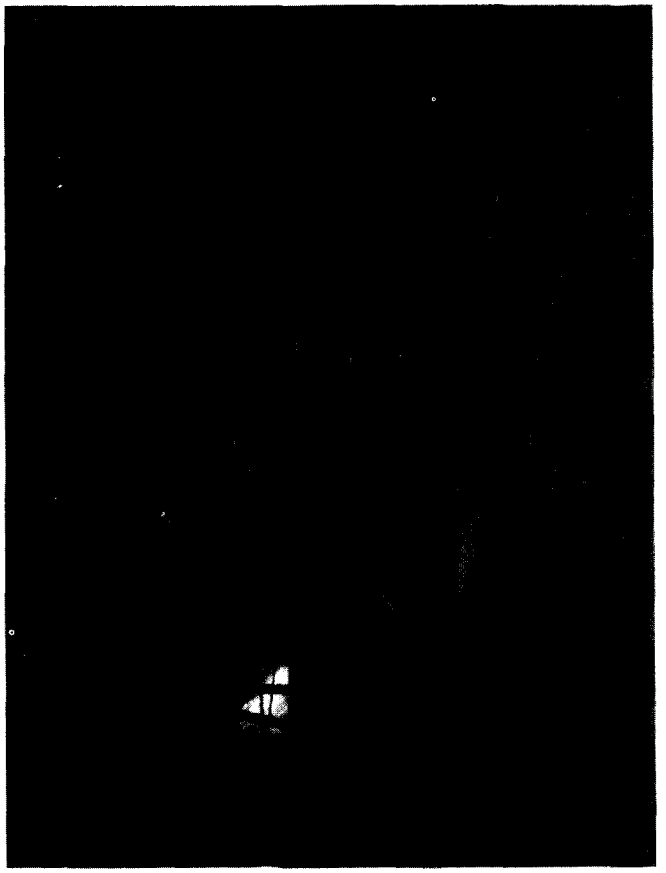

(c)

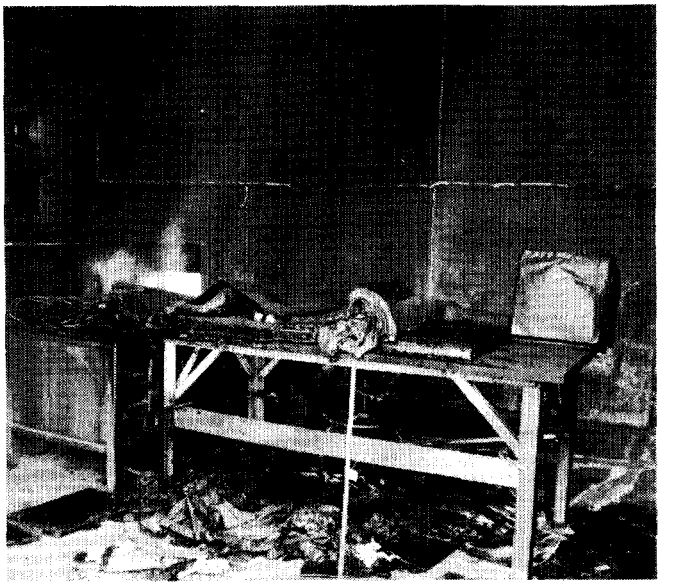

(d)

Figure A-1 Test No. 1. (a) Fuel array; (b) fire at 0.5 min; (c) fire at 1 min; (fuel after burn (loss about 23 kg); (e) external view during test.

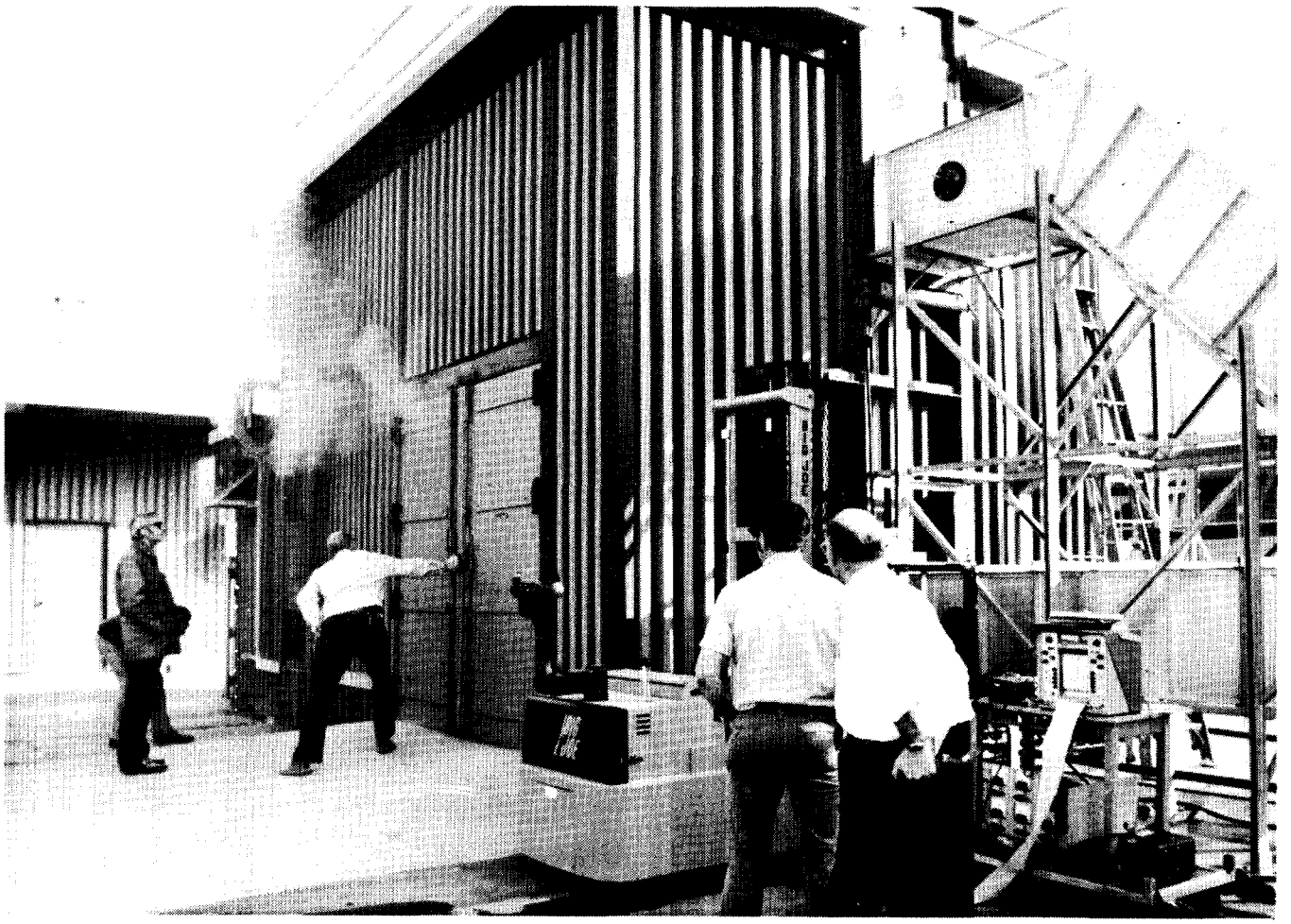

(e)

Figure A-1 (continued)

PRELIMINARY BURN NO. 2 DATE Feb. 13, 1976

PURPOSE To minimize overpressurization; to determine effects of clean, moderately heavy fuel load.

FUEL Surplus Laboratory furnishings and equipment

LOADING 10.5 kg/m^2 D/C RATIO 0.57

INITIAL VENTILATION 250 ℓ/s (9 changes/hr) EXHAUST high

IGNITION Plastic waste basket containing milk cartons & paper soaked with acetone.

RESULTS

SUMMARY Clean fire until polyester hood ignited; then very sooty; attempts to depressurize room by increasing exh. ventil. unsuccessful because filter plugged (1.0 kg of soot); fuel loss: 9.1% of total; 6.6% clean; 12.3% dirty.

DETAILS

Maximum Temperatures (°C)

In Cell ND In Cell at ceiling ND

In Cell at exhaust ND In Duct at HEPA ND

Cell Pressure See narrative

Optical Density

Exhaust Ventilation Flow 250 → 500 → < 150 ℓ/s

P HEPA (Pa) ND

Smoke Particulates-Concentration(mg/m^3) 3375 at 16 min.

"Size" (μm) 3/75% %

PRELIMINARY BURN NO. 4 DATE March 26, 1976

PURPOSE To evaluate effect of free-burning diesel fuel on smoke-particulate production, filter clogging, and combustion rate.

FUEL 25-mm layer (13 kg) diesel fuel on water in 914-mm diam. pan

LOADING 0.55 kg/m^2 D/C RATIO –

INITIAL VENTILATION 250 ℓ/s EXHAUST high

IGNITION 500-m/gasoline floated on surface of fuel; ignited with torch.

RESULTS

SUMMARY Fuel burned ∿20 min; then extinguished; dense smoke; ventilation decreased & filter plugged ∿20 min.
Fuel loss: 8 kg (∿62%)

DETAILS

Maximum Temperatures (°C)

In Cell 500 center midheight In Cell at ceiling 320

In Cell at exhaust 160 In Duct at HEPA 60

Cell Pressure

Optical Density Heavy in ∿1 min

Exhaust Ventilation Flow 250 → 125 ℓ/s in 20 min

P HEPA (Pa) → 2200 (loading 0.3 kg)

Smoke Particulates-Concentration(mg/m^3) ∿1000 at min.

"Size" (μm) <1/50% %

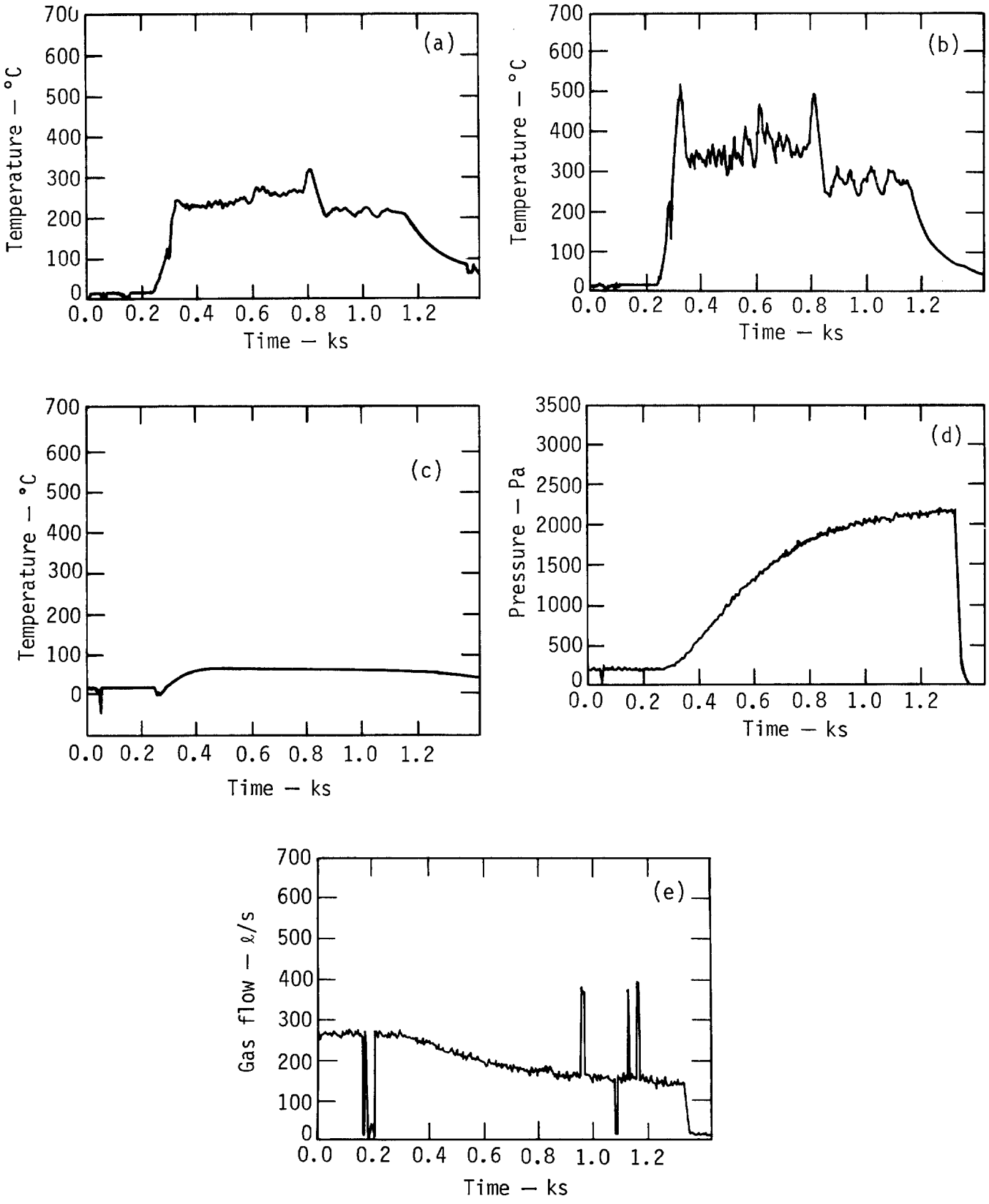

Figure A-2 Test No. 4. (a) Temperature in center of cell 3.7 m above floor; (b) temperature in center of cell 2.2 m above floor; (c) temperature in duct ahead of HEPA filter; (d) pressure drop across HEPA filter; (e) gas flow in exhaust duct.

PRELIMINARY BURN NO. 5 DATE April 22, 1976

PURPOSE To determine effects of very dirty, moderately heavy fuel loading; to test gas sampling/analytical system; to demonstrate system to local media.

FUEL Surplus Laboratory furnishings and equipment

LOADING 10.5 kg/m^2 D/C RATIO 5.1

INITIAL VENTILATION 250 ℓ/s EXHAUST high

IGNITION 3-ℓ of acetone in pans on floor ignited remotely using spark coil.

RESULTS

SUMMARY Room pressurized/vision obscured in 1.5 min; fire decayed at 3 min (lack of oxygen) for 12 min when hood burned through then flared up. Vent switched to APC increase in fire level. Extinguished at 21 min. Fuel loss: total 9%; clean 1.5%; dirty 10%.

DETAILS

Maximum Temperatures (°C)

In Cell 700 in flame In Cell at ceiling 550

In Cell at exhaust 300 In Duct at HEPA 80

Cell Pressure Positive after 1.5 min

Optical Density Dense smoke

Exhaust Ventilation Flow 250 → 220 ℓ/s in 10 min

P HEPA (Pa) Lost data

Smoke Particulates-Concentration(mg/m^3) 1000 at ___ min.

"Size" (μm) 3/44% %

Exhaust-gas Analysis

Unburned hydrocarbons	(ppm methane)	3200/5 min	MAX
Carbon monoxide	(ppm CO)	3600/5 min	MAX
Carbon dioxide	(% CO_2)	ND	MAX
Oxygen	(% O_2)	11.5 min	MIN

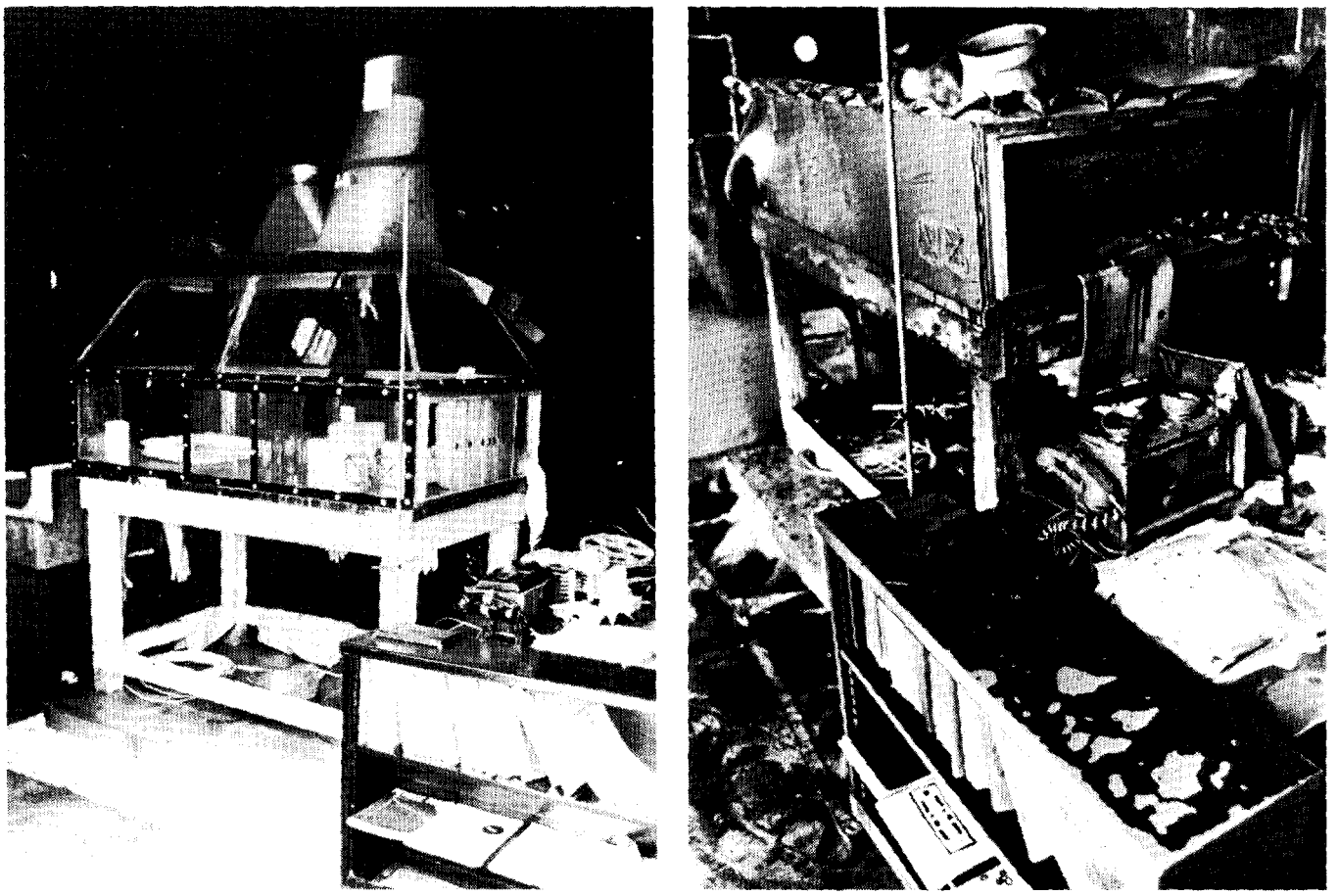

(a) (b)

Figure A-3 Test No. 5. (a) Fuel load before fire; (b) fuel load after fire.

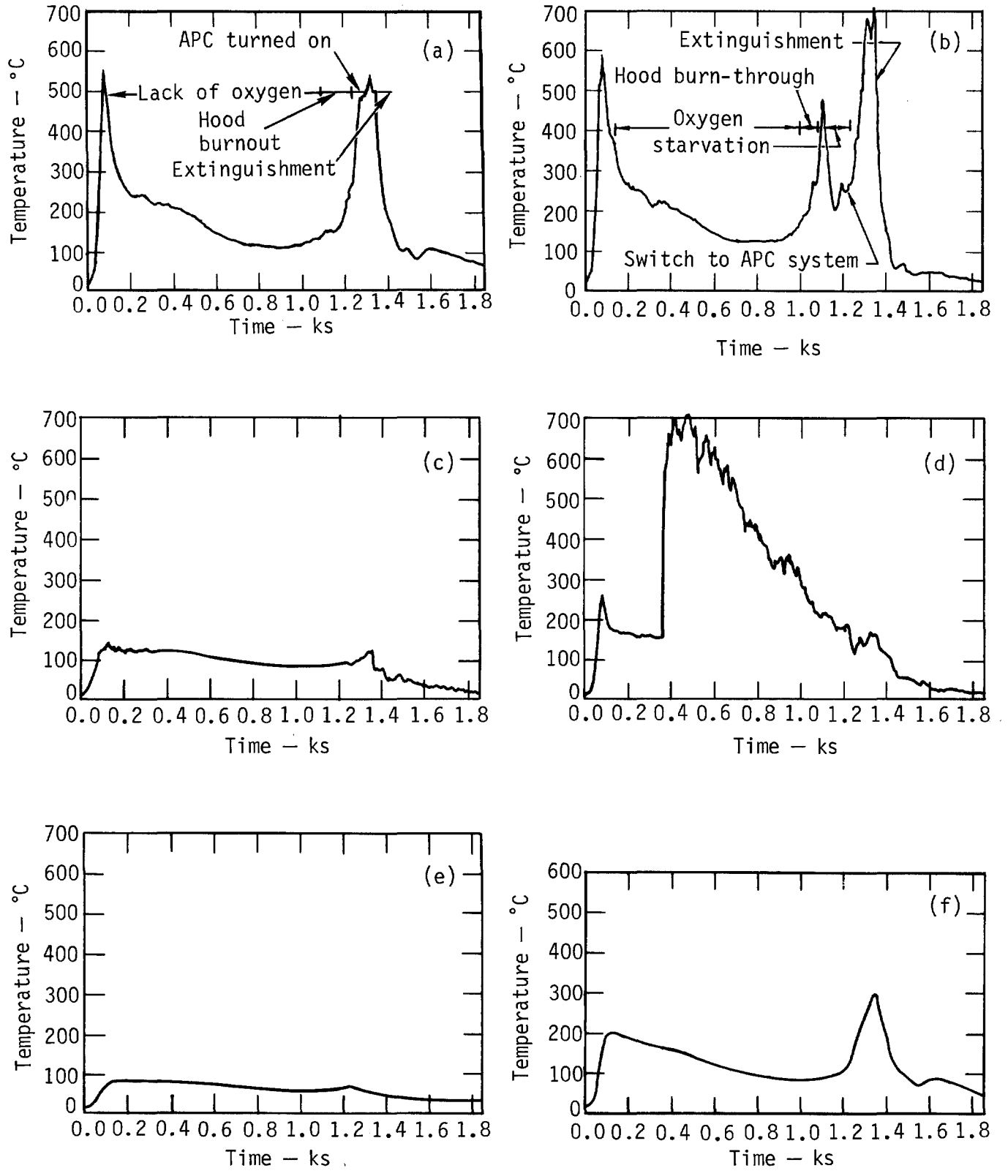

Figure A-4 Test No. 5. (a) Temperature in center of cell 3.7 m above floor; (b) temperature in center of cell 2.2 m above floor; (c) temperature in southwest corner of cell 0.5 m above floor; (d) temperature in hood; (e) temperature in duct ahead of HEPA filter; (f) temperature at cell outlet in duct.

PRELIMINARY BURN NO. 6 DATE May 7, 1976

PURPOSE Effect on filter plugging of oversize filter using diesel fuel- two-part burn

FUEL 14-kg diesel, first part - 14-kg diesel, second part

LOADING 0.59 kg/m^2 D/C RATIO -

INITIAL VENTILATION 250 ℓ/s for each test EXHAUST high

IGNITION 500-ml gasoline floated on diesel; ignited remotely.

Note: Filter rated at 500 ℓ/s was used.

RESULTS

SUMMARY First fire burned well and burned out in 19 min. Second fire burned 3.3 min when filter reptured.

Fuel loss: 0.73 kg/min.

DETAILS

Maximum Temperatures (°C)

In Cell 600 (above fire) In Cell at ceiling 300

In Cell at exhaust – In Duct at HEPA 80

Cell Pressure –

Optical Density 1.5 m

	Part 1	Part 2
Exhaust Ventilation Flow	250 → 180 ℓ/s	250 → 210 ℓ/s
	first part	second part
P HEPA (Pa)	30 → 1800	2600 → 2750 (rupture)

Smoke Particulates-Concentration(mg/m^3) ∿1000 at 5 min.

"Size" (μm) <1/40%; >3/∿25% %

Exhaust-gas Analysis

Unburned hydrocarbons	(ppm methane)	2800/20 min	MAX
Carbon monoxide	(ppm CO)	2000/20-min	MAX
Carbon dioxide	(% CO_2)	ND	MAX
Oxygen	(% O_2)	10/20-min	MIN

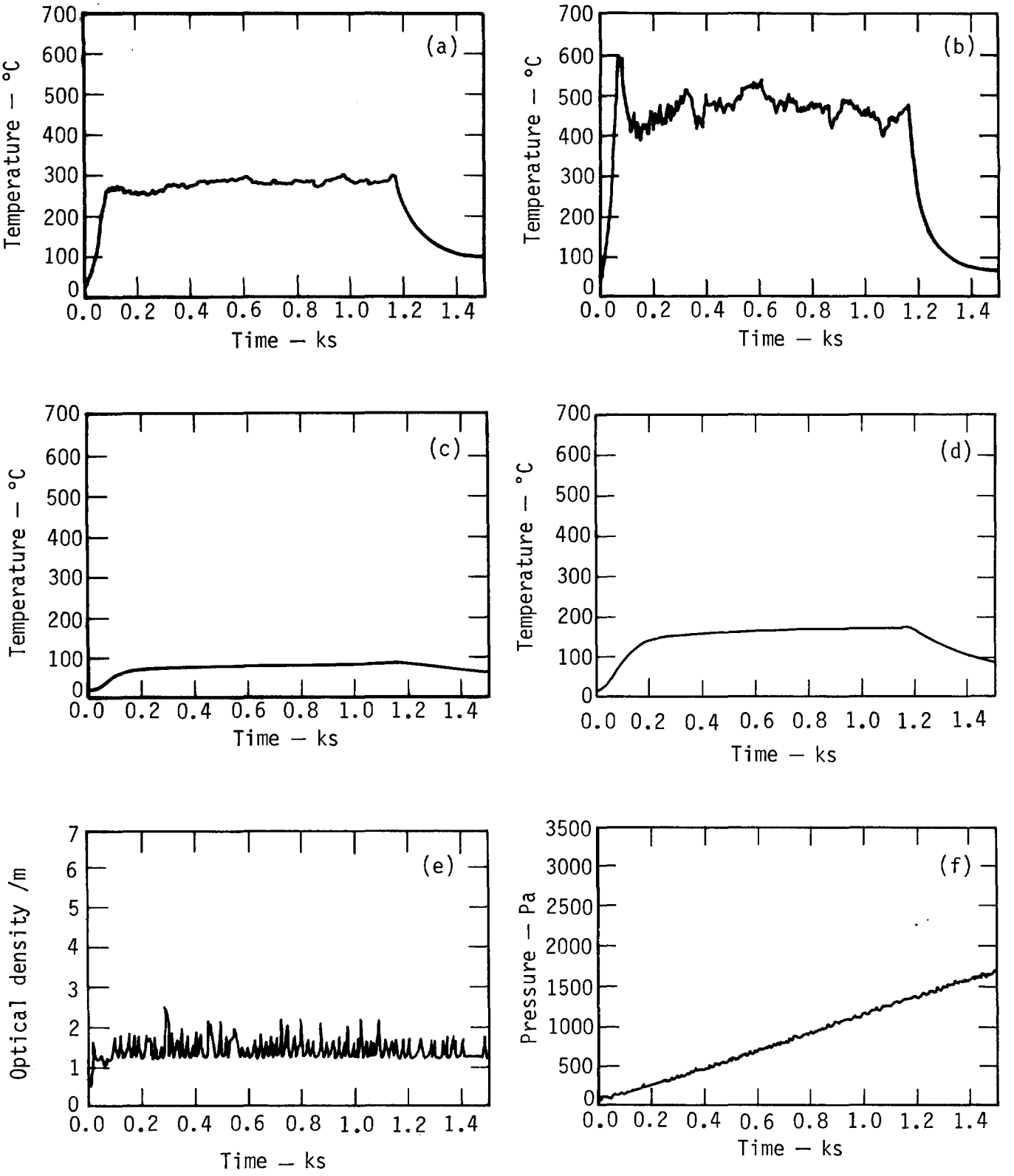

Figure A-5 Test No. 6. (a) Temperature in center of cell 3.7 m above floor; (b) temperature in center of cell 2.2 m above floor; (c) temperature in duct ahead of HEPA filter; (d) temperature in duct 1 m from cell exhaust; (e) optical density in cell 2.2 m above floor; (f) pressure drop across HEPA filter; (g) gas flow in exhaust duct; (h) fuel weight loss.

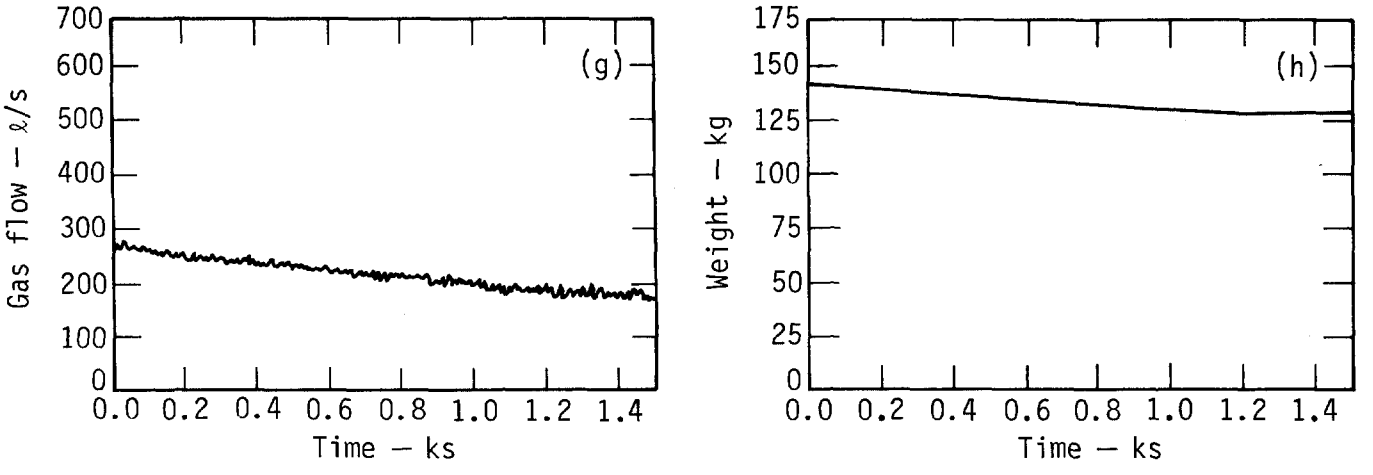

Figure A-5 (continued)

PRELIMINARY BURN NO. 7 DATE May 28, 1976

PURPOSE Effect on filter plugging of well ventilated clean burning fuel (Douglas-fir, wood crib) plus natural gas

FUEL Douglas fir crib 0.914 × 1.22 × 0.81 m high made up of 51 × 51-mm cross section sticks

LOADING 8.2 kg/m^2 D/C RATIO 0

INITIAL VENTILATION 500 ℓ/s (18 changes/hr) EXHAUST high

IGNITION Premixed natural gas fire (ignited remotely) under crib at 100 ℓ/min, used throughout test.

RESULTS

SUMMARY Fire burned well for ∿16 min and was then extinguished; little evidence of filter plugging; higher than usual temperatures noted.

DETAILS

Maximum Temperatures (°C)

In Cell ∿720-above flame In Cell at ceiling 630

In Cell at exhaust 300 In Duct at HEPA 200

Cell Pressure ∿20-30 Pa (negative)

Optical Density ND

Exhaust Ventilation Flow 530 → 470 ℓ/s

P HEPA (Pa) 250 → 420

Smoke Particulates-Concentration(mg/m^3) 1000 at 8 min.

"Size" (μm) >3/80% %

Exhaust-gas Analysis

Unburned hydrocarbons	(ppm methane)	ND	MAX
Carbon monoxide	(ppm CO)	30,000	MAX
Carbon dioxide	(% CO_2)	ND	MAX
Oxygen	(% O_2)	6	MIN

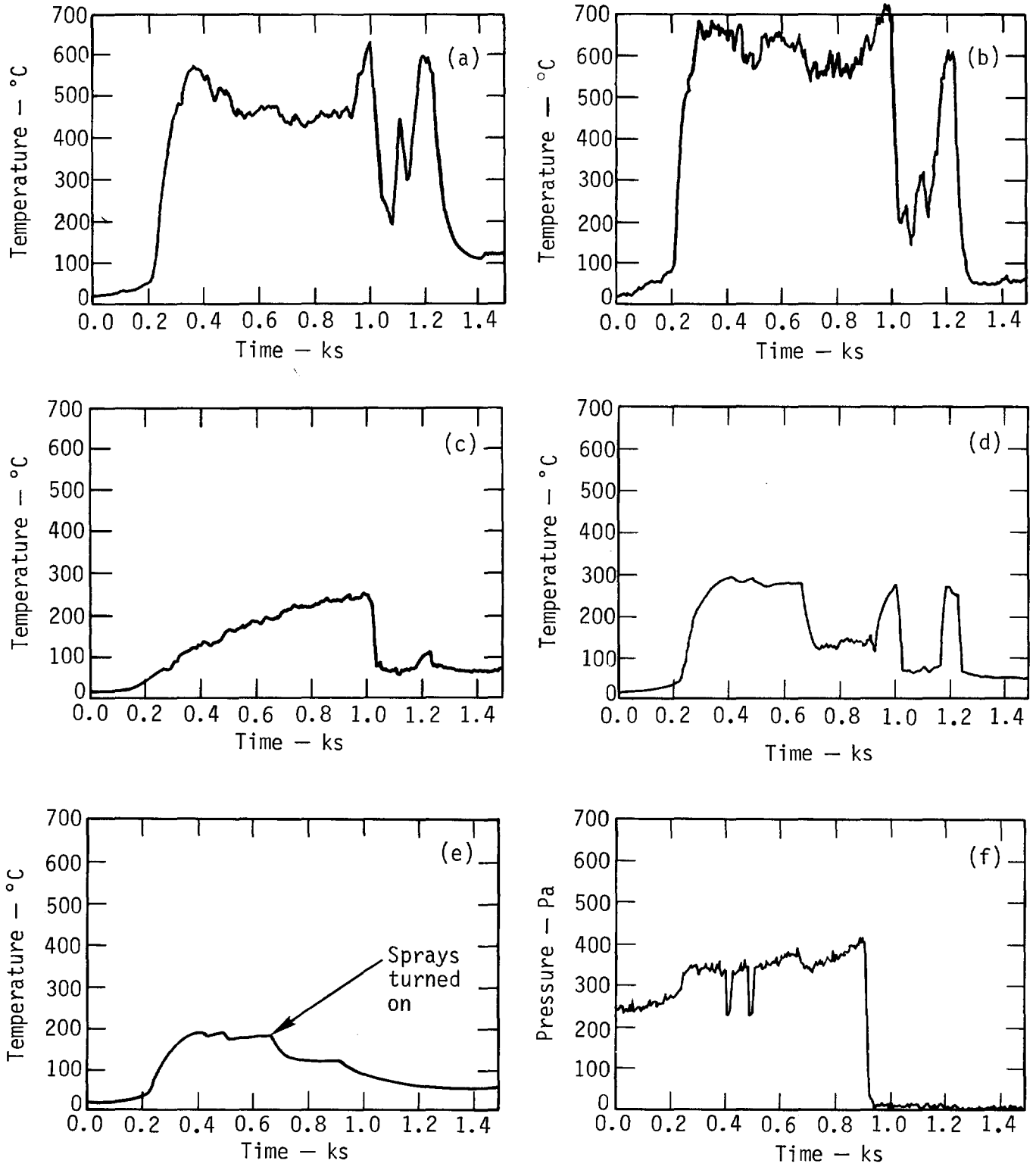

Figure A-6 Test No. 7. (a) Temperature in center of cell 3.7 m above floor; (b) temperature in center of cell 2.2 m above floor; (c) temperature at west end of cell 0.5 m above floor; (d) temperature in duct 1 m from cell exhaust; (e) temperature in duct ahead of HEPA filter; (f) pressure drop across HEPA filter; (g) gas flow in exhaust duct; (h) fuel weight loss; (i) percent oxygen in duct at cell exhaust.

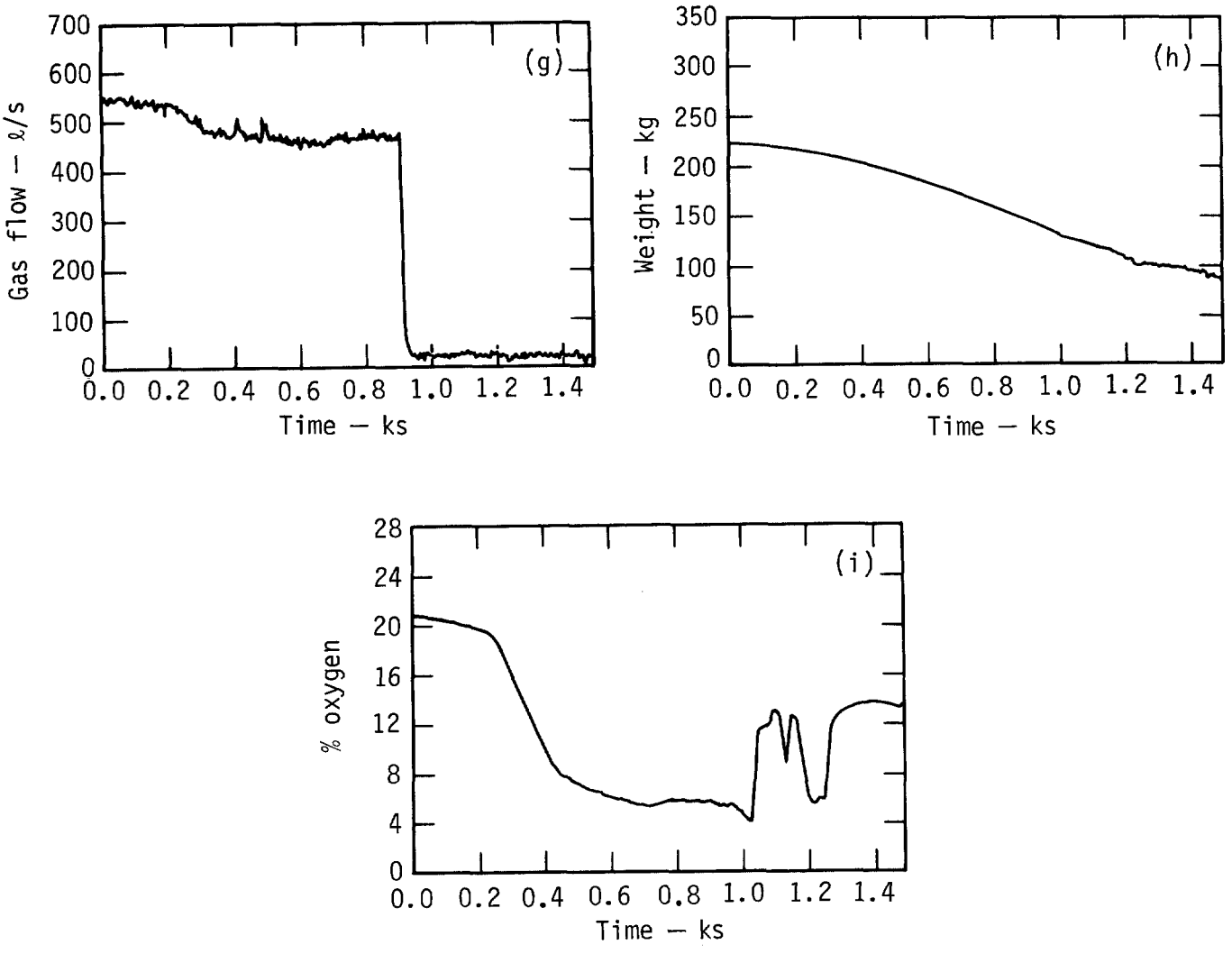

Figure A-6 (continued)

PRELIMINARY BURN NO. 8 DATE June 22, 1976

PURPOSE To determine effect on filter plugging of moderately well ventilated, clean burning fuel. (Douglas fir wood crib) plus premixed natural gas flame.

FUEL Douglas fir crib, similar to that used in PB-7 plus premixed natural gas flame

LOADING 8.3 kg/m^2 D/C RATIO 0

INITIAL VENTILATION 250 ℓ/s (9 changes/hr) EXHAUST high

IGNITION Premixed natural gas (ignited remotely) located under crib and kept burning using 100 ℓ/min of gas throughout test.

RESULTS

SUMMARY Good burning for 5 min; decay to lower steady state for 14 min; brief flareup during APC switchover; extinguished at 20 min. Overpressurization at 2-3 min; dense, acrid, liquid-particulate smoke.

DETAILS

Maximum Temperatures (°C)

In Cell 700 over crib In Cell at ceiling 550

In Cell at exhaust 280 In Duct at HEPA 100

Cell Pressure 20 Pa negative

Optical Density 1/m

Exhaust Ventilation Flow 250 → 100 ℓ/s in 15 min

P HEPA (Pa) 200 → 2000/15 min

Smoke Particulates-Concentration(mg/m^3) 12 000 at 16 min.

"Size" (μm) >2/70% %

Exhaust-gas Analysis

Unburned hydrocarbons	(ppm methane) ND	MAX
Carbon monoxide	(ppm CO) 60 000/20 min	MAX
Carbon dioxide	(% CO_2) ND	MAX
Oxygen	(% O_2) 4.4%/21	MIN

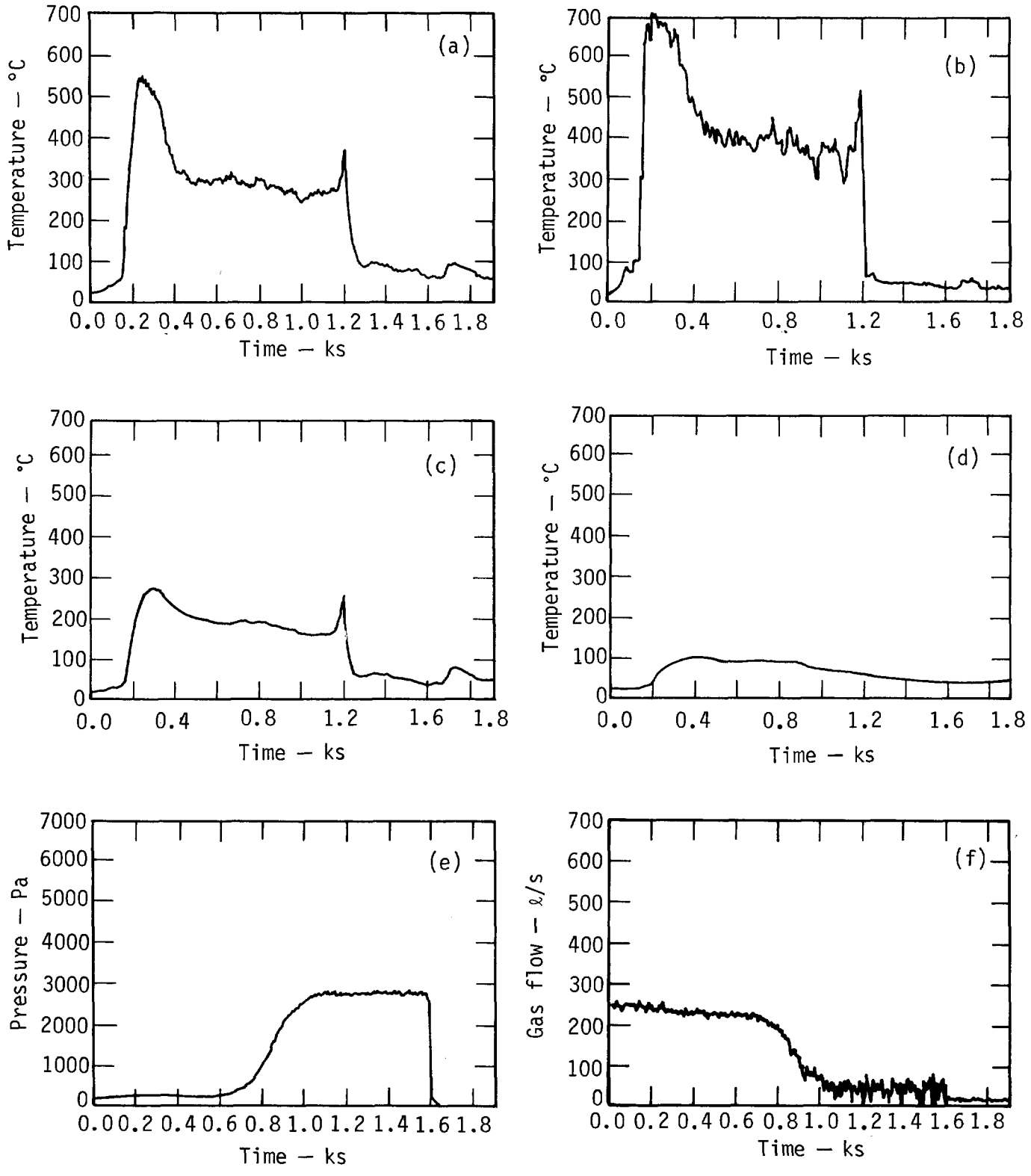

Figure A-7 Test No. 8. (a) Temperature in center of cell 3.7 m above floor; (b) temperature in center of cell 2.2 m above floor; (c) temperature in duct 1 m from cell exhaust; (d) temperature in duct ahead of HEPA filter; (e) pressure drop across HEPA filter; (f) gas flow in exhaust duct; (g) percent oxygen in duct at cell exhaust; (h) percent carbon monoxide in duct at cell exhaust; (i) fuel weight loss.

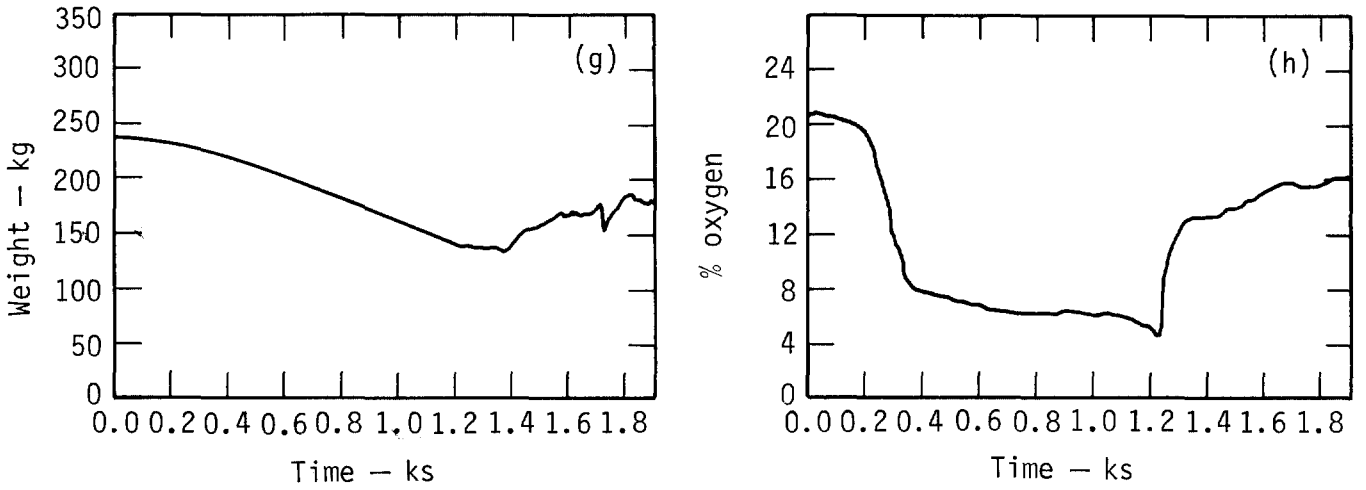

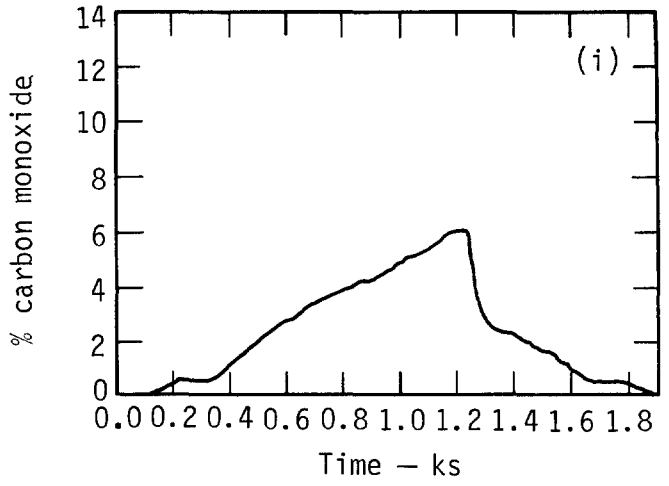

Figure A-7 (continued)

DISCUSSION

BALSMEYER: You talked about filter plugging. Is there any standard definition we can use?

GASKILL: Yes. Three years ago, at an ERDA conference, it was agreed somewhat arbitrarily that after one starts off at a rate of flow, say, 250 liters a second, when one reaches 125 liters per second, the filter is considered to be plugged. Empirically, we have found that this is tantamount to a pressure differential of about 2,100 to 2,300 Pascals across the filter.

BALSMEYER: On filter plugging, did you notice filter breaching or anything else from high pressure flow?

GASKILL: Only in the one case we illustrated. In the other cases, we have stopped short of that. When the filter is plugged, we just say, "That is it", and stop the test. But in the one case where we had the Diesel fuel fire, we were up to around 2,000 Pascals differential at the end of the first fire. The second fire went for three minutes, and we were reading something like 2,800 Pascals when the filter ruptured.

FIRST: I am wondering why you don't go into a more sophisticated filter system by using deep beds of fibers or granules which would have a capacity to protect the absolute filter more capably than is shown.

GASKILL: We may come to that. We have some ideas on scrubbing techniques which we have deferred up to now because our previous work showed that we were dealing with what I will call embryonic particles, mostly of submicron size. Our work now shows they are apparently in the micron size and may be amenable to some of the techniques we have in mind and will be checking. On the other hand, if these are unsuccessful, we will have to use more expensive methods.

W.C. BROWN: I have a question regarding an ERDA interpretation that requires sprinklers in the filter exhaust ahead of the HEPA filters. About two years ago, we designed a system with two stages. Now we are confronted with the possibility that their thinking has changed and that only one stage of sprinklers will be required. The sprinklers will be followed by a demister-prefilter section which tends to protect the HEPA's from carry-over of moisture. Would that be satisfactory?

GASKILL: I don't know that I can completely comment on that. However, as we reported two years ago, using a two-fluid nozzle, we can get 100 per cent evaporation of the water. On a steady basis, with intake gases of 800 degrees Celsius, we can reduce the temperature to 150 degrees Celsius, which I understand is satisfactory, in a distance of about a meter and a half of duct length. We didn't find it necessary to use demisters at that point. On the other hand, I should mention that if, in our scrubbing techniques, we find it necessary to go back to the old inefficient method of spraying where there is a lot of water carry-over, then demisters would probably be indicated. But that remains to be seen.

TORNADO DEPRESSURIZATION AND AIR CLEANING SYSTEMS

W. S. Gregory, K. H. Duerre, P. R. Smith*, and R. W. Andrae
Staff Members, Los Alamos Scientific Laboratory
Los Alamos, New Mexico

Abstract

Results from analytical and experimental investigations of tornado depressurization effects on air cleaning systems are presented. Development and use of a computer code that simulates the internal pressures and flows within an arbitrary ventilation system is described. The formulation of fluid motion equations is based upon lumped component response, isothermal or adiabatic compression of air, and conservation of mass. A computer generated movie is shown illustrating the flows and pressures in a simple system.

Also described are experimental investigations to determine air cleaning component response to high flow rates caused by tornado depressurization. HEPA filter is the principal component under investigation. A description of the experimental apparatus is given and preliminary test results presented.

I. Introduction

Air cleaning systems in nuclear fuel cycle facilities must maintain confinement during such natural phenomena as earthquakes and tornados. The operation of a nuclear facility ventilation system is highly dependent on stable atmospheric pressure to maintain proper pressure differentials between containment zones. Atmospheric pressure drops as large as 20.7-kPa (3-psi) are associated with tornados, so that generation of undesirable pressures and flow rates within a ventilation system is possible. Large pressure drops could cause filtration failures, duct collapse or damper failures. Failure of these components in air cleaning systems could result in release of radioactive material to the environment.

Tornado depressurization effects on air cleaning systems are being studied both experimentally and analytically at the Los Alamos Scientific Laboratory and New Mexico State University. A computer code that will predict the magnitude of the pressures and flows within an air cleaning system is the objective of the analytical effort. Experimental testing has centered on evaluating critical air cleaning component response to large pressure pulses. The experimental data obtained will establish empirical relationships for the computer code, and provide structural response information. The status of the experimental and analytical work will be described in the following sections of this paper.

*Professor, New Mexico State University, Las Cruces, New Mexico.

II. Experimental Work

Preliminary Experimental Testing

Small-scale testing of 0.2-by 0.2-m (8-by 8-in.) HEPA filters has been performed at New Mexico State University[1]. A blow-down system was used to impose a 20.7-kPa (3-psi) pressure differential across the test filters for three seconds. A pressurized tank (Fig. 1) supplied the air needed to create the required pressure pulse.

The mass flow rate was regulated by sonically choking the flow, and expanding to the desired pressure in a chamber. The chamber served to slow the flow and allow the prefiltering system to operate within design capacity. The flow was exited through a test section of sufficient length to achieve uniform flow before impinging upon the test filter. Flow timing was accomplished by controlling the opening rate of a pneumatically operated ball valve upstream from the sonic orifice.

New 0.2-by 0.2-m (8-by 8-in.) HEPA filters were tested at over-pressures of 20.7-kPa (3-psi) with a 6.9-kPa/s (one-psi/s) pressurization rate. Characteristic flow-resistance data were obtained for the filters. The following conclusions were made from these tests.

- A pressurization rate of 6.9-kPa/s (one-psi/s) did not cause physical damage to the filters.
- In some tests, the pressurization rate was larger than 6.9-kPa/s (one-psi/s), which led to failure of the filter. The 0.6-by 0.6-m (24-by 24-in.) filters would be even more susceptible to structural failure because of their larger span.
- At high flow rates the pressure drop across the filter depends upon the duct cross-sectional area, and not on filter depth (Fig. 2).
- Air seems to pass through only a small portion of the filter during the pressure transient. This raises the question of filter effectiveness even if structural failure does not occur (Fig. 3).

Present Experimental Testing

The small filter experiments provided basic information for designing an experimental facility to test 0.6-by 0.6-m (24-by 24-in.) HEPA filters. Results of the small filter tests have led to speculation that high flow rates through HEPA filters can also lead to filter failure. The high velocity air through the folded ends of the fiber mat may open up mat fibers allowing high flow rate air to pass through, and then close after the transient with no evidence of structural failure. (See the change in filter resistance in Fig. 2). Entrapment of particles by the velocity-dependent diffusion mechanism may not occur during turbulent air flow through the fibers. Re-entrainment of smaller particles without a second entrapment could also occur under reversed high flow rate conditions.

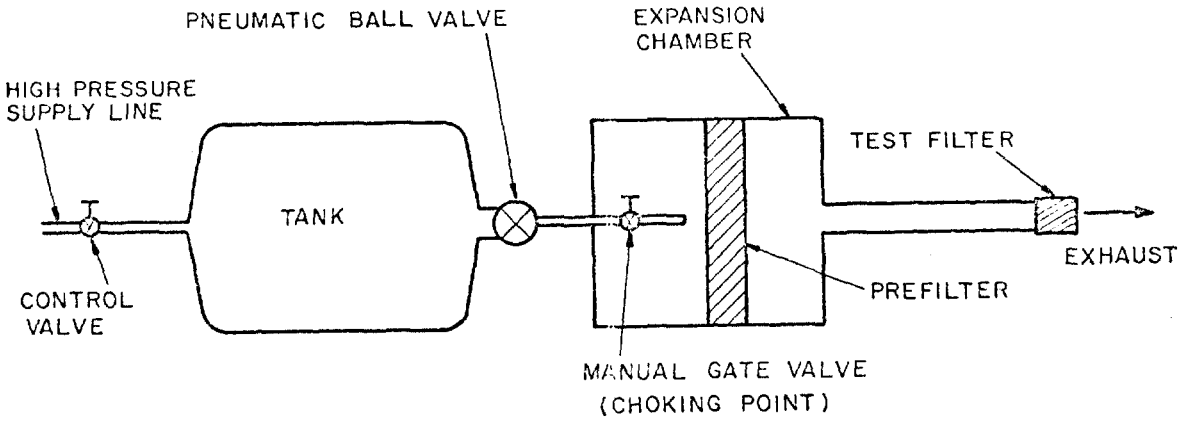

Fig. 1. Small filter experimental apparatus.

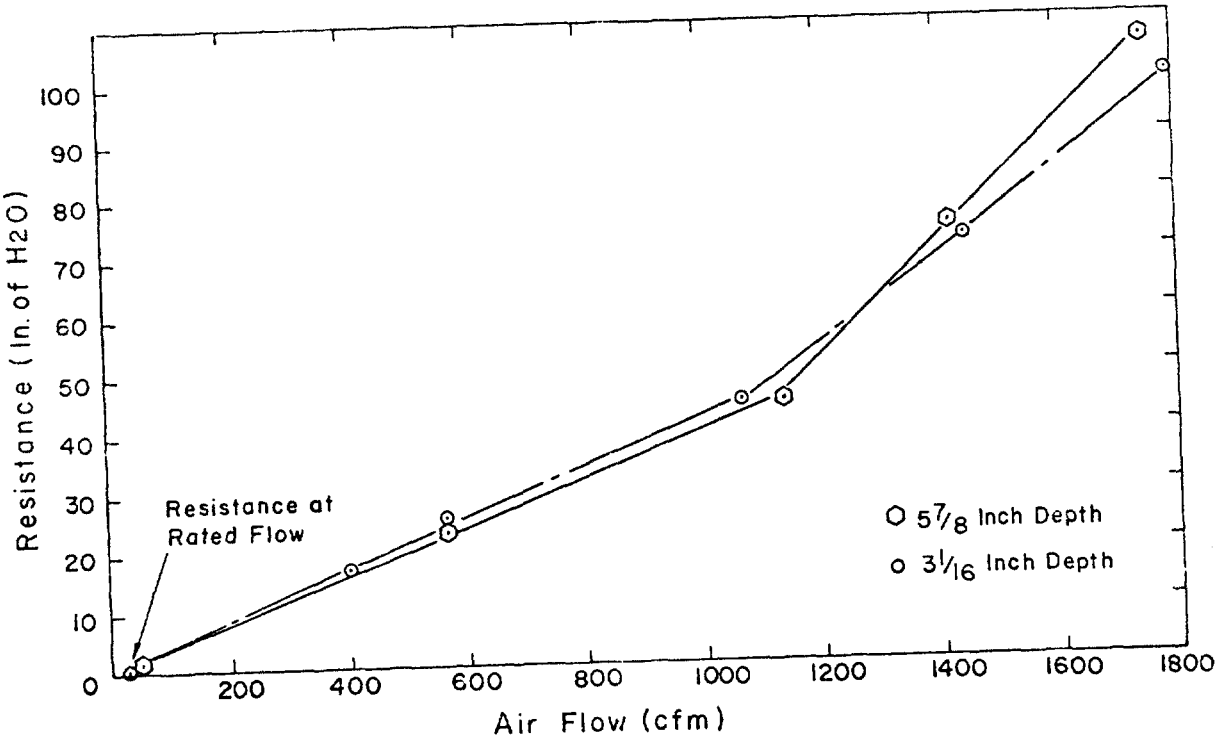

Fig. 2. Flow-resistance curve.

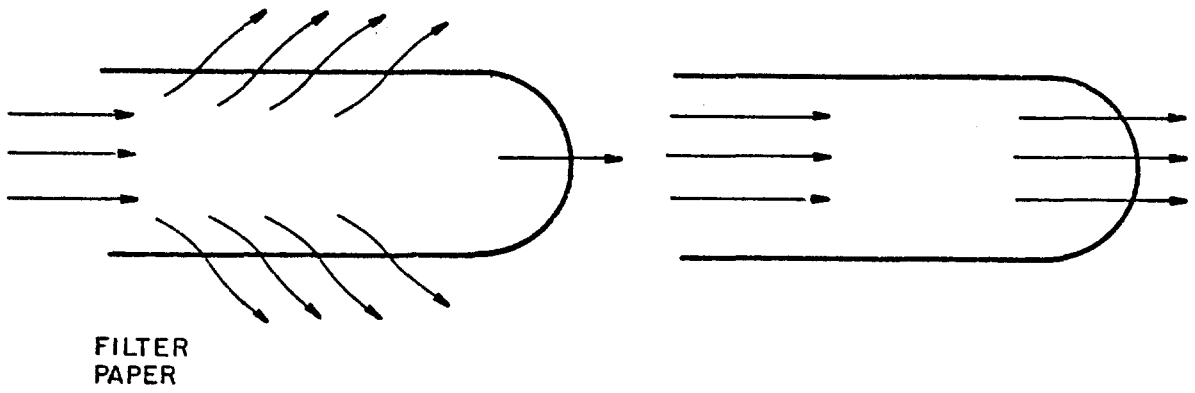

Fig. 3. Flow patterns through HEPA filter.

Objective of the present test program will be to determine the response of 0.6-by 0.6-m (24- by 24-in.) HEPA filters subjected to pressure pulses simulating a NRC Region I tornado (Fig. 4). Two possible failure modes will be investigated; failure from structural damage such that the physical integrity of the filter is destroyed and filter degradation under the NRC Region I tornado pressure conditions.

The experimental program will attempt to answer the following questions:

- Will the structural integrity of the filters be maintained during the pressure pulse?
- How critical is the rise-time of the pressure pulse? When, or at what rate of the pressure rise will the filters invariably fail?
- What is the actual flow-path through the filters during the transient pressure pulse? How does the porosity of the filters change during the pulse?
- If the filters do not fail structurally, is filter effectiveness maintained during the transient pressure pulse? Is filter effectiveness different after the pressure pulse?
- How effective are "loaded" filters during the pressure pulse? Does degree of loading have an effect upon structural failure of the filters?
- How much "release" can be expected during the transient pressure pulse for various degrees of loading?

Proposed Test Methods and Equipment. The equipment to be used to test the 0.6-by 0.6-m (24-by 24 in.) HEPA filters will be a scaled-up version of the preliminary experimental equipment. Two large pressure tanks and compressor equipment were obtained from the Nevada Test Site, and are now located at New Mexico State University at

Las Cruces, New Mexico. The pressure tanks are each 1.5-m (5 ft.) in diameter and 19.8-m (65 ft.) long (Fig. 5). They were made to contain oxygen at pressures to 19.3-MPa (2800-psi.). The compressor is capable of supplying air at 1.7-MPa (250-psi). A pressure of 1.3-MPa (200-psi) in the tanks will provide enough air for one pressure pulse. After each pressure pulse is applied, the tanks will be re-pressurized for the next pulse.

As in the small filter experiment, the mass flow rate will be regulated by sonically choking the flow and expanding into a 3.1-by 3.1-m (10-by 10-ft.) chamber (Fig. 6). The expansion chamber will contain 25 HEPA filters for prefiltering the air. The air will travel through a duct of sufficient length to achieve uniform flow before impinging on the test filter.

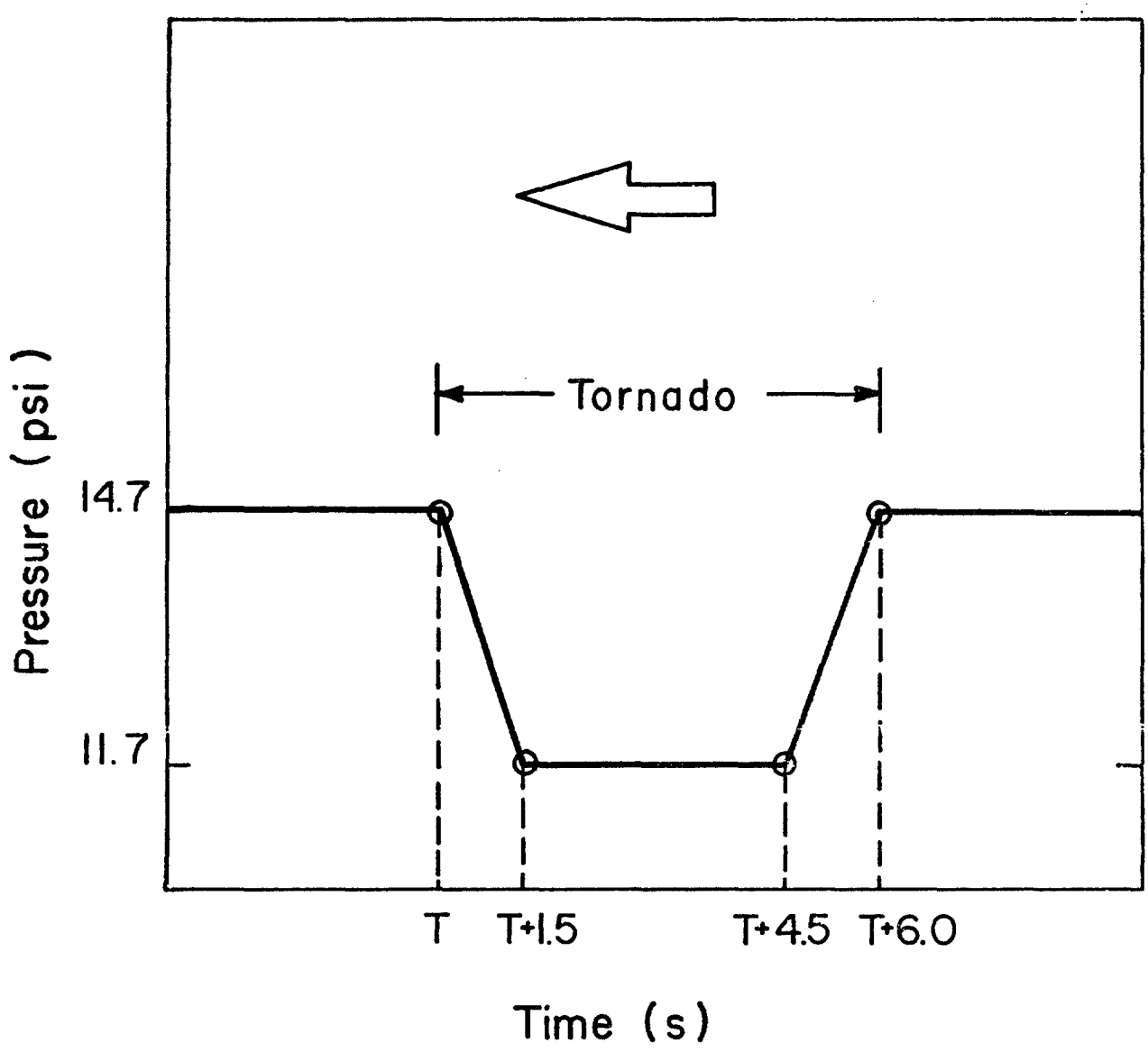

Fig. 4. Assumed pressure transient for Region I Tornado[2].

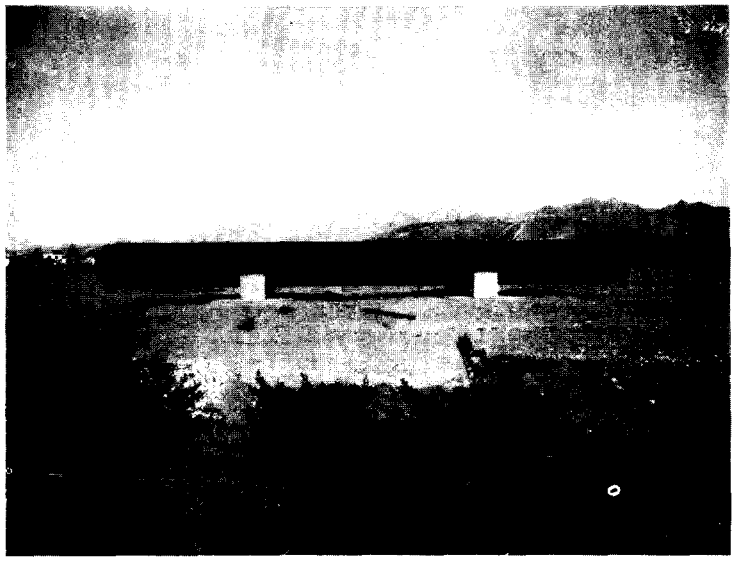

Fig. 5. Pressure tanks.

Fig. 6. Expansion chamber under construction.

The pressure pulse rise-time will be regulated by controlling the opening rate of valves between the expansion chamber and the high pressure air supply tanks. A pneumatically operated ball valve will be used with a closely regulated air pressure to actuate the control mechanism. A multiple valve arrangement is also being evaluated to achieve pressure rise times shorter than the NRC Region I tornado of 1.5 seconds.

The key to obtaining answers on questions of effective filtration is an ability to measure filter behavior during a transient pressure pulse. This can be accomplished by injecting particles of uniform size into the supply duct upstream of the filter, and simultaneously measuring particle density upstream and downstream from the filter. Care must be taken to distribute the particles uniformly across the cross-section of the duct. Also, particles of a size and density comparable with reprocessing ventilation systems should be used.

Several methods for determining the particle density upstream and downstream of the filter during the pressure were considered. These included nuclear tracer methods, x-ray defraction methods, and light diffusion or scattering methods. The safety problems inherent with the handling of radioactive materials and x-ray equipment as well as the expense of the instrumentation needed for these methods essentially eliminated them from consideration. The further requirement that the porosity of the filter material be investigated during a transient pressure pulse virtually demanded use of a light scattering method. The fact that particle density must be measured in an airstream having a velocity of 61-m/sec (200-ft/sec) during a time interval of approximately 3 seconds led to the consideration of a Laser Doppler Velocimeter (LDV) as both a particle counter and velocity meter. A slight modification on the optical system of the LDV will allow investigation of a filter porosity using a single laser beam.

The measured particle density will be related to the number of particles passing through a small volume per unit time. The data rate measured by the LDV is proportional to the number of particles passing through its measurement volume per unit time. Hence, the difference in data rate upstream to downstream across the filter gives the filter effectiveness (F_{eff}) during the pulse.

$$F_{eff} = \frac{\text{Data Rate Upstream - Data Rate Downstream}}{\text{Data Rate Upstream}} \qquad (1)$$

A possible configuration of such a system is shown in Fig. 7. We believe that the LDV system could monitor the effectiveness of clean and loaded filters during a pressure pulse. Further, it could give a quantitative measurement of particles released from loaded filters during a pressure transient.

The LDV system would give the mean flow velocity upstream and downstream of the filters, as well as the turbulance level at these points. Furthermore, by traversing the LDV measuring volume (the crossing point of the beams) across the cross-section of the duct downstream of the filters, the flow path of the air through the filters can be determined. Porosity of the filter material during the pressure pulse could be investigated by passing a laser beam through the filter and measuring the change in beam intensity.

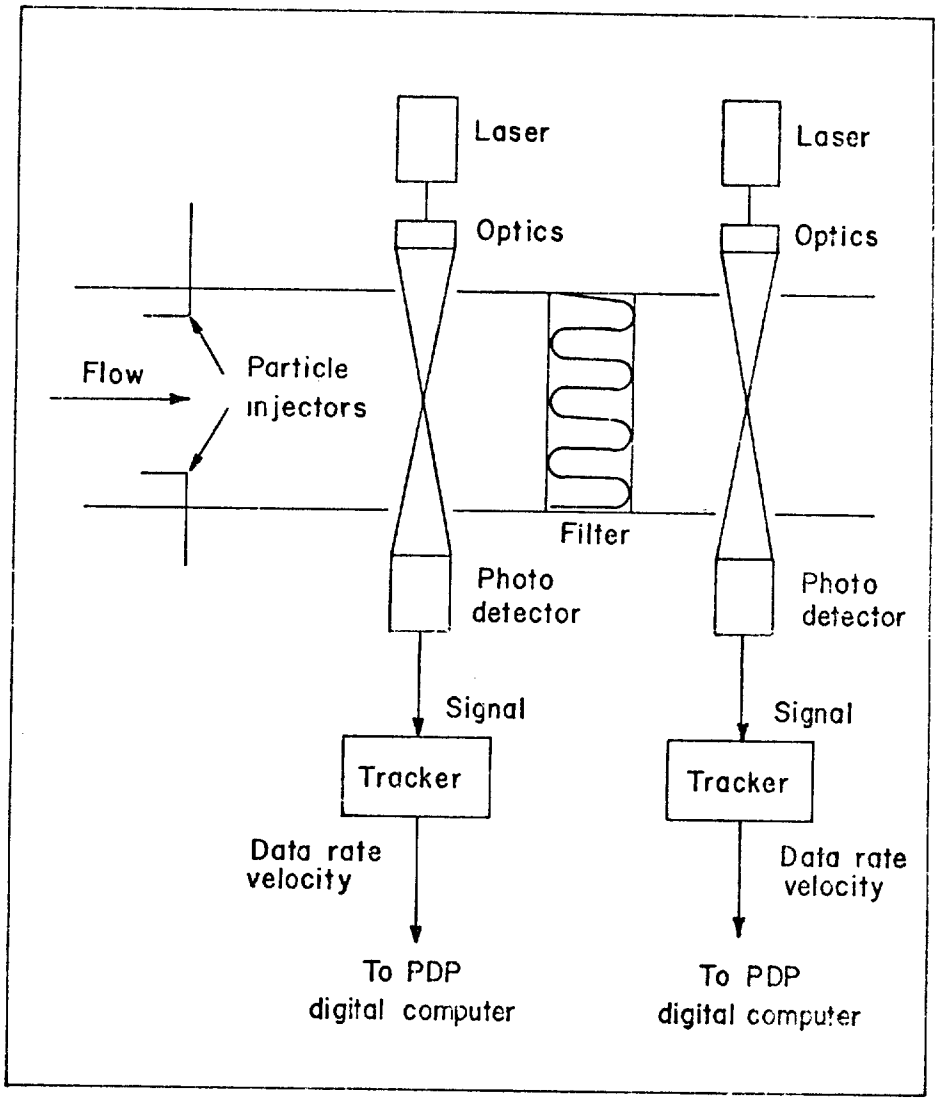

Fig. 7. Laser instrumentation system.

Future Investigations

Further investigations will examine the behavior of other ventilation system components during tornado induced pressure transients. Considerable uncertainty exists concerning the response of a fan or blower to a change in atmospheric pressure. Blowers on either the exhaust or supply side, are probably the components closest to the full impact of tornado depressurization. Blower operation under conditions of out-running flow and flow reversal are not well known.

III. Analytical Work

General

Calculation of pressures and flows, within an air cleaning system for a tornado depressurization requires solution of general fluid dynamic equations, involving the conservation of momentum,

energy, and mass. These equations are not easily solved numerically, but they do provide a basis for development of a simplified set of working equations. Analysis of these equations showing the importance of inertia and shock terms has been described elsewhere[3]. Simplification and coupling of these equations with empirical fluid-flow relationships, allows development of equations that can be used to calculate the fluid dynamics in a network of connecting ducts and components.

A digital computer code "TVENT" has been developed that utilizes the equations derived in the following section to predict the transient response of arbitrary ventilation systems to tornado induced pressure transients.

Formulation of Equations

The equations are formulated using a "lumped" parameter approximation that neglects spatial distribution of variables. The following equations types will result upon application of the lumped parameter approach:

- a simultaneous set of coupled nonlinear algebraic equations, and
- a simultaneous set of ordinary differential equations.

The lumped parameter approach includes a number of system elements or branches joined together at points called nodes. The nodes are the connection points at the upstream and downstream ends of the branches. The pressure variable of the system is lumped into the nodes. Air cleaning system components such as dampers, filters and blowers, that have a resistive nature, are located within the branches of the system. A branch without a component (the duct work) also has a resistive nature. The frictional resistance to flow in the ductwork and system components is lumped within the branches of the network. An empirical pressure-flow relationship suitable for the elements is used for all branches in the system. This relationship can be written as:

$$Q(K) = \alpha(K) + \beta(K)(P(J) - P(I))^{\gamma(K)} \qquad (2)$$

where
- K = branch K,
- $Q(K)$ = flow rate through a branch,
- $\gamma(K)$ = constants for a particular branch,
- $P(I)$ = pressure at node I, and
- $\alpha(K), \beta(K)$, $P(J)$ = pressure at an upstream node J so that $P(J) > P(I)$.

Application of Eq. (2) for the system components will yield a number of forms. These forms are summarized in Table I.

At any particular time, the branch flow and the pressures at the upstream and downstream nodes are unknown. Coupling all branch equations at a particular node through use of a continuity equation, allows the flow variable to be eliminated. Only the system pressures remain to be determined. An iterative process, ideally suited for the digital computer, is used with a linearized form of Eq. (2) to

Table I Pressure-Flow Relationships for Various Branch Components.

Branch Component	$\alpha(K)$	$\beta(K)$	$\gamma(K)$	Flow Equation	Eq. No.
Duct Friction	0	Variable	0.5	$\beta(K)(P(J)-P(J))^{\gamma(K)}$	(3)
Filter (low flows)	0	Variable	1	$\beta(K)(P(J)-(P(I))$	(4)
Damper	0	Variable	0.5	$\beta(K)(P(J)-P(I))^{\gamma(K)}$	(5)
Blower (linear approximation)	Variable	Variable	1	$\alpha(K)+\beta(K)(P(J)-(P(I))$	(6)

determine a pressure correction (ΔP) at each node. The process is repeated many times until the pressures at the nodes are within an acceptable tolerance.

Calculation of the pressure correction parallels Streeter's procedure for determining the pressures and flows in the steady-state portion of a water-hammer computer code[4]. Streeter located pumps at nodes, whereas this analysis requires all components to be located within the branch connections. In addition, this formulation is a transient analysis with allowance for storage of fluid at particular nodes. This condition requires derivation of a different algorithm for calculation of ΔP at fluid storage nodes.

The pressure correction for a node is calculated assuming that the true pressure at node I is equal to $P(I) + \Delta P$. Using this approximation, Eq. (2) becomes:

$$Q(K) \approx \beta(K)\,[P(J) - (P(I) + \Delta P)]^{\gamma(K)} \pm \alpha(K). \tag{7}$$

Using a bionomial expansion of Eq. (7), neglecting higher order terms and considering P(I) to be the value of pressure at node I for the previous iteration, Eq. (7) becomes:

$$Q(K) \approx \beta(K)[P(J) - P(I)]^{\gamma(K)}\left[1 - \frac{\beta(K)\,\Delta P}{P(J) - P(I)}\right] \pm \alpha(K), \tag{8}$$

or

$$Q(K) \approx A - C\Delta P. \tag{9}$$

where A and C are known constants from the previous iteration and are equal to:

$$A = \beta(K)[P(J) - P(I)]^{\gamma(K)} \pm \alpha(K) \tag{10}$$

$$C = \beta(K)\gamma(K)[P(I) - P(J)]^{\gamma(K)-1} \tag{11}$$

If $P(I) > P(J)$*, the values of A and C become:

$$A = -\beta(K)[P(I) - P(J)]^{\gamma(K)} \pm \alpha(K), \text{ and} \tag{12}$$

*J refers to downstream node in this case.

$$C = \beta(K)\gamma(K)[P(I) - P(J)]^{\gamma(K)-1}. \quad (13)$$

Components that have a relatively large volume such as rooms, gloveboxes, and plenums are located at the nodes. These nodes exhibit a capacity for fluid storage and are called capacitance nodes. The compressibility of the system is accounted for by allowing fluid storage at the capacitance nodes. However, in all cases the conservation of mass must hold at the nodes. For an ordinary node, with no storage or blower connection, conservation of mass yields:

$$\Sigma Q(K) = 0, \quad (14)$$

or

$$\Sigma A - \Sigma C\ \Delta P = 0. \quad (15)$$

Solving for the pressure correction ΔP gives:

$$\Delta P = \frac{\Sigma C}{\Sigma A}. \quad (16)$$

Equation (16) is used to determine successive pressure corrections for an ordinary node without storage. When a node is connected to a duct containing a blower, the constant $\alpha(K)$ must be added or subtracted from ΣA before the correction is calculated. In all other cases $\alpha(K)$ is equal to zero.

If only steady-state values of pressure and flow are of interest, Eq. (16) is sufficient for arriving at the correct pressures. However, during a transient, mass-in does not equal mass-out at nodes containing rooms, gloveboxes or plenums. The equation of state is used at these storage nodes in addition to the continuity equation. The equation of state can be written as:

$$P(I) = \rho RT, \quad (17)$$

where

ρ = density of air at the node,
R = gas constant for air, and
T = absolute temperature of the air.

Differentiation of this equation with respect to time yields:

$$\frac{dP(I)}{dt} = CF(Q_{in} - Q_{out}), \quad (18)$$

or

$$\frac{dP(I)}{dt} = CF\ \Sigma\ Q(K), \quad (19)$$

where

$$\begin{aligned} CF &= \rho RT/V, \\ Q_{in} &= \text{flow rate into node}, \\ Q_{out} &= \text{flow rate out of node}, \end{aligned} \tag{20}$$

and V is the volume of the node under consideration.

Using finite differencing, Eq. (19) can be written as:

$$\Sigma Q(K) = \frac{1}{CF} \frac{P(I)^n - P(I)^{n-1}}{\Delta t}, \tag{21}$$

where

$$\begin{aligned} P(I)^n &= \text{present iterative value of pressure}, \\ P(I)^{n-1} &= \text{past iterative value of pressure, and} \\ \Delta t &= \text{discrete time step}. \end{aligned}$$

Substituting $P(I)^n + \Delta P$ for $P(I)^n$ in Eq. (21) yields the following equation for determination of the pressure correction at a storage node:

$$\Delta P = \frac{CF\ \Delta t\ \Sigma A + P(I)^{n-1} - P(I)^n}{1 + CF\ \Delta t\ \Sigma C}. \tag{22}$$

Eqs. (16) and (22) are incorporated within the computer code TVENT so that successive pressures are calculated until the true pressures that balance the system are obtained. After convergence has been achieved, the flows that result from the calculated pressure distribution are computed from the branch component equations.

Modeling Technique

Several facility ventilation systems were reviewed to determine the complexity of these systems and to identify typical components and subsystems [5,6]. A small fictitious test-case ventilation system was devised containing many of the components and subsystems common to facility ventilation systems. This test-case ventilation system (Fig. 8 and Fig. 9) was used to test the computer code. The test-case features:

- Natural bypass around rooms,
- Recirculation similar to that used in the Westinghouse Recycle Fuels Plant,
- Combinations of series and parallel arrangements of components,
- Rooms (confinement volumes) with multiple inlets and outlets,
- Duct friction, and
- A network consisting of 30 components and 25 nodal points.

Some components have been omitted from Fig. 8 for clarity, but are included in the schematic of Fig. 9.

A branch is defined as a connecting member between two nodes and includes only one component. Boundary conditions (pressure as a function of time) and capacitance are prescribed at nodal points. The branch and node labeling are somewhat arbitrary, however numbers may not be skipped.

Following the lumped parameter approach, all of the pressure losses for a branch are ascribed to the component contributing the largest pressure loss. Thus, the duct loss may be lumped with the damper loss characterized by Eq. (5) of Table I for Branch 1 of Fig. 9. Similarly the duct pressure loss in Branch 2 of Fig. 9 may be lumped with the filter pressure loss. An inspection of the $\gamma(K)$ Table I shows that Branch 1 is modeled more accurately than Branch 2. A branch should be added to the model if the duct pressure loss is a significant fraction of the component pressure loss.

The blower pressure-flow relationship is approximated by a series of linear segments (Fig. 10). The coefficients (Eq.(6) of Table I)

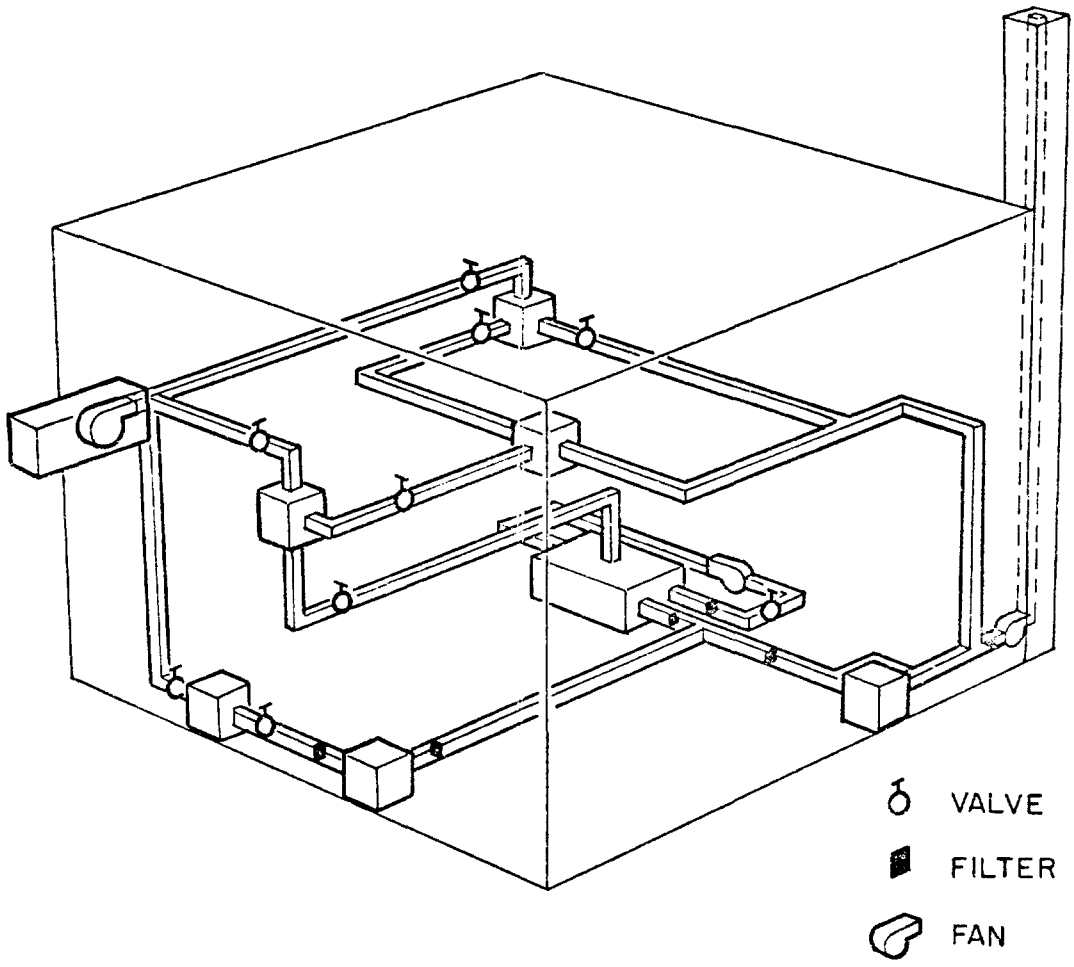

Fig. 8. Fictitious ventilation system within building.

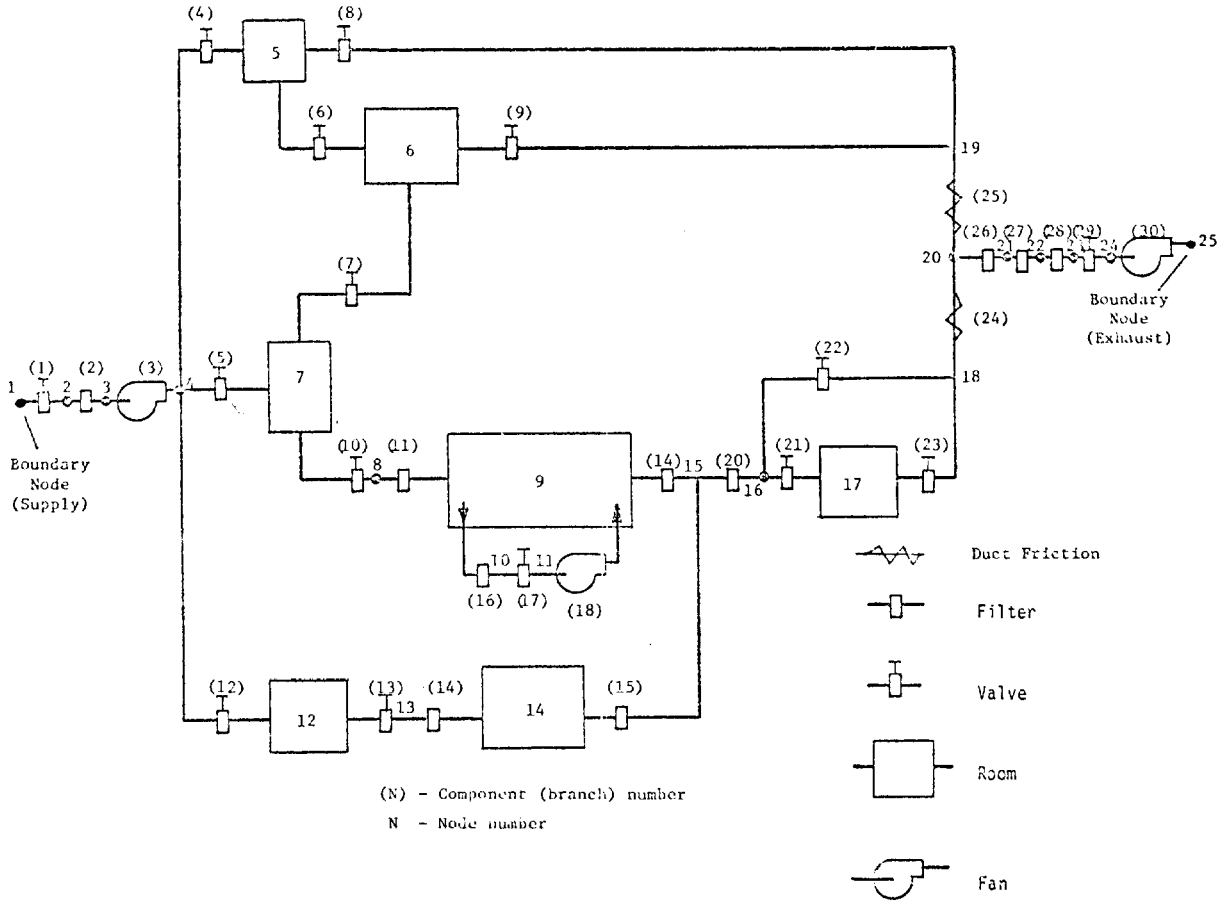

Fig. 9. Lumped parameter model of ventilation system.

are checked at every time-step and changed if necessary to obtain consistant flows and nodal pressures. This technique may also be used for filters with low and high flows as better experimental data become available.

Infiltration or leakage may be specified by the addition of a boundary node attached to a fictitious branch connected to the room with the leak. The resistance can be calculated from the design leak, the design room pressure and the boundary pressure. In this way a variable leakage rate is achieved for the transient.

Duct volumes are checked against the smallest room volume detected by the computer code. An informative message is given if a duct volume exceeds half the smallest room volume, since this would probably indicate a modeling error. Consideration should then be given to adding a capacitance node or possibly eliminating the smallest room(s).

The Computer Program "TVENT"

General. The program is written in the FORTRAN IV language and is designed to be "portable", that is, easily transferred from one computer to another with a minimum of change. Runs have been performed on the CDC 7600 computer and the IBM 360 computer to demonstrate this capability. The portability requirement precludes free format input and film plotting options that are not found on some systems.

The program is structured as a one level overlay (Fig. 11) to permit its use on smaller computers and to allow expansion.

Input. The input consists of two parts: 1) control information specifying how the problem is to be run and 2) a physical description of the system to be analyzed. An attempt has been made to organize and format the input in a way that is "natural" to the designer or engineer preparing the data for analysis. Several common methods exist for designing ventilation systems [7,8]. The branch description (Fig. 12) is similar to the working tables given in the above references.

A more common method of representing the pressure-flow relationship is:

$$\Delta H = R \cdot Q^m, \tag{23}$$

where

ΔH = pressure drop across the component (measured or calculated),

R = resistance coefficient,

Q = branch design or measured flow, and

m = flow exponent (equals $1/\gamma(K)$ of Table I).

Equation (23) is used for branch description input and for calculating resistance of leakage nodes. The resistance R, if specified, overrides the resistance normally calculated by the computer using input values of pressure drop and design flow in Eq. (23). Pressures may be specified directly, in which case pressure drops are determined from these pressures and the branch descriptions.

Output. The output produced during problem set-up and transient calculations encompasses:

- Informational and diagnostic messages indicating input or modeling errors.
- Input return in the form of a card-image listing (Fig. 13) and lists associated with arrays generated from the input and used in the system solver.

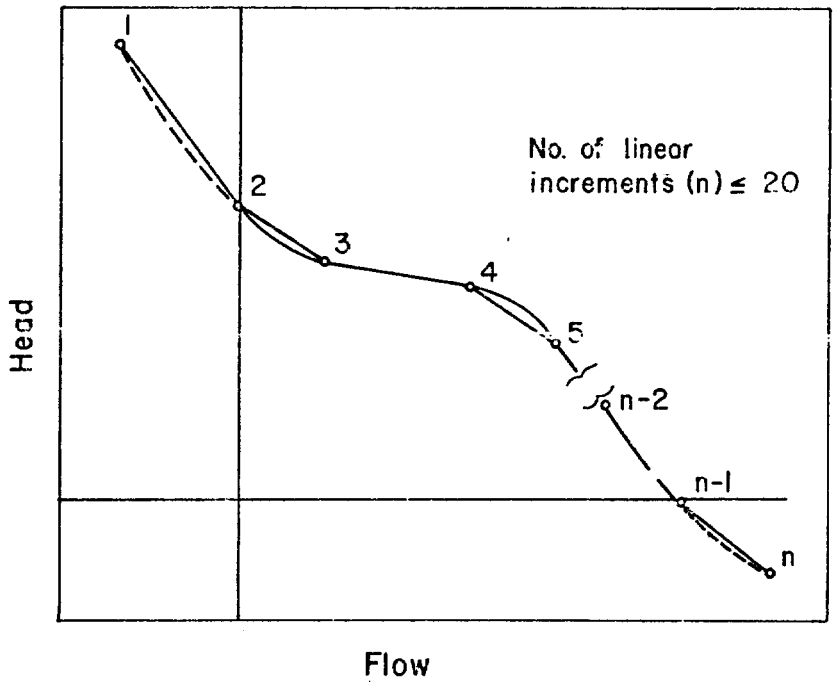

Fig. 10. TVENT blower characteristics.

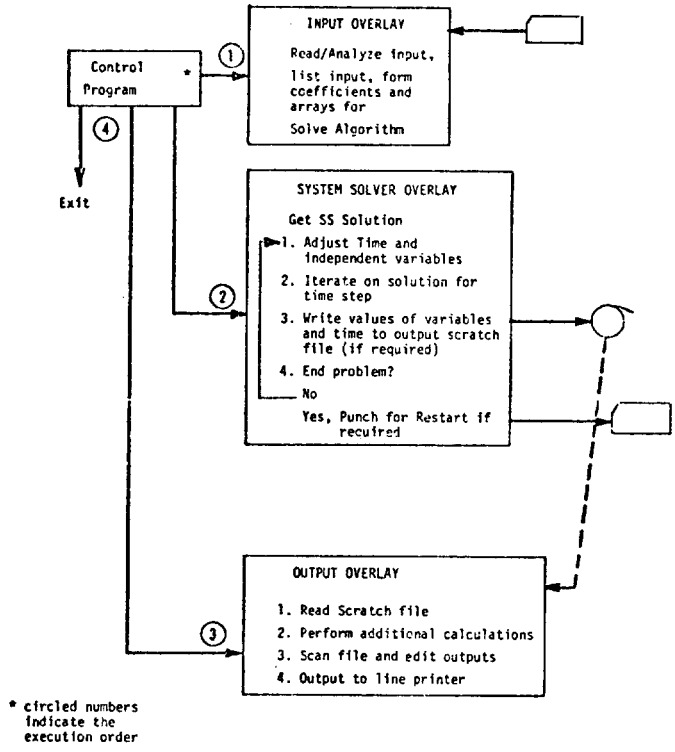

Fig. 11. TVENT program flow and overlay structure.

BRANCH DATA

NO.	IN NODE	OUT NODE	INITIAL FLOW	HYDRL RADIUS	COMP TYPE	BLOWER CURVE	EXP Q P	RESIST VALUE	BLOWER INTERCEPT,	INITIAL DELTA-P
1	1	2	388.000	0.000	VALV	0	.50	1.203E+03	0.	.104000
2	2	3	388.000	0.000	FILT	0	1.00	1.003E+03	0.	.387000
3	3	4	388.000	0.000	BLWR	1	1.00	2.500E+02	1.0000E+03	2.448000
4	4	5	0.000	0.000	VALV	0	.50	1.000E+02	0.	1.000000
5	4	7	156.100	0.000	VALV	0	.50	1.201E+03	0.	.016900
6	5	6	0.000	0.000	VALV	0	.50	1.200E+03	0.	.000050
7	7	6	0.000	0.000	VALV	0	.50	1.000E+02	0.	1.000000
8	5	19	0.000	0.000	VALV	0	.50	1.200E+03	0.	.007000
9	6	19	0.000	0.000	VALV	0	.50	1.200E+03	0.	.007000
10	7	8	57.400	0.000	VALV	0	.50	1.202E+03	0.	.002280
11	8	9	57.400	0.000	FILT	0	1.00	3.005E+02	0.	.191000
12	4	12	103.000	0.000	VALV	0	.50	1.220E+03	0.	.006944
13	12	13	100.000	0.000	VALV	0	.50	1.200E+03	0.	.006944
14	13	14	100.000	0.000	FILT	0	1.00	6.993E+02	0.	.143000
15	14	15	100.000	0.000	FILT	0	1.00	6.993E+02	0.	.143000
16	9	10	179.800	0.000	FILT	0	1.00	6.996E+02	0.	.257000
17	10	11	180.100	0.000	VALV	0	.50	1.201E+03	0.	.022500
18	11	9	200.000	0.000	BLWR	2	1.00	2.500E+02	2.5000E+02	.220000
19	9	15	57.900	0.000	FILT	0	1.00	3.016E+02	0.	.192000
20	15	16	198.500	0.000	FILT	0	1.00	3.000E+02	0.	.635000
21	16	17	79.300	0.000	VALV	0	.50	1.201E+03	0.	.004360
22	16	18	112.800	0.000	VALV	0	.50	1.200E+03	0.	.008830
23	17	18	80.200	0.000	VALV	0	.50	1.201E+03	0.	.004460
24	18	20	193.800	0.000	DUCT	0	.50	1.807E+03	0.	.011500
25	19	20	0.000	0.000	DUCT	0	.50	1.000E+03	0.	.053000
26	20	21	395.800	0.000	FILT	0	1.00	7.005E+02	0.	.565000
27	21	22	395.800	0.000	FILT	0	1.00	3.021E+02	0.	1.310000
28	22	23	395.800	0.000	FILT	0	1.00	3.021E+02	0.	1.310000
29	23	24	395.800	0.000	VALV	0	.50	1.204E+03	0.	.108000
30	24	25	395.800	0.000	BLWR	3	1.00	2.500E+02	1.0000E+03	2.416800

Fig. 12. Branch description of input data.

```
                              TVENT      JAN 76   LASL
         10        20        30        40        50        60        70        80
12345678901234567890123456789012345678901234567890123456789012345678901234567890
   A REGION I TORNADO AT THE AIR SUPPLY
     .1875 12.      4


   14.3                    1    2
    1                 1
   25
    1    5
                       1,5        -83.067    4,5        -83.067
  6,                   9.0
   30   25    3    7    3
    1    1    2  388.0                          V    .104
    2    2    3  388.0                          F    .387
    3    3    4  388.                           B                              1
    4    4    5                                 V    1.0          1.000E-04
    5    4    7  156.1                          V    .0169
    6    5    6                                 V    .00005       6.944E-07
    7    7    6                                 V    1.0          1.000E-04
    8    5   19                                 V    .007         6.944E-07
    9    6   19                                 V    .007         6.944E-07
   10    7    8  57.4                           V    .00228
   11    8    9  57.4                           F    .191
   12    4   12  100.000                        V                 6.944E-07
   13   12   13  100.000                        V                 6.944E-07
   14   13   14  100.000                        F                 1.430E-03
   15   14   15  100.000                        F                 1.430E-03
   16    9   10  179.8                          F    .257
   17   10   11  180.1                          V    .0225
   18   11    9  220.                           B                              2
   19    9   15  57.9                           F    .192
   20   15   16  190.5                          F    .635
   21   16   17  79.3                           V    .00436
   22   16   18  112.8                          V    .00883
   23   17   18  80.2                           V    .00446
   24   18   20  193.800                        D    .0115
   25   19   20                                      .05          1.000E-06
   26   20   21  395.8                          F    .565
   27   21   22  395.8                          F    1.31
   28   22   23  395.8                          F    1.31
   29   23   24  395.8                          V    .108
   30   24   25  395.8                          B                              3
    5   20.       10.       25.
    6   20.       10.       25.
    7   20.       10.       25.
    9   20.       10.       25.
   12   20.       10.       25.
   14   20.       10.       25.
   17   20.       10.       25.
    1    2
            4.0       1000.
    2    2
     0.0       1.0        250.       0.0
    3    2
       0.0       4.0       1000.       0.0
```

Fig. 13. Card-image listing of input.

- The following lists of steady-state and transient results as shown in Figs. 14 and 15 may be obtained (transient-output times must be requested).
    - pressures and flows for all nodal points and branches, respectively,
    - differential pressures across filters,
    - flows through filters,
    - differential pressures across dampers,
    - differential pressures between rooms, and
    - a summary of peak values.
- A limited number of pressure or flow versus time line-printer plots upon request.

Special Features.

- The input processor accepts an output frequency based on total problem-time less the problem start-restart time with additional special output times (up to 5). The latter are useful when doubt may exist whether a maximum or minimum value of some variable may have been missed.
- A problem may be stopped and subsequently restarted, which is useful for unusually large systems or long transients. It is also useful in simulating duct or filter failures during a transient.
- The input is sufficiently flexible to permit runs for verification of an existing design, and parameter studies for insight into the effects of changing design values.
- The program is easily modified. This is an asset when experimental data may dictate changes in modeling techniques.

IV. Discussion and Results

A computer generated movie has been prepared from four runs made with TVENT for the test case ventilation system.

These runs included:

1. A Region I tornado* occurs at the air supply,
2. A Region I tornado occurs at the exhaust,
3. A Region I tornado occurs simultaneously at both the air supply and exhaust, and
4. A Region I tornado occurs at the air supply, and after a six second delay appears at the exhaust.

A REGION I TORNADO AT THE AIR SUPPLY

NODAL PRESSURES FOR TIME = 6.00000

	0	1	2	3	4	5	6	7	8	9
0		0.00000	-2.29290	-4.11000	-7.39740	-1.90970	-1.90970	-8.23790	-7.85330	-5.37240
10	-5.62970	-5.65220	-8.03090	-7.24290	-5.71960	-4.83680	-2.24870	-2.13180	-2.14000	-1.94050
20	-2.11820	-2.33890	-2.85080	-3.36280	-3.37940	-0.00000				

BRANCH FLOWS

	0	1	2	3	4	5	6	7	8	9
0		1821.8	1821.8	1821.8	-234.3	1100.9	8.7	-251.6	210.8	210.6
10	-745.5	-745.5	955.2	-1065.3	-1065.3	-617.3	180.8	180.1	180.1	-161.5
20	-778.8	-397.9	-381.0	114.1	-266.9	421.5	154.6	154.7	154.7	155.1
30	155.1									

DIFFERENTIAL PRESSURE (D.P.) ACROSS FILTER

BRANCH	D. P.	BRANCH	D. P.	BRANCH	D. P.	BRANCH	D. P.
2	1.817100	11	2.480900	14	1.523300	15	.882800
16	.257300	19	.535600	20	2.596100	26	.220700
27	.511900	28	.512000				

FLOW THROUGH FILTER

BRANCH	FLOW	BRANCH	FLOW	BRANCH	FLOW	BRANCH	FLOW
2	1821.8	11	-745.5	14	-1065.3	15	-617.3
16	180.8	19	-161.5	20	-778.8	26	154.6
27	154.7	28	154.7				

DIFFERENTIAL PRESSURE (D.P.) ACROSS DAMPER

BRANCH	D. P.	BRANCH	D. P.	BRANCH	D. P.	BRANCH	D. P.
1	2.292900	4	5.487700	5	.840500	6	0.000000
7	6.328200	8	.030800	9	.030800	10	.384600
12	.633500	13	.788000	17	.022500	21	.109700
22	.100700	23	.009000	29	.016600		

Fig. 14. Composite of output listings.

A REGION I TORNADO AT THE AIR SUPPLY

DIFFERENTIAL PRESSURE BETWEEN ROOMS FOR TIME = 6.00000

NODE	ROOM	1	2	3	4	5	6	7
5	1	0.00000	0.00000	6.32820	3.46270	6.12120	3.80990	.22130
6	2	0.00000	0.00000	6.32820	3.46270	6.12120	3.80990	.22130
7	3	-6.32820	-6.32820	0.00000	-2.86550	-.20700	-2.51830	-6.10690
9	4	-3.46270	-3.46270	2.86550	0.00000	2.65850	.34720	-3.24140
12	5	-6.12120	-6.12120	.20700	-2.65850	0.00000	-2.31130	-5.89990
14	6	-3.80990	-3.80990	2.51830	-.34720	2.31130	0.00000	-3.58860
17	7	-.22130	-.22130	6.10690	3.24140	5.89990	3.58860	0.00000

S U M M A R Y

* * * * * * * * * * * * * *

* HIGHEST PRESSURE OF -0.00000 OCCURS AT NODE 25

* LOWEST PRESSURE OF -8.23790 OCCURS AT NODE 7

* LARGEST POSITIVE FLOW OF 1821.80 OCCURS IN BRANCH 3

* LARGEST NEGATIVE FLOW OF -6823.30 OCCURS IN BRANCH 3

* FILTER WITH LARGEST PRESSURE DIFFERENTIAL OF 2.596100 IS IN BRANCH 20

* FILTER WITH LARGEST FLOW OF 1821.80 IS IN BRANCH 2

* DAMPER WITH LARGEST PRESSURE DIFFERENTIAL OF 6.328200 IS IN BRANCH 7

* ROOM NO. 0 HAS THE HIGHEST POSITIVE PRESSURE OF 0.00000

* ROOM NO. 3 HAS THE LOWEST NEGATIVE PRESSURE OF -8.23790

Fig. 15. Composite of output listings.

Some preliminary observations can be made based on studies of the test case ventilation system:

- A convergence tolerance of 0.025-Pa (1.0×10^{-4} in. of water) (that is nodal pressures changing by less than this amount on successive iterations) appears to be adequate for accuracy. This has been checked against different algorithms.

- Branches containing small pressure drops (less than five times convergence tolerance) exhibit significant errors. A decrease in the tolerance does not improve the solution.

- Solution accuracy is not a strong function of time-step size.

- The use of linear segments to approximate the blower characteristic curves has not caused convergence problems at those points where the algorithm might tend to search for the correct segment of the blower curve during the transient.

- The CDC 7600 computer time to real time ratio is about one half with a time step of 0.1 second for the test case problem.

V. Summary and Conclusions

The analytical and experimental investigations described in this paper will provide the analyst with some insight into the effects of tornado depressurization on air cleaning systems. The results obtained thus far are preliminary, as the analytical and experimental tools needed to investigate the problem are under development.

Interpretation of preliminary experimental results indicates that there may be a loss of material through the HEPA filters from either filter degredation or structural failure. Further experimental work at the Las Cruces Test facility will be aimed at accurately determining HEPA filter failure mechanisms under tornado conditions.

Analytical investigations with the computer code "TVENT", can provide information on overall air cleaning system response to tornado depressurization. However, this code has not been applied to an actual system. Future plans include its application to an actual system as well as incorporating experimental results for individual components. A second level of analysis using a distributed parameter approach is also planned.

Acknowledgements

The authors would like to express their appreciation for the support provided by the Energy Research and Development Administration, Division of Operational Safety and the Nuclear Regulatory Commission, Division of Safeguards Fuel Cycle and Environmental Research.

References

1. Gregory, W.S., HEPA Filter Effectiveness during Tornado Conditions, LA-5352-MS, Los Alamos Scientific Laboratory, 1973.

2. Markee, E. H. Jr., Beckerley, J. G., Sanders, K. E., Technical Basis for Interim Regional Tornado Criteria, U.S. Atomic Energy Commission Office of Regulation, Wash-1300, 1974.

3. Gregory, W. S., Smith, P. R., Duerre, K. H., "Effect of Tornados on Mechanical Systems", Proceedings Symposium on Tornados, Lubbock, Texas, 1976.

4. Streeter, V. L., "Water-Hammer Analysis of Distribution Systems", American Society of Civil Engineers, HY5, Sept. 1967.

5. Gregory, W. S., Bennett, G. A., Ventilation Systems Analysis During Tornado Conditions - July through December 1974, LA-5894-PR, Los Alamos Scientific Laboratory, March 1975.

6. Bennett, G. A., Gregory, W. S., Smith, P. R., Ventilation Systems Analysis During Tornado Conditions - January - June 1975, LA-6120-PR, Los Alamos Scientific Laboratory, Nov. 1975.

7. ASHRAE Handbook of Fundamentals (Chapter 25), American Society of Heating, Refrigeration and Air Conditioning Engineers, 1972.

8. Carrier Air Conditioning Company, "Air Duct Design", Handbook of Air Conditioning System Design, McGraw Hill Book Company, New York, 1965.

DISCUSSION

OLSON: I would like to know why you are using one and a half seconds for pressure drop rather than three seconds, which I believe is used by NRC.

GREGORY: In the past, the Region 1 tornado criteria have been over a three-second period and, in fact, we did test the small filters over a three second period or with a 1 psi per second ramp. Since then, we are using the interim Region 1 tornado criteria, which, I believe, are in WASH-1300. In the Region 1 tornado, there is a 2 psi per second depressurization which would occur over a one and a half second period, I believe. The computer program will take any kind of condition for any particular transient that you would like to apply.

DESIGN AND ANALYSIS OF THE SANDIA LABORATORIES HOT CELL FACILITY SAFETY VENTILATION SYSTEM

E. A. Bernard and H. B. Burress
Sandia Laboratories
Albuquerque, New Mexico 87115

Abstract

Sandia Laboratories has designed a Hot Cell Facility (HCF) to support a variety of experimental programs. This facility will provide an on-site capability to conduct glove box experiments with irradiated samples having intermediate levels of radioactivity- 2,000 curies of fission products and 200 curies of plutonium.

The HCF uses a combination of existing and new construction to minimize costs and maximize usage of existing facilities. A new safety ventilation system has been designed to service the HCF.

The ventilation system consists of three zones as required by the Plutonium Facilities General Design Criteria, Appendix 6301 (GDC). In conforming with this GDC, the HCF can accommodate several hundred curies of plutonium while actual Sandia requirements are for 1-5 curies.

The maximum credible accident for the HCF is a hypereze (liquid cutting compound) fire. A combination of experimental data and calculational procedures are used to define the fire environment, predict the impact on the ventilation system components and determine the overall system effectiveness in case of such an accident.

I. Introduction

This report describes the Hot Cell Facility (HCF) designed by Sandia Laboratories. The HCF is composed of three steel confinement boxes (SCB's), the hot cell, a support area, the safety ventilation system and a fire protection system. This facility provides Sandia Laboratories with an on-site capability to analyze irradiated samples containing up to 2,000 curies of fission products and 200 curies of plutonium.

The HCF is located in the basement of Building 6580 which is in one of Sandia's major technical areas. Figure 1 shows the floor plan of the HCF. There are three safety ventilation systems serving the HCF. The first system (Zone 1) serves the SCB's and the second (Zone 2A) serves the hot cell. Both of these systems are once-through systems. The third system is a partial recirculation system and serves the support area (Zone 2). The three SCB's are located next to the manipulator wall, the west wall of the hot cell. The separation distance between the SCB's and the other walls of the hot cell allows sufficient space in which to position and unload the sample containers and transfer samples within the hot cell. The walls of the hot cell are 1.07 m (3.5 ft) thick and made of reinforced concrete. An airlock is located at the north end of the hot cell. This airlock permits

access to the hot cell from the support area. The support area (Zone 2) which surrounds the hot cell is used for storage of casks prior to moving them into the hot cell. The area adjacent to the HCF (Zone 3) is not considered a part of the HCF. Make-up air for the safety ventilation system is drawn from the building ventilation system.

The HCF is composed of pre-existing and new construction. The SCB's, the west manipulator wall and part of the south hot cell wall were present before construction of the HCF. The south wall was extended to the ceiling and the new east wall was added to form the walls of the hot cell. The airlock at the north end of the hot cell was added to provide for access into the hot cell. In order to enclose the support area, a new wall was added at the southeast and south boundaries of the HCF. This addition also contains the outside airlock for access into the HCF. A second airlock into the HCF is located adjacent to Room 106.

The mechanical equipment room (MER) which is located above the HCF at ground level has been added to house the HCF ventilation equipment.

Emergency electrical power for critical systems, the fire protection system, evacuation alarms, public address and radiation monitoring systems in Building 6580 have been extended or modified to meet the HCF requirements. A nitrogen fire protection system has been added in Zones 1 and 2A.

The HCF is primarily designed to be a post-irradiation facility for the study of moderately radioactive materials. It is designed to permit safe handling and experimentation with these materials. Several research programs at Sandia--material studies, fuel studies, safety studies and waste solidification studies--require that radioactive materials be analyzed. The HCF meets these requirements.

II. Ventilation System

Functional Requirements

The ventilation system (Figure 2) maintains a safe operating environment within the facility by ensuring that proper differential pressures are maintained so that leakage is from zones of lesser contamination to zones of greater contamination. These zones are as follows:

Zone 1 - Normally Contaminated Area.

Zone 2A - Potentially Contaminated Area.

Zone 2 - Non-contaminated Area.

Exhaust gases from each of these zones are filtered through high efficiency particulate (HEPA) filters to reduce the off-site plutonium exposures to levels less than the Chapter 0524 limits.

Motor control circuits have been designed to provide sequential start-up of all the ventilation fans so that negative pressures are first established in the innermost zones, thus causing any leakage to be from a zone of lesser contamination to one of greater contaimination. Interlocks are employed to shut down the necessary fans to avoid an adverse pressure differential if any fan should fail during operation.

The Zone 1 exhaust fans, the Zone 2A exhaust fans, and the Zone 2 make-up fans have modulating devices to control exhaust air quantities and to aid in maintaining proper static pressure within their respective zones. The Zone 2A make-up fans and Zone 2 recirculating fan will have manually adjusted dampers to provide essentially constant flow through the units. All Zone 1 SCB's have manually adjustable dampers for initial adjustment of air flows. In addition, all Zone 1 supply and exhaust dampers are provided with pneumatic operators which are controlled by energized or de-energized solenoid valves. Some of these dampers are fail-open type and some are fail-closed type.

Pressure differentials between zones are as follows:

Zone 3 - Ambient Condition.

Zone 3 - Zone 2 -0.10 inch w.g.

Zone 2 - Zone 2A -0.25 inch w.g.

Zone 2A - Zone 1 -1.00 inch w.g.

Zone 2 Ventilation System

The Zone 2 area (Figure 3) is maintained at a -0.10 inch w.g. with respect to the Zone 3 area. Zone 2 consists of Rooms 110, 111, and 112, in the east section and Rooms 105, 106, and 107 in the west section.

The Zone 2 make-up damper MUD-2-13 is modulated to maintain -0.10 inch w.g. pressure between Zone 2 (east section) and Zone 3 (Room 114). A differential pressure controller (DPC), with low input located in Room 111 and high input located in Room 114 modulates the make-up damper located on the discharge side of the Zone 2 make-up blower. The west section of Zone 2 is maintained at -0.10 inch w.g. by a DPC with low input in Room 107 and high input located in Room 114 which modulates the return air damper RD-2-12 located in the return air duct downstream of the return air blower.

A majority of the air supplied to the west section of Zone 2 is exhausted through a hood exhaust in Room 106 and the Scanning Electron Microscope System located in Room 105. These exhaust systems discharge into the existing hot exhaust system and are filtered through two HEPA filter banks, one at the glove box and one located at the area stack.

The make-up air unit supplying Zone 2 receives its air from the existing building distribution system. The volume of make-up air is determined by the amount of air exhausted from the east and west Zone 2 areas, the amount of make-up air supplied to Zone 2A, which includes the Zone 1 supply air, less the amount of infiltration air into Zone 2.

The Zone 2 recirculating blower supplies air to both the east and west sections of Zone 2. In addition to maintaining the correct pressure differential, the Zone 2 system maintains the required number of air changes in the area and supplies the needed heating and cooling. The volume of recirculated air is regulated by a manual intake damper located in the intake duct of the Zone 2 Filter and Cooling Coil Unit.

A cooling coil located in the Zone 2 unit with the controlling thermostat located in Room 107 maintains temperature in the Zone 2 areas. This thermostat also controls the reheat coil located in the building air supply duct to prevent the room temperature from dropping below 68°F during winter and no-load conditions. The water cooling coil is supplied chilled water from the existing building system. A manual by-pass damper in the Zone 2 unit maintains a fixed flow of air through the coil.

Zone 2A Ventilation System

The Zone 2A area (Figure 4) is maintained at -0.25 inch w.g. with respect to the Zone 2 area. Zone 2A is surrounded by the west and east sections of Zone 2.

The Zone 2A exhaust damper ED-2A-8-9 (Figure 4) is modulated to maintain -0.25 inch w.g. pressure differential with respect to Zone 2 (Room 111). This damper is modulated by a DPC, with low input located in Zone 2 (Room 111) and high input located in Zone 2A. The damper is located on the exhaust duct upstream of the Zone 2A exhaust blowers. Effluents are discharged through the exhaust filters at the area stack to the atmosphere.

The make-up air unit supplying Zone 2A draws its air from Zone 2 (east). The volume of make-up air through the Zone 2A make-up unit is controlled by manually adjusting damper MU-D-2A-10 (Figure 4). The volume of make-up air is determined by the supply demands of the Zone 1 SCB's and the air required to meet the cooling requirements of Zone 2A and the Zone 1 SCB's

The exhaust blowers B-8 and B-9 maximum air quantity is set by adjusting the manual damper MD-2A to prevent overloading of the blowers by excess volume of air through the system.

Only cooling, no heating is required in Zone 2A. The make-up air from Zone 2 east (Room 111) is normally maintained within the 69°F to 74°F range.

The heat generated within the Zone 2A comes from lighting of Zone 2A, crane motor and/or other equipment, infiltration, and

by convection and conduction loads from the SCB's. Some air is drawn through the SCB's and removes some SCB heat, but the amount of air through the SCB's is usually very low. Also, if a nitrogen atmosphere is maintained in SCB 1 and SCB 2, very little flow enters the Zone 1 exhaust, resulting in the Zone 2A cooling system handling the total load of Zone 2A and Zone 1. A cooling coil in the Zone 2A make-up air unit, with the controlling thermostat bulb located in the Zone 2A exhaust duct controls the zone temperature. The cooling coil is supplied cooling water from the building chilled water system. Normally Zone 2A is maintained at 68°F but under full load the temperature within the zone can rise to 85°F. This is within the design and operating limits of the Zone 2A area and Zone 1 SCB's.

The exhaust blowers B-8 and B-9 are controlled by a Blower Selector Switch which automatically selects the alternate blower in case of failure of the primary blower, thus assuring continuous exhaust.

Zone 1 Ventilation System

The Zone 1 area (Figure 5) consists of the three SCB's located within the area designated as Zone 2A. These are referred to as SCB 1, SCB 2 and SCB 3. The Zone 1 SCB's are maintained at -1.0 inch w.g. with respect to the Zone 2A area. Zone 2A surrounds Zone 1.

The exhaust of each SCB is connected to the Zone 1 exhaust manifold. The pressure differential between this manifold and Zone 2A is maintained at -2.0 inch w.g. by DPC EM-1. This controller modulates a damper located on the upstream duct of the Zone 1 exhaust blowers which discharge into the existing hot exhaust system. Each SCB is maintained at its designed negative pressure by a DPC that modulates an exhaust damper located on the exhaust duct between the cell and the exhaust manifold.

The exhaust blowers B-6 and B-7 maintain the required static pressure in the exhaust manifold and have sufficient capacity for exhausting the required CFM necessary for purging with air or nitrogen.

Make-up air to the SCB's is drawn from the discharge duct of the Zone 2A Make-up Air Unit. To assure that the supply to the Zone 1 Make-up Air Filter Banks will have sufficient head, a manual damper downstream of the Zone 1 take-off is adjusted to maintain this required head. Each SCB has a pneumatic operated damper on its air supply duct. The volume of air to the SCB is governed by a manual positioning switch in the control line to the damper of the supply duct to the SCB. The maximum open position of each SCB damper will be determined to prevent excessive air flow into the SCB's and to prevent the combined maximum flows of the SCB's from overloading the capacity of Zone 1 blowers B-6 and/or B-7.

In addition, each SCB has a nitrogen supply system, in the event the operations within the SCB demand a nitrogen atmosphere.

The controls for these nitrogen systems will be located on the control console of the SCB. Each SCB has a control console.

The above SCB control console is located on the operator side (west wall) of the manipulator wall. The following items of the Zone 1 ventilation control system of the SCB are located in this console. For each SCB there is:

(a) A differential pressure indicator to indicate the pressure differential between the SCB and Zone 2A with high and low limit light and alarms.

(b) A manual positioning switch to regulate volume of make-up air into SCB from "no flow" to "full flow."

(c) Controls for the nitrogen supply to the SCB.

Cooling of the SCB's is by heat transfer to the Zone 1 air flow and by heat transfer to the air of Zone 2A surrounding the SCB's.

Ventilation Controls

The operating controls for the HCF ventilation system are located in Room 106 adjacent to the existing control panel for the hot and cold exhaust systems. These controls consist of on-off (or automatic) switches, monitor lights and alarm indicators (Alarms are relayed to the area guardhouse.) for the various components of the ventilation system. The electrical motor control center is located in the MER, where disconnect switches are to be used for shutting down the blowers for maintenance purposes. The mechanical control panel for the HCF ventilation system is located in the MER. This panel contains the zone differential pressure controllers and associated auxiliary equipment for the ventilation system operation.

III. Facility Electrical, Radiation and Fire Protection Systems

The electrical service to the HCF is obtained from the Building 6580 service. Critical loads fed by the electrical service (ventilation equipment, including the SCB nitrogen system, selected lighting, and receptacles in containment boxes, monitor and alarm system, remotely-operable airlock doors, etc.) will be served from the existing Building 6580 Emergency Generator System. The emergency generator system starts automatically and picks up the critical loads when the normal power source is interrupted. The system is tested weekly by simulating a normal power source interruption and allowing the generator to automatically start and pick up the critical loads. A new diesel-powered generator was installed in July 1975.

Radiation Protection Systems

Systems. Radiation monitoring is provided by two basic systems, the Remote Area Monitoring System (RAMS) and the Constant Air Monitoring System (CAMS). There is also a stack gas monitor

for the area stack. Selected RAMS and CAMS will be specifically required by the HCF Technical Specifications operating regulations. CAMS will monitor exhaust and environment air in the HCF.

RAMS. The RAMS is designed to monitor radiation levels at locations remote from a central readout station in the Health Physics Office. Each RAMS unit has a local meter readout, a visible alarm, an audible alarm, plus the remote readout in the Health Physics Office. The range for all RAMS units is 1 mr/hr to 100 r/hr. Trip points for each location are established at levels consistent with the values necessary for compliance with Chapter 0524 criteria.

Each RAMS unit employs transistorized circuitry coupled to a detector which responds to gamma radiation. The unit also includes backup power in the form of a battery which has a minimum capacity of 100 hours in no-alarm condition and 8 hours in alarm condition and is capable of full recharge. Batteries presently employed in the RAMS units are Glob Gel/Cel; however, a continuous in-service maintenance program evaluates new battery types, capabilities, etc., and replacements are made when superior batteries are found.

CAMS. The CAMS consist of portable monitors which monitor the air and exhaust for gross beta and gamma activity. CAMS units are located in areas adjacent to the HCF and in adjoining passageways. CAMS units may be placed at other locations at the discretion of the health physicists.

Fire Protection Systems

Systems. The Building 6580 Fire Protection System is utilized for the HCF. Fire Protection is provided within Zone 1 and Zone 2A by limiting the amount of combustibles within the areas, and providing an inert atmosphere when working with pyrophoric materials. Additional protection in the form of nitrogen fire suppression systems is provided inside the SCB's and the hot cell, and water sprays used in conjunction with metal screen scrubbers and demistors in the ventilation exhaust ducts of the SCB's and hot cell.

A wet pipe automatic sprinkler system is provided in Zone 2.

Hot Cell and SCB Fire Protection System. The hot cell has heat detectors to initiate a fire alarm. In addition, these detectors initiate the nitrogen purge system of the hot cell. Control interlocks prevent further introduction of make-up air and maintain negative pressure within the cell through control of the exhaust damper.

SCB 1 and SCB 2 (those involved with examination of capsules containing enriched uranium-dioxide and sodium) have a nitrogen atmosphere for these operations and are also equipped with containers of MET-L-X. SCB 3 (involved with waste solidification studies) has an air atmosphere, but is also equipped for nitrogen

atmosphere operation. All SCB's have heat detectors to initiate a fire alarm and a nitrogen fire suppression system identical to the hot cell system.

Nitrogen Fire Suppression System. The nitrogen fire suppression system is incorporated in the HCF to serve Zone 1 (SCB's) and Zone 2A (hot cell) areas. A 4,400 gallon liquid nitrogen storage tank, located adjacent to the MER, provides nitrogen for daily operation and the fire suppression systems to Zones 1 and 2A. When actuated either manually or by the Zone 1 and Zone 2A fire detection system, nitrogen gas flows into these zones, electrical interlocks prevent further introduction of make-up air and the ventilation controls continue operation of the exhaust fans, maintaining the area negative pressure. Pressure regulators and orifice plates regulate the volume of nitrogen flow into the zones. Within a few minutes after initiation of the nitrogen flow, the oxygen content is low enough to suppress the type of fire that may occur within Zone 1 or 2A.

HEPA Fire Protection System. To protect the HEPA filters from heat damage, a water spray system, including scrubbers, water spray nozzles, and demistors, are incorporated into the Zone 1 and Zone 2A exhaust lines to assure that air temperatures to the HEPA filters is less than 300°F. Temperature sensors are located in the exhaust duct and actuate the water sprays, providing the necessary water flow required to reduce the air temperature to an acceptable level for flow through the HEPA filter. A final water spray, manually operated, is located in the MER filter banks. These filter banks also have a temperature sensor located in the supply air ducts to initiate an alarm within the facility Fire Alarm System.

The residual water, after passing through the spray system, is drained into a storage tank where it is monitored for radioactive content.

IV. Discussion

GDC Conformance

In the early design stage for the HCF it was determined that the GDC would apply in that three ventilation zones would be required. At that time only 1-5 curies were considered to be the upper limit for the plutonium inventory. We considered eliminating Zone 2A but this was not pursued because ERDA/ALO's position was that 5 curies did represent a substantial quantity of plutonium and the GDC requirement for three zones should be met. They also maintained that Zone 2A was necessary to prevent the contamination of Zone 2 (essentially all of the HCF) in the event of a serious incident in the SCB's. In addition, the elimination of Zone 2A would be a major redesign effort. Time was short and sufficient resources were not available to do the redesign work. Also the savings in construction cost were found to represent only a few percent of the total cost. Because of these factors it was decided to retain the three

ventilation zones. However, we did increase the plutonium limit to 200 curies and were permitted to remove one HEPA filter each from the Zone 1 and 2A banks.

In retrospect the early design work was at a disadvantage because the plutonium inventory limit was not well defined. This uncertainty plus the position that 1-5 curies of plutonium is a substantial quantity lead to conservatism in the design and to the three ventilation zones. Consequently, the three zone system required for the New Plutonium Recovery Facility at Rocky Flats and the DP West Plutonium Processing Facility at Los Alamos, both of which can handle significantly more plutonium than is planned for the HCF, is nonetheless still required.

We have three suggestions which might avoid what we consider to be the over design problems which we have encountered with the HCF. (1) Attempt to quantify the meaning of "substantial quantities of in-process plutonium". The disparity that exist between the quantities of plutonium associated with the HCF and major plutonium facilities is such that some modification of the three zone ventilation requirement appears to be justified. We intend to pursue this point with ERDA/ALO. (2) Develop firm upper limit inventories before proceeding with preliminary design of the facility. Thus one can avoid incorporating excessive design margins to deal with the uncertainty in the inventories. (3) Reduce the area devoted to support activities within the confines of any future facilities. The argument about extensive clean-up requirements in case of an incident is certainly valid. The Zone 2 Support Area is probably larger than required because of the constraints of pre-existing construction. If the hot cell boundary was slightly enlarged to accommodate storage of casks and transfer containers, it is conceivable that only two ventilation zones would be needed.

Fire Analysis

In performing the hazards analysis associated with a fire in the SCB's we established an SCB limit of 1 lb of hypereze cutting compound, a high quality kerosine, having a heat of combustion of about 20,000 BTU/lb. With the air available an upper limit burn rate of about 0.5 lb/min could be sustained. Tests at Sandia showed that a maximum flame temperature of 2,000°F existed in the upper position of the flame. Hence our fire environment was defined to be one with a heat release rate of 10,000 BTU/min which lasted two minutes. Air temperature from the flame was assumed to be 2,000°F.

Attempts were made to incorporate a metallic heat sink in the exhaust duct to protect the HEPA filters. The heat sink was found to be very effective in initially cooling the exhaust air. But subsequent to the fire, the heat sink was cooled by the air flow and the temperature rise in the air was enough to present a hazard to the HEPA filters. Two alternatives were considered, an active cooling system for the heat sink (radiator-like system) and bypassing the heat sink once the fire was extinguished. These seemed complex with respect to the conventional water

sprays which we decided to use. However, we are pursuing this concept and intend to incorporate a heat sink alternative if a practical one is developed.

V. Summary

We believe that the HCF is too conservatively designed. Part of this conservatism has been removed by increasing the plutonium limits to 200 curies. Alternatives of two ventilation zone systems and reduced support areas would be considered if the HCF were redesigned. The heat sink concept appears to be a viable option to water sprays for HEPA filters. However this concept does need further development.

References:

Appendix 6301, General Design Criteria, Plutonium Facilities.

ORNL-NSIC-65, Design, Construction and Testing of High Efficiency Air Filtration System for Nuclear Application, January 1970.

UCRL-23800, Fire Protection of HEPA Filters by Using Water Sprays, July 1972.

Argonne National Laboratory, Liquid Nitrogen Fire Extinguishing System Test Report, J. A. Beidelman, May 1972.

SLA-74-0345, Test Results on the Effect of Heating a Confined High Explosive, A. B. Donaldson and D. O. Lee, August 1974.

U. S. ERDA Manual, Chapter 0524, Standards for Radiation Protection, January 1975.

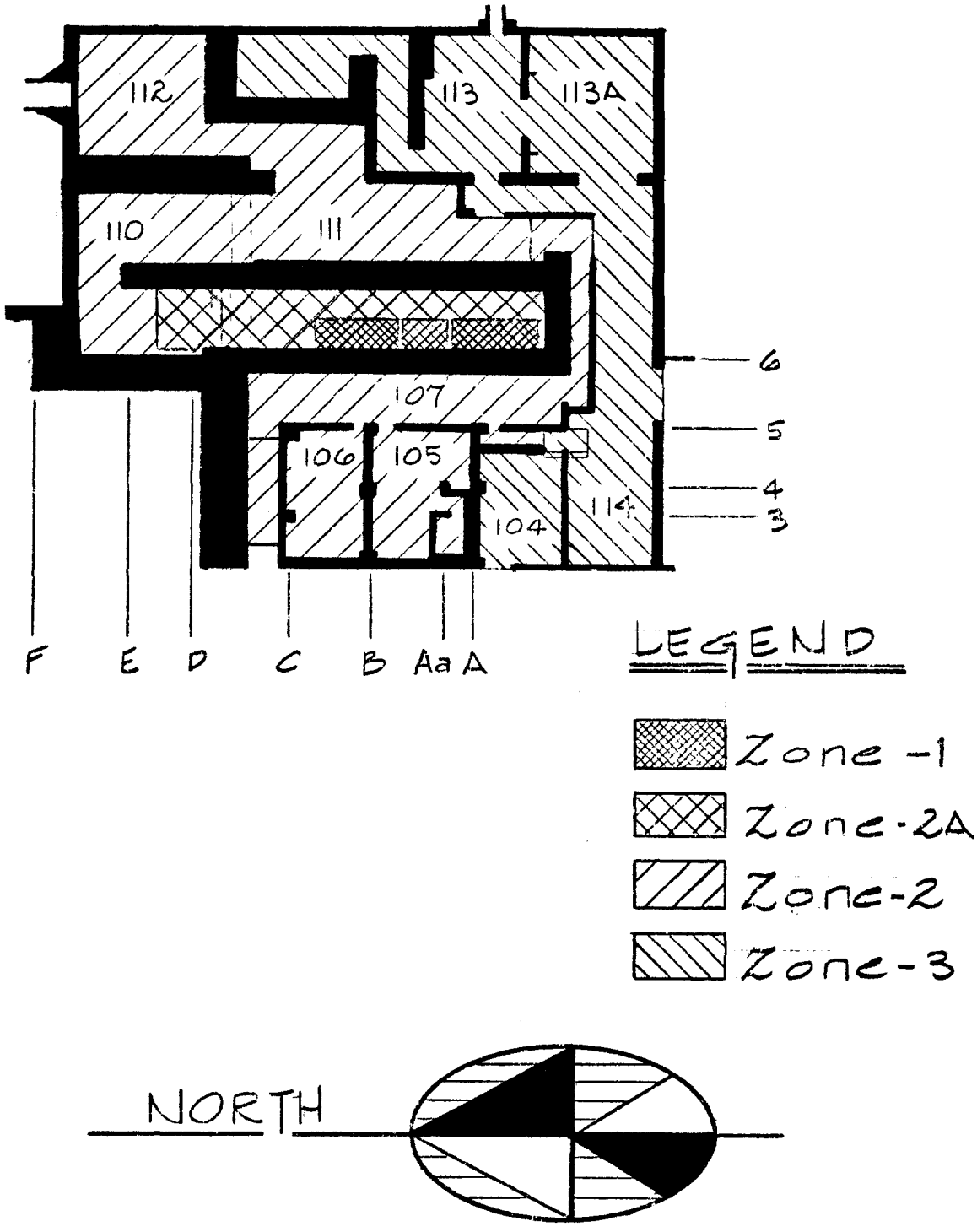

FIGURE 1

HCF FLOOR PLAN

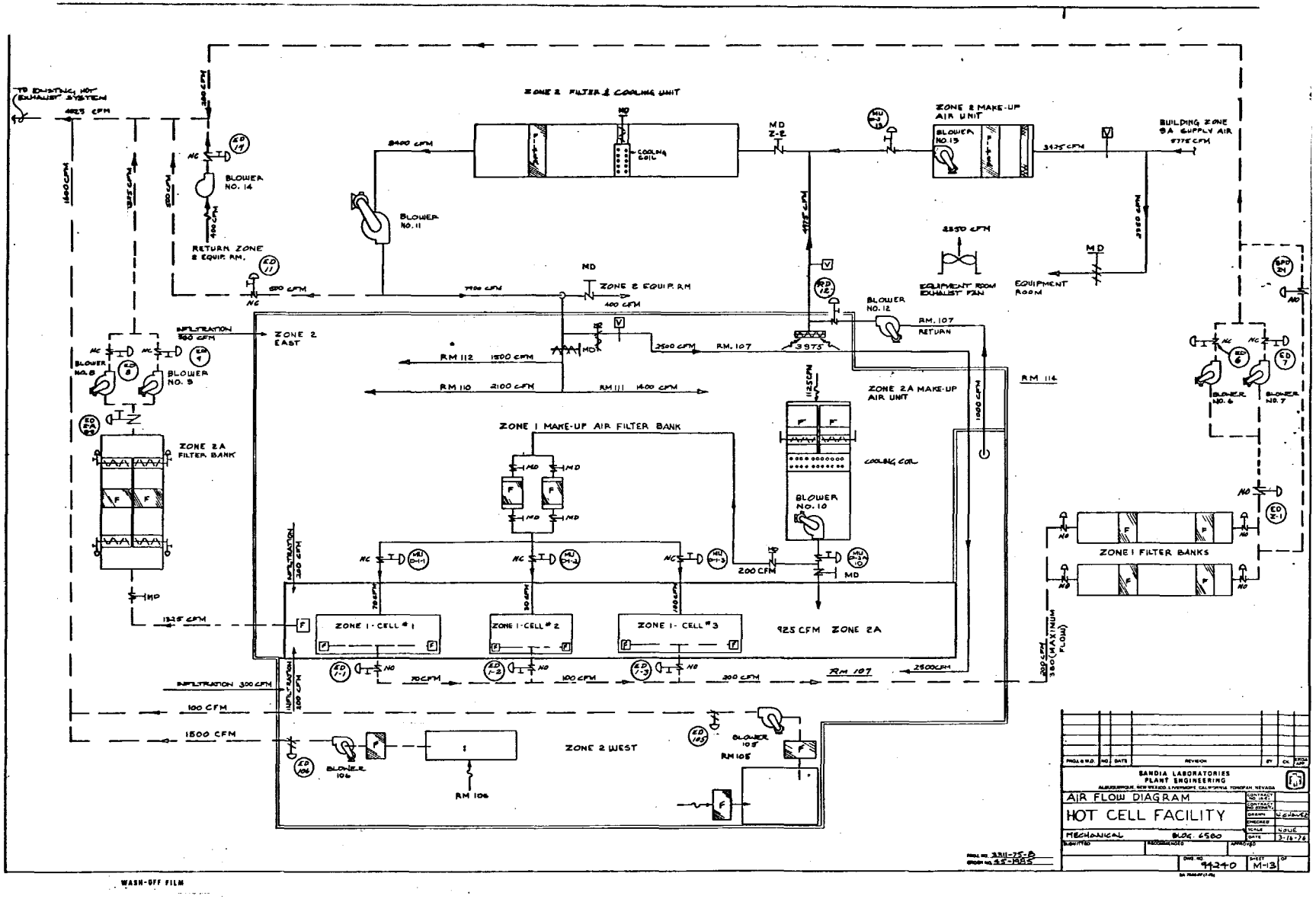

FIGURE 2

VENTILATION SYSTEM

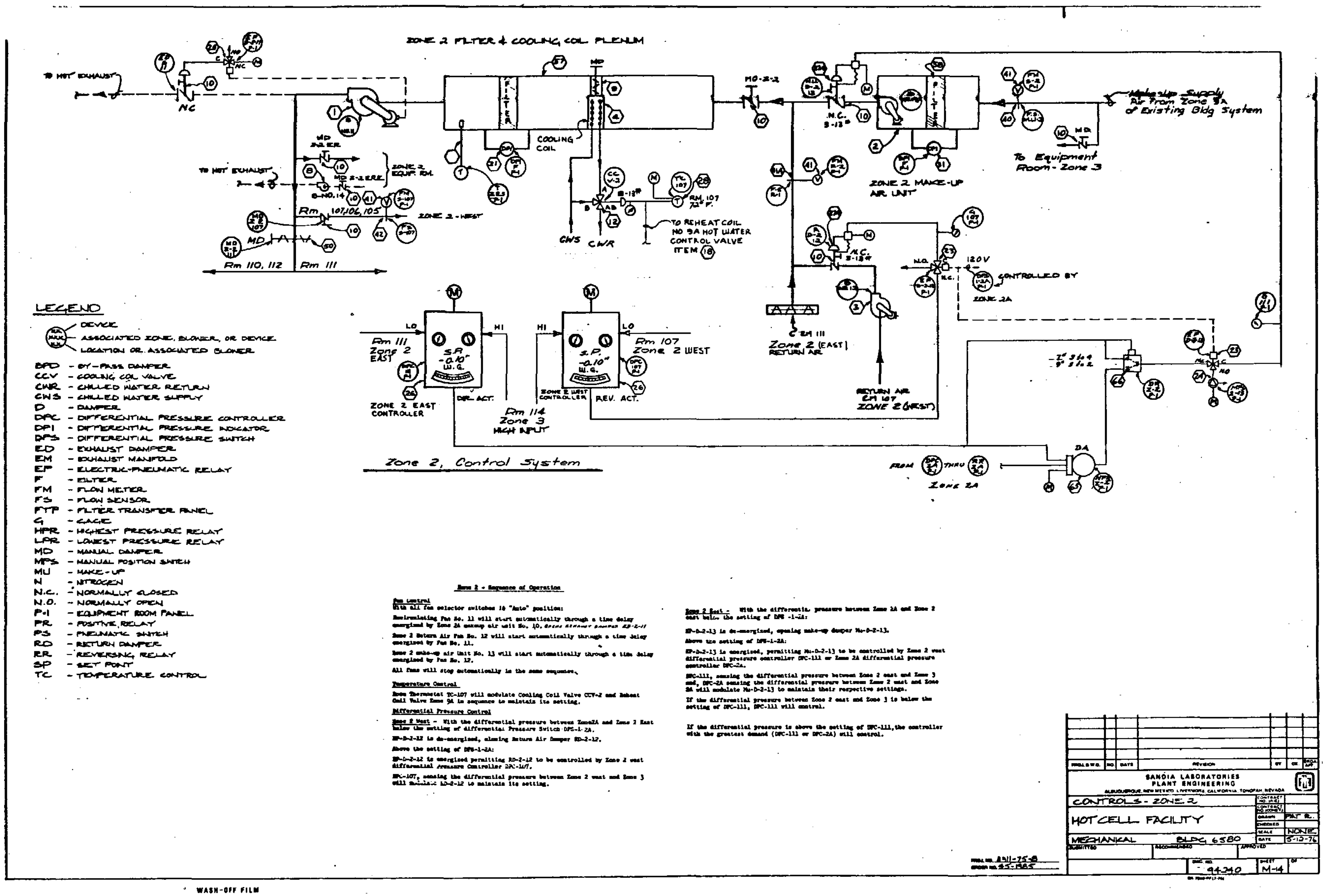

FIGURE 3
ZONE 2

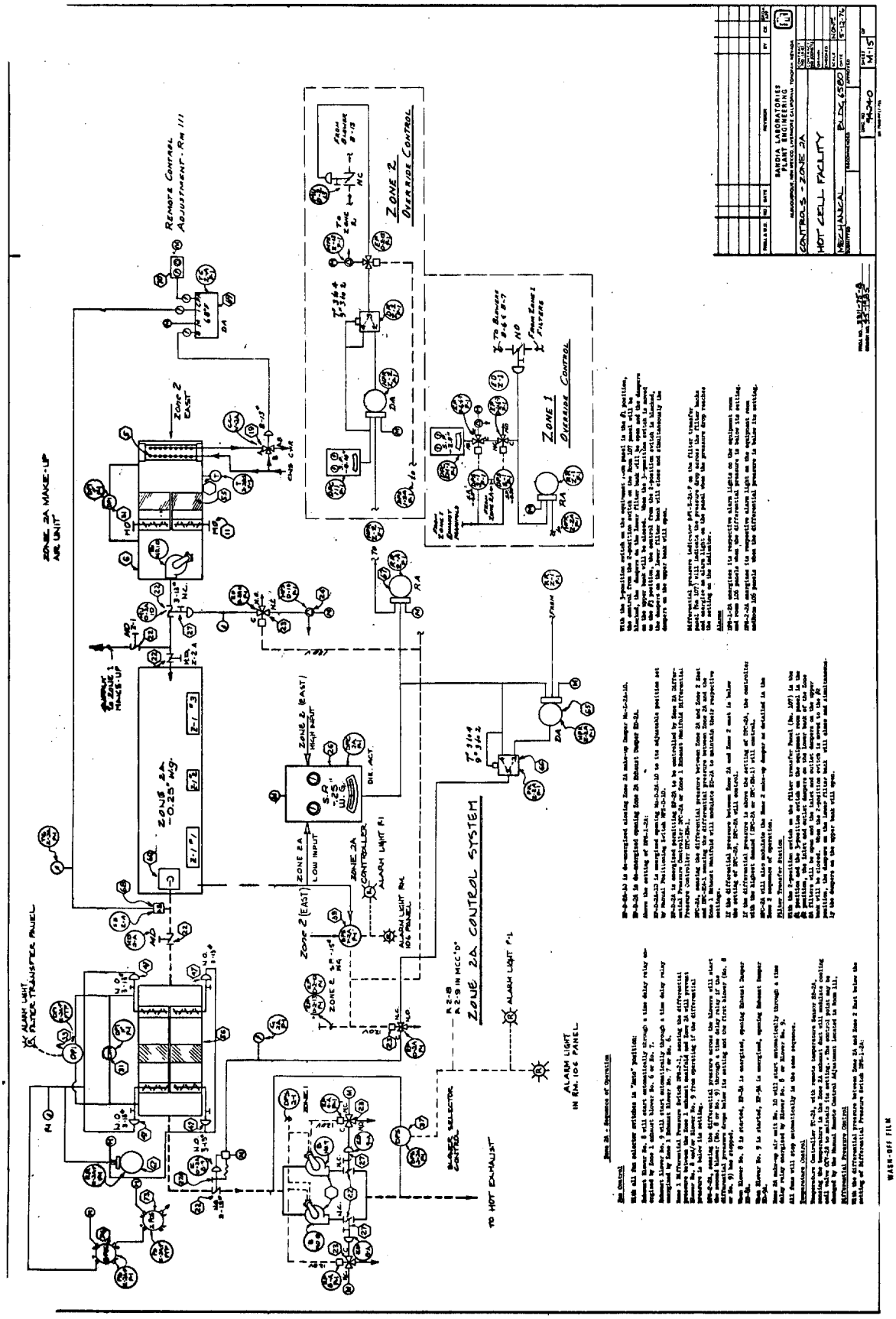

FIGURE 4
ZONE 2A

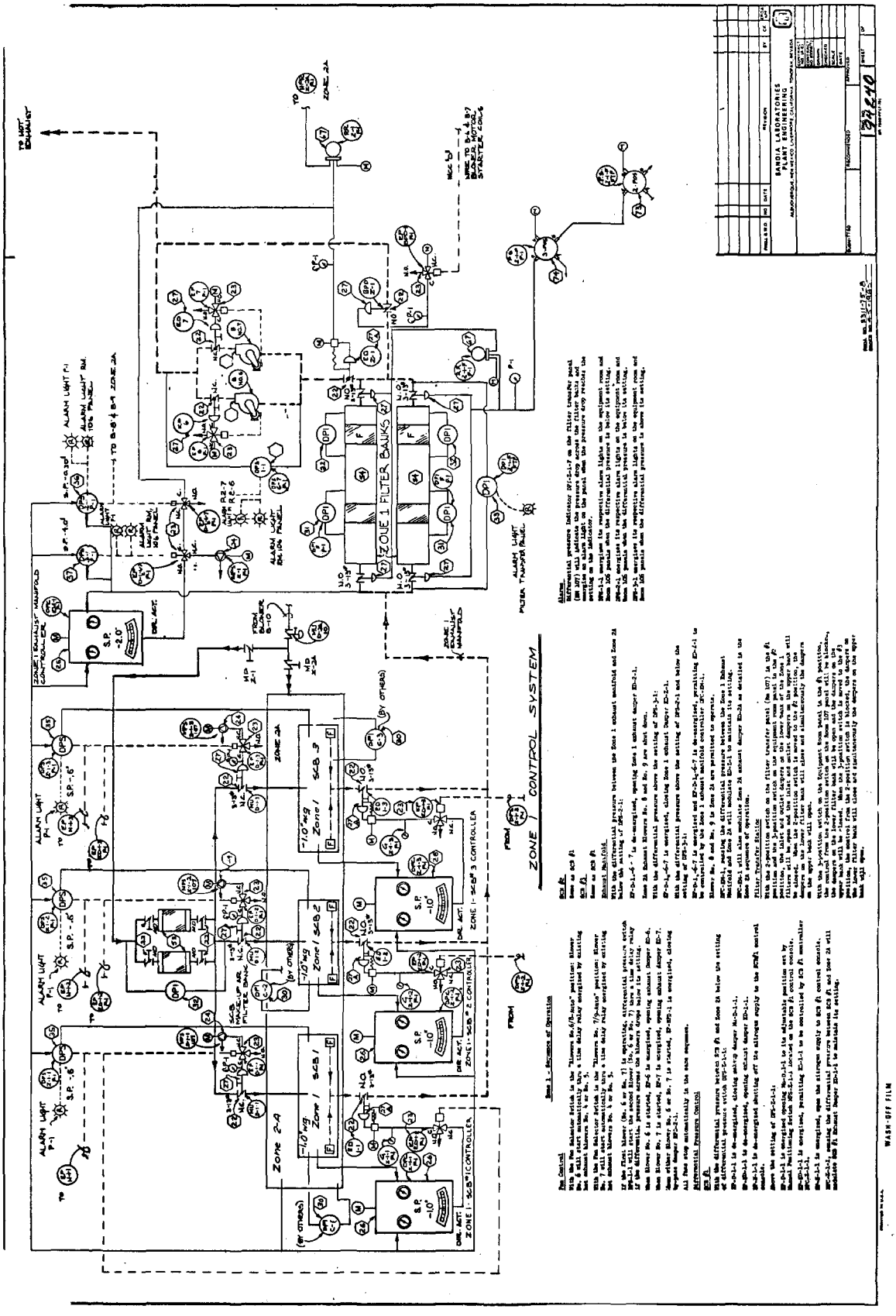

FIGURE 5
ZONE 1

DISCUSSION

BURCHSTED: You mentioned you had water sprays on your filters. Do these sprays permit impingement of water on the filter itself, and if so, could the droplets puncture the filter?

BURRESS: The first set of sprays is located in a spray chamber and is about 25 feet from our first bank of filters, both in Zone 1 and Zone 2A. In Zone 2, we do not have a water spray system on the filter. I don't believe we will get any water carry-over on the Zone 2 bank. Also, ERDA has asked us to put a final manual spray on the filter banks in the event that heating continues in spite of the sprays.

BURCHSTED: That might be a last-ditch type of thing. If you have a fire, you put the fire out regardless of what happens to the filter?

BERNARD: Yes. About four failures are needed to produce this situation.

EFFECTS OF EXPLOSION-GENERATED SHOCK WAVES IN DUCTS*

M. R. Busby**
Tennessee State University
Nashville, Tennessee

J. E. Kahn and J. P. Belk
Union Carbide Corporation–Nuclear Division
Oak Ridge National Laboratory
Oak Ridge, Tennessee

Abstract

An explosion in a space causes an increase in temperature and pressure. To quantify the challenge that will be presented to essential components in a ventilation system, it is necessary to analyze the dynamics of a shock wave generated by an explosion, with attention directed to the propagation of such a wave in a duct.

Using the equations of unsteady flow and shock tube theory, a theoretical model has been formulated to provide flow properties behind moving shock waves that have interacted with various changes in duct geometry. Empirical equations have been derived to calculate air pressure, temperature, Mach number, and velocity in a duct following an explosion.

I. Introduction

A comprehensive safety analysis should evaluate the effects of a localized detonation on essential air-cleaning components in an exhaust system. The analysis should predict the capability of critical air-cleaning apparatus to remain functional following a detonation, even if the location of the actual incident is distant from those components and connected to them by a complex path. In order to describe an explosion, it will be necessary to differentiate between normal burning and detonation.

Description of Explosions

Normal burning is a result of heating an optimal volume of a combustible gas mixture to the ignition temperature by an external source, after which the flame propagates through the entire volume.[1] The maximum flame front speed for normal burning of a hydrogen-air mixture is 320 cm/sec, and the maximum post- to precombustion pressure ratio is 8.[2,3] However, detonation differs from normal burning in that the velocity of flame propagation and pressure ratio are significantly higher (e.g., for a 40% hydrogen-air mixture the detonation wave velocity is 2100 m/sec, and the pressure ratio is approximately 20).[4,5] Although the phenomenon is not completely understood at present, the steady detonation wave has been modeled as a shock front, followed, after a short time interval, by a combustion zone, and then a region of hot gases in equilibrium. This model has been

*Research sponsored by the U.S. Nuclear Regulatory Commission under contract with Union Carbide Corporation under Union Carbide Corporation's contract with the Energy Research and Development Administration.

**Consultant to Oak Ridge National Laboratory.

used successfully to predict the detonation wave velocities for various gas mixtures.[6] Detonation velocity depends on the reaction-kinetic properties of the mixture.[7] Because of the tremendous pressures that such equipment would experience upon wave impact, detonation can be more damaging to air-cleaning components than normal burning.

Initiation and Propagation of Detonation

If an explosive mixture is present in a duct system, there exists the possibility of spontaneous transition from normal burning to detonation at some "induction distance."[8,9] This phenomenon occurs because, as a flame propagates down a duct, the burning rate increases continuously due to the turbulence of the mixture in front of the flame and the increase in flame surface area. The rapid burning creates a shock wave in the unburned mixture, which ignites the gas downstream from the flame front.

Of particular interest also is the likelihood of detonation waves propagating from a smaller duct to a larger one. From generalizations of earlier experiments,[10,11] it was erroneously concluded that it is impossible for a detonation wave to propagate to the larger duct.[9] However, if a detonation wave is transmitted to a large volume or duct from a smaller duct or tube whose cross section is sufficiently large, the detonation wave can propagate into the large duct. For example, Zel'dovich has shown experimentally that the initiation of spherical detonation in an explosive gas mixture is possible by means of a plane detonation wave from a tube, only if the tube diameter is equal to or greater than a certain critical diameter (e.g., for a hydrogen-air mixture, the critical diameter is 19 mm).[12] If the diameter of the tube is less than the critical diameter, a plane detonation wave collapses, and normal burning of the gas takes place. Zel'dovich thus concluded that, at a point where the tube diameter changes, a plane detonation wave can either be attenuated, transformed to slow burning, or transformed to a spherical wave that will propagate within the volume, with all the consequences that follow.

The conclusion concerning attenuation has led to a proposed detonation-control measure by placing orifices with diameters less than the critical diameter for detonation at intervals in a duct less than the "induction distance."[8] In this paper, less consideration is given to the probability of occurence of a detonation than to the effects produced by such a phenomenon.

Hydrogen-Air Mixtures

Because a hydrogen-air mixture has so many prevalent possible sources (e.g., radiolytic or thermal disassociation of water, metal fires in the presence of water, sodium-water reaction, etc.) its detonation properties are of major interest. The actual explosive mixture might be air-hydrogen-steam, and a theoretical phase diagram for such a mixture is presented in Figure 1. Theoretically, in an air-hydrogen-steam mixture, 11% steam is sufficient to suppress any detonation.[13] However, using a "third explosion limit theory", Mathews shows that the water molecule is only as effective as the hydrogen molecule in suppressing the active radicals in a hydrogen-air mixture.[14] Thus the effectiveness of water vapor in suppressing detonations is still open to question, and experimental verification is lacking. In the present analysis, the effect of steam is neglected, and since the water molecule is more effective than the nitrogen molecule in suppressing the active radicals in the hydrogen-air mixtures,[15] an air-hydrogen mixture should have a more destructive potential.

Experimental data for the detonation properties of hydrogen-air mixtures for various percentages of hydrogen are used in the analysis given here. The molecular weight of the mixture, the detonation velocity, the Mach number, and the Mach number based on 100% air are given in Table I.[12,4] The detonation wave Mach number is defined as the ratio of the wave velocity to the speed of sound in the gas ahead of the wave. The effect of a shock wave passing through a duct containing a nonexplosive gas is independent of the explosive mixture at the initiation of the explosion and

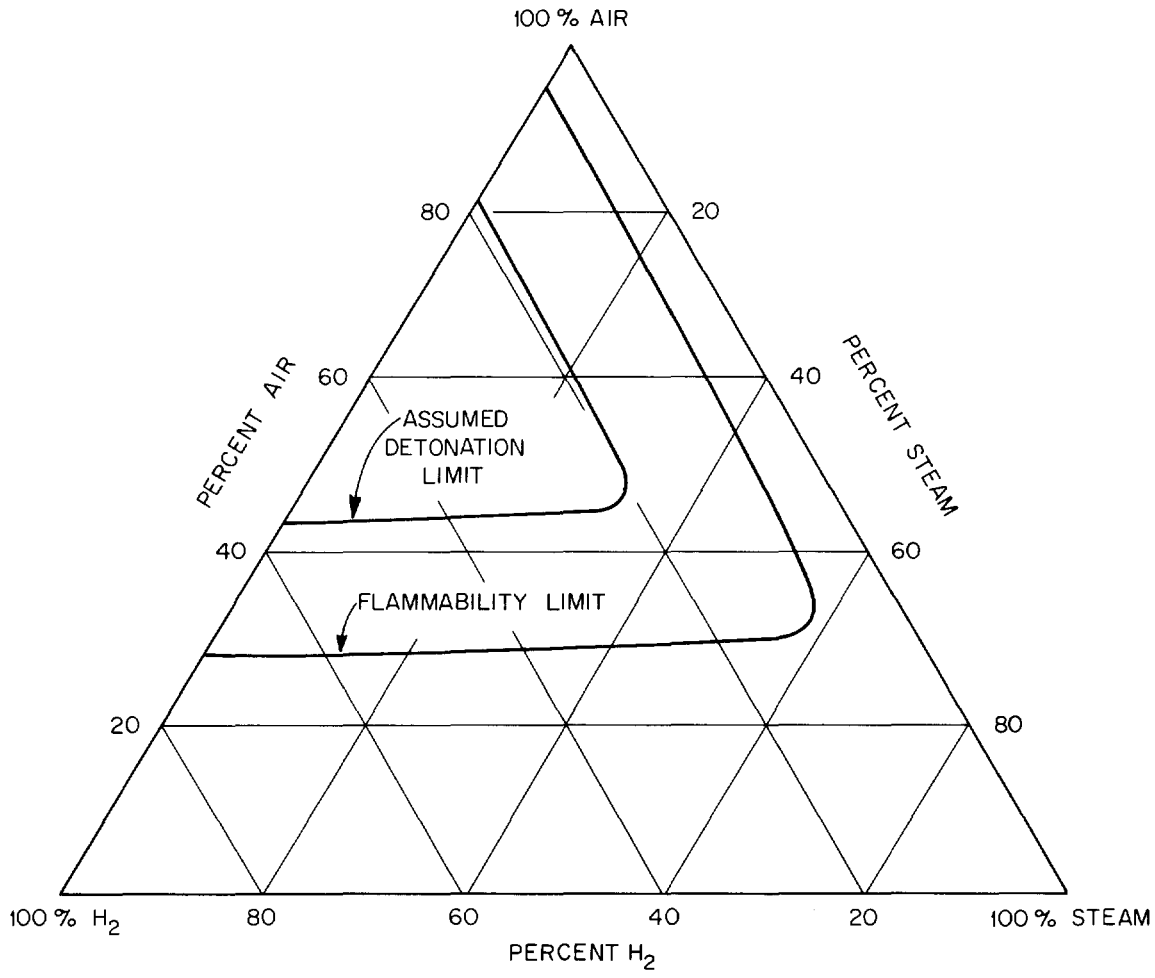

Figure 1: Detonation and flammability limits for air-hydrogen-steam mixtures (ref. 15).

Table I. Detonation data for hydrogen-air mixtures
(1 atm; 300° K)

H_2 (percent by volume)	Mixture molecular wt.	Detonation velocity m/sec	Wave Mach Number (based on mixture)	Wave Mach Number (based on 100% air)
18.5[a]	23.98	1300	4.11	3.74
18.8[a]	23.90	1483	4.70	4.27
19.0[b]	23.85	1480	4.70	4.26
19.9[b]	23.60	1650	5.26	4.75
35[b]	19.53	1950	6.84	5.62
42[b]	17.64	2100	7.75	6.05
55[b]	14.14	2200	9.07	6.34
58.9[b]	13.08	2190	9.39	6.31

[a]R. Wendlandt, *Z. Physik Chem.*, 110, 637 (1924).
[b]J. Brenton, *Ann. Office Nat'l. Combustibles Liquids,* 11, 487 (1936).

depends only on the incident shock wave Mach number and the gas-mixture properties and configuration within the duct.

II. The Duct-Detonation Wave Model

For the theoretical model, it is assumed that detonation occurs in a localized section of a duct where a hydrogen-air mixture is present. The blast wave is established and advance with a velocity corresponding to the hydrogen composition as given in Table I. It is assumed that in the duct there exists an imaginary plane which divides the detonable mixture from 100% air. As the detonation wave crosses this plane into the air, combustion ceases, and the shock wave is then governed by those equations applicable to moving shock systems. Therefore, the Mach number of the wave as it travels in the noncombustible region is based on the speed of sound in 100% air. The variation of Mach number with hydrogen composition is presented in Figure 2. As predicted by this assumption, the values of pressure, temperature, and density behind the wave would be those related to the von Neumann "spike" and are consistent with the assumed model of the detonation wave (i.e., a shock front, followed by a combustion zone, and then a region of hot gases in equilibrium).[2]

The interactions of the moving shock wave with sudden or gradual duct contractions or enlargements are calculated by utilizing a shock-tube digital-computer program in which the area ratio between duct stages is an independent variable. The program employs the unsteady flow and shock tube equations to determine by an iterative technique the flow conditions as the duct area changes.[16,2] A variety of flow conditions may be established after the passage of the shock wave. Once the area ratio and gas properties are fixed, the computer program will provide the flow condition that reflects what actually occurs. The program is limited to the unsteady one-dimensional flow of real and ideal gases. The energy- and momentum-dissipative effects of heat transfer and friction at the duct walls have not been considered in the calculation of shock wave properties. Since these effects tend to weaken the wave, neglecting them provides conservative results. Also, for the same reason, the possibility of reflected rarefraction waves overtaking and weakening the shock system has not been included in the model.

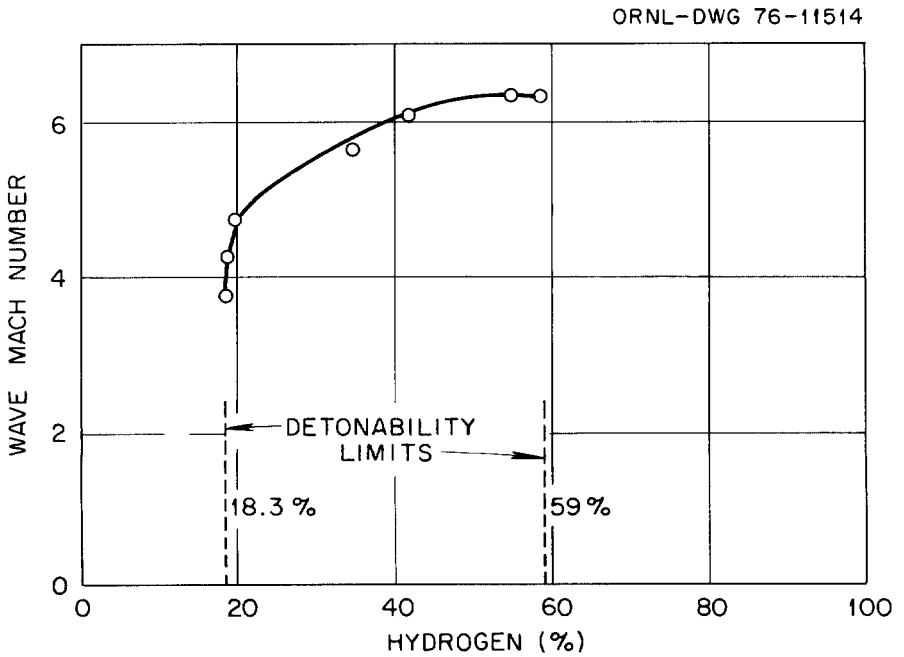

Figure 2: Detonation wave Mach numbers for hydrogen-air mixtures (refs. 4 and 12).

A time-displacement diagram for a typical sudden contraction is presented in Figure 3. As the incoming shock impinges upon the area change, another shock wave is reflected upstream while a stronger shock (i.e., higher Mach number) is transmitted downstream in the smaller duct. A contact surface and an unsteady expansion follow the transmitted wave. For a sudden enlargement, a typical time-dependent diagram is given in Figure 4. As the incident shock wave encounters the sudden

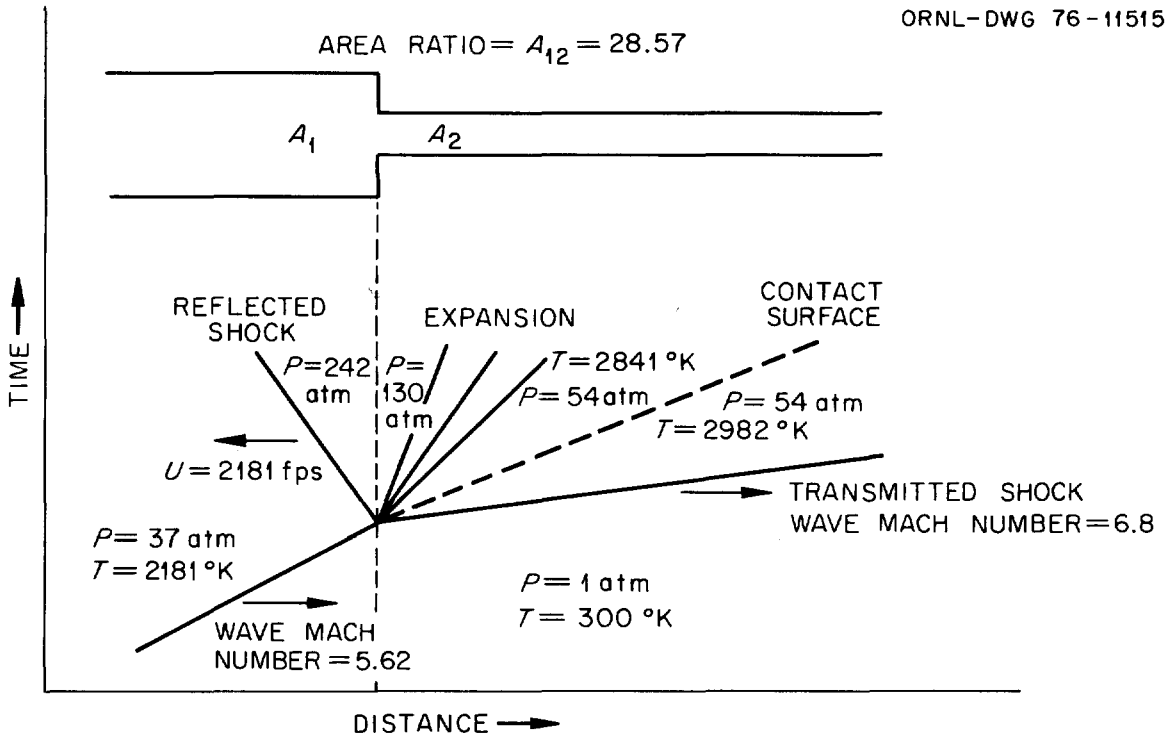

Figure 3: Shock wave interaction with sudden contraction.

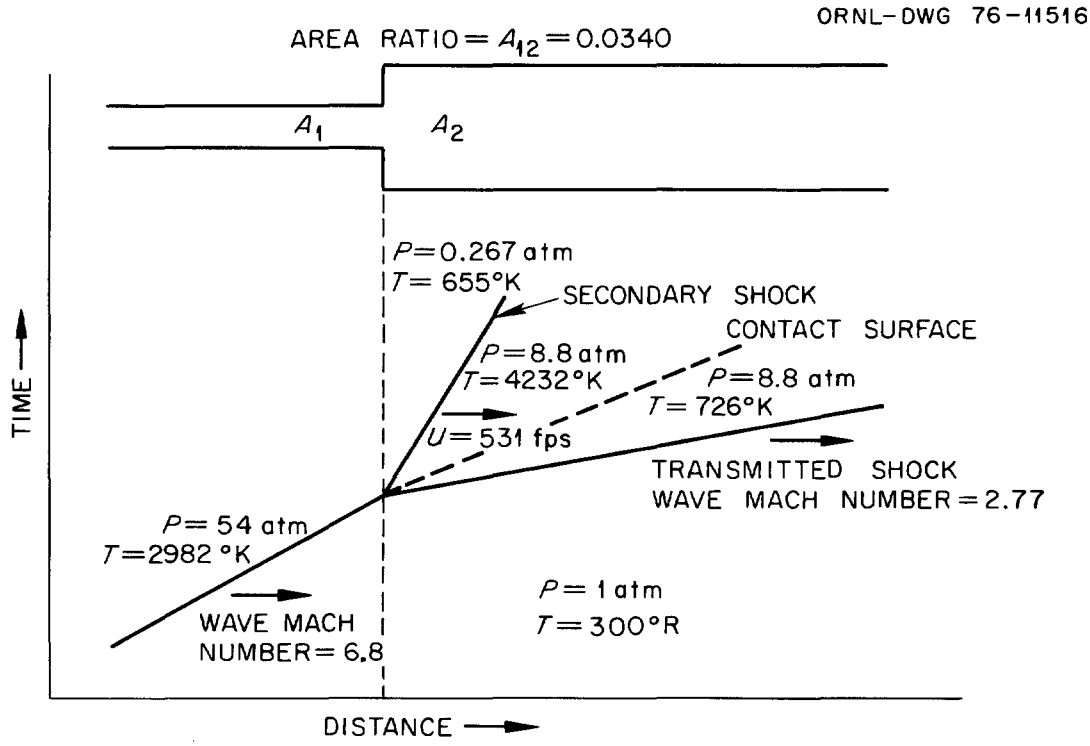

Figure 4: Shock wave interaction with sudden enlargement.

enlargement, a weaker shock wave is transmitted which is followed by a contact surface and a secondary shock that is swept downstream. With assumed ideal air and by utilizing the computer program, surfaces may be constructed in a three-dimensional plot of area ratio vs incident Mach number vs transmitted Mach number, static pressure, static temperature, or velocity. Empirical equations for these surfaces have been derived and are given below for a sudden area contraction or enlargement:

$$M_T = M_S (1 + a_1 \ln A_{12}) \tag{1}$$

$$P_T = a_2 + (M_S)^2 [b_2 + c_2 (\ln A_{12}) + d_2 (\ln A_{12})^2] \tag{2}$$

$$T_T = a_3 + b_3(M_S)^2 + c_3(M_S)^{-2} + (\ln A_{12}) [d_3 + e_3(M_S)^2] + (\ln A_{12})^2[f_3 + g_3(M_S)^2] \tag{3}$$

$$U_T = a_4 + b_4(M_S) + c_4(M_S)^{-1} + (\ln A_{12}) [d_4 + e_4(M_S)] + (\ln A_{12})^2[f_4 + g_4(M_S)^{-1}] \tag{4}$$

where

dependent variables are:

M_T = transmitted shock wave Mach number;
P_T = transmitted static pressure behind wave, atm;
T_T = transmitted static temperature behind wave, °K;
U_T = transmitted velocity behind wave, fps;

and independent variables are:

M_S = incident shock wave Mach number;
A_{12} = area ratio, upstream area/downstream area.

The coefficients and range of applicability for the appropriate geometry are given in Table II. It must be emphasized that these equations are empirical, and no inference concerning property functional

Table II. Coefficients and limits for transmitted flow property equations [eqns. (1) to (4)]

Transmitted property	Eqn. no. and subscript	Coefficients						
		a	b	c	d	e	f	g
For sudden contraction limit of applicability: $A_{12} > 1.0$, $M_S > 2.1$								
Mach No., M_T	1	0.070						
Pressure, P_T	2	−0.728	1.19	0.362	−0.066			
Temperature, T_T	3	277	58.7	13.0	−14.7	18.2	2.66	−3.23
Velocity, U_T	4	108	950	−1360	227	91.1	−156	143
For sudden enlargement limit of applicability: $A_{12} > 0.13$, $M_S > 2.5$								
Mach No., M_T	1	0.182						
Pressure, P_T	2	−0.120	1.16	0.443	0.046			
Temperature, T_T	3	288	58.1	−64.1	1.76	22.1	−1.02	2.32
Velocity, U_T	4	19.1	947	−970	72.4	175	37.1	−142

relationships is intended. All the properties behind the shock wave may be determined from the above equations. The equations apply only to ideal air ahead of the shock wave (though the computer program can apply to other ideal and real gases) and are presented in order to facilitate design and safety analyses. The results from the equations agree within about 5% of the computer results.

If a sudden enlargement results in a secondary shock which attempts to propagate upstream (i.e., $A_{12} < 0.13$ and $M_S < 2.5$), the computer program will not calculate the flow-field properties. For such cases, three-dimensional flow-field effects are significant but are beyond the scope of the assumed model. However, if these sudden enlargements are modeled as gradually expanding channels with pre- to post-enlargement ratios equal to that of the actual sudden enlargements, the expansion properties may be estimated for the actual cases. In this model, a stationary shock wave is allowed to stand at some calculated area ratio in the diverging duct, and its presence will adjust the downstream properties to match the flow requirements for the primary shock wave. Specifically, the solution for such a case may be constructed on a pressure–velocity (P–U) diagram in the following way:

1. A stationary normal shock is assumed to stand at a given duct area ratio.
2. An isentropic, steady expansion is assumed up to the shock.[16]
3. The normal shock relations are used to calculate flow properties across the shock.[16]
4. An isentropic steady expansion is assumed downstream of the shock until the final area is traversed. The pressure and velocity at the final area are plotted on the P-U diagram.
5. By assuming different shock locations, a locus of points may be constructed.
6. The pressure and velocity behind the primary shock wave are given in terms of conditions ahead of the wave by the following relation:[16]

$$\frac{U_T}{C_1} = \frac{\frac{P_T}{P_1} - 1}{\gamma\sqrt{1 + \frac{\gamma+1}{2\gamma}\left(\frac{P_T}{P_1} - 1\right)}} \tag{5}$$

Also the upstream or transmitted pressure behind the shock wave, P_T, is given in terms of the shock wave Mach number as:[2]

$$\frac{P_T}{P_1} = \frac{2\gamma M_T^2 - (\gamma - 1)}{(\gamma + 1)} \tag{6}$$

where

γ = specific heat ratio, C_P/C_V;
M_T = transmitted shock wave Mach number;
U_T = transmitted velocity behind shock wave, fps;
C_1 = speed of sound in gas downstream, fps;
P_1 = pressure in gas downstream, atm;
P_T = transmitted static pressure behind shock wave, atm.

By assuming various values of P_T when P_1 and C_1 are given, a shock polar may be constructed on the P–U diagram.

7. The intersection of the shock polar with the previously constructed curve will give the pressure and velocity behind the primary shock wave.

An example of this procedure applied to a specific duct enlargement is presented in Figure 5. Because the assumption of a gradual enlargement should yield a stronger transmitted shock than that formed in a sudden enlargement, this formulation is conservative (as desired in a safety analysis).

The limits of applicability for a sudden contraction are $A_{12} > 1.0$ and $M_S > 2.1$. Cases for $M_S < 2.1$ are being investigated. Since sudden contractions always produce a stronger transmitted wave, a conservative estimate is made for cases where $M_S < 2.1$ if the incident Mach number is assumed to be 2.1.

The flow properties should also be affected by other geometrical duct arrangements such as bends, tees, valves, or long runs of straight duct. However, in an experimental study of detonation in hydrogen-air mixtures in Savannah River process equipment, Porter found that pipe bends up to 90° had no apparent effect on the formation or propagation of detonation waves.[5] In addition, a combination of $^1/_2$- and 2-in. pipe in a "Y" configuration had no significant effect on the detonation process. Similar results were found by Hishida and Hori for the propagation of pressure waves in water in pipes of various geometries.[17] Thus, experimentally, there appears to be no measurable shock-wave suppression effects in bends or tees. Even though these geometries must have flow losses associated with them, the effects cannot be calculated with the present model; and since these losses appear to be experimentally insignificant, they will be neglected in the present analysis.

As an example, a duct system consisting of contractions and enlargements (Figure 6) will be analyzed for detonation effects. It is assumed that a detonation wave is established near the entrance of the duct and enters a nondetonable mixture (i.e., air) as shown. A sudden contraction at *a* and sudden enlargements at *b* and *c* are encountered. The time-displacement conditions are shown in Figure 6. At point *c* the gradual enlargement assumption is invoked. It is observed that such a duct

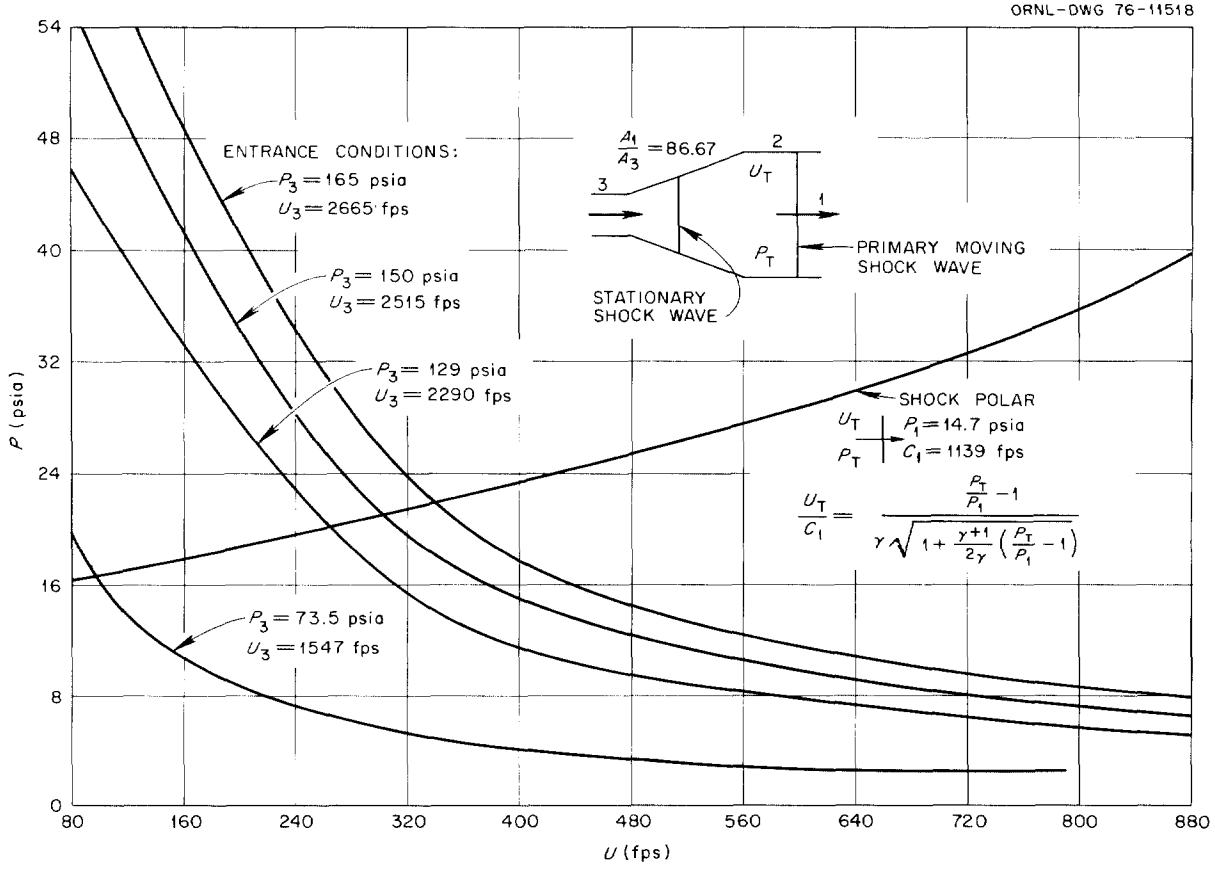

Figure 5: Estimation of conditions behind shock wave propagating through a gradual duct enlargement.

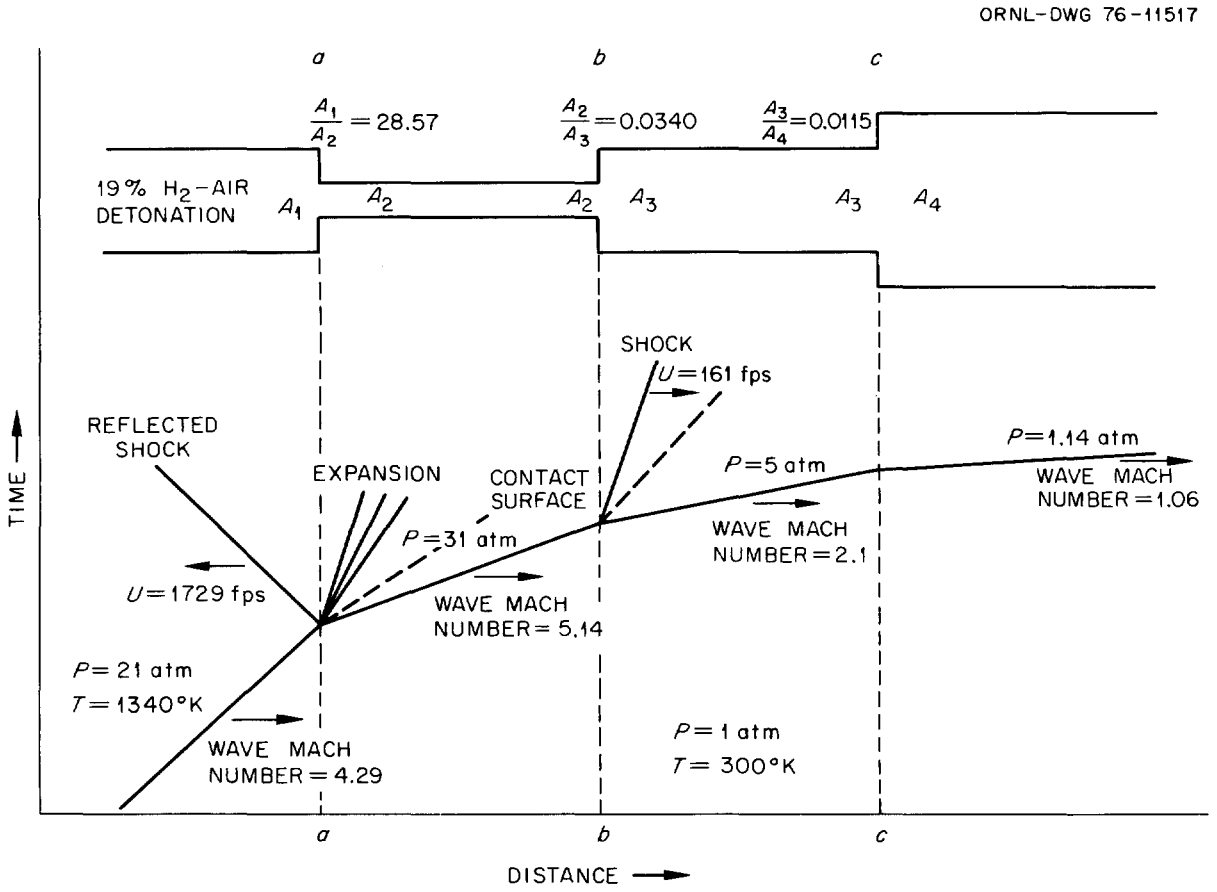

Figure 6: Duct system analysis.

arrangement for the given initial shock condition (i.e., a shock of $M_S = 4.29$ moving into air at 1 atm and 300° K) would produce a pressure drop from 21 to 1.14 atm. Any number of such duct contractions or enlargements may be joined together and analyzed for the final flow properties.

III. Conclusions

A theoretical model has been presented which should aid in a comprehensive safety analysis of explosion-induced shock waves in ducts of various geometries. Empirical equations for a range of sudden duct contractions and enlargements virtually eliminate the necessity of computer computations for the flow-field properties behind the primary shock wave. Also, a method has been presented which can conservatively estimate the flow properties for enlargements outside the range of the computer model applicability. Damage to air-cleaning components in duct systems due to wave impact can be estimated.

References

1. Ia. B. Zel'dovich and N. M. Simonov, *J. Phys. Chem. (USSR),* 11, 1361 (1949).

2. A. G. Gaydon and I. R. Hurle, *The Shock Tube in High-Temperature Chemical Physics,* Reinhold Publishing Corp., N.Y., 1963, pp. 251–787.

3. W. S. Young and N. W. Kruse, "Properties of Explosive Gas Mixtures," *Trans. Am. Inst. Chem. Engrs.* 35, 337–358 (1939).

4. J. Brenton, *Ann. Office Nat'l Combustibles Liquids,* 11, 487 (1936).

5. J. B. Porter, *Analysis of Hydrogen Explosion Hazards,* DP-1295, E. I. DuPont de Nemours and Co., Savannah River Laboratory, Aiken, S.C. (July 1972).

6. B. Lewis and G. von Elbe, *Combustion, Flames, and Explosions,* Academic Press, N.Y., 1951, p. 606.

7. Ia B. Zel'dovich, S. M. Kogardo, and N. N. Simonov, "An Experimental Investigation of Spherical Detonation in Gases," *Soviet Phys.—Tech Phys.,* 1, 1689–1713 (1956).

8. B. Lee, J. Lee, and R. Knystautas, "Transmission of Detonation Waves Through Orifices," *AIAA Journal,* 4,(2), 365-367 (1966).

9. W. Jost, *Explosion and Combustion Processes in Gases,* McGraw Hill, N.Y., 1946, pp. 160–209.

10. P. Laffitte, *Comptes rend.* 177, 178 (1923).

11. P. Laffitte, *Comptes rend.* 179, 1934 (1924).

12. R. Wendlandt, *Z. Physik Chem,* 110, 637 (1924).

13. J. G. Moore and E. V. Gilby, *A Review of Problems Arising from the Combustion of Hydrogen in a Water Reactor Containment,* UKAEA Report AHSB(S) R101, Authority Health and Safety Branch (1966).

14. R. L. Mathews, *Explosion and Detonation Limits for an Oxygen-Hydrogen-Water Vapor System,* USAEC Report KAPL-M-6564, Knolls Atomic Power Laboratory (June 1966).

15. H. A. McLain, *Potential Metal-Water Reactions in Light Water-Cooled Power Reactors,* ORNL-NSIC-23 (August 1968), p. 90.

16. A. H. Shapiro, *Dynamics and Thermodynamics of Compressible Fluid Flow,* Vols. 1 and 2, Ronald, N.Y., 1953.

17. M. Hishida and M. Hori, *Experiment on Pressure Wave Propagation. I. The Result of Experiments on Branches and Bends,* United States–Japanese Fast Reactor Exchange Program, JAPFNR-137 (November 1974).

DISCUSSION

ETTINGER: Since ventilation systems normally have tapered rather than sudden expansions or contractions, what is the magnitude of the difference between your model for sudden changes in duct size versus the real situation in ventilation systems?

BUSBY: For tapered geometries, the losses would be less than for sudden expansions or contractions. The particular computer model that we have can calculate the flow through tapered geometries.

MURROW: If the shock wave was not such a serious one, but a shock wave generated by an abrupt closing of a valve in a moving air stream, the Mach number might not be 2.1. Would the computer code be able to handle this kind of problem and generate the pressures, the reflected pressures, and the less-than-ambient downstream pressure from the closing valve?

BUSBY: If a moving shock wave has a Mach number less than 2.07, the flow behind the shock wave is subsonic. In some particular cases the flow may be assumed to be incompressible and those corresponding equations will apply. For the closing of a valve, if the incident conditions are known, the reflected conditions can be found from the equations of shock tube theory.

ORTH: Since your calculations, as you've mentioned, are conservative, do you know of any plans to run some experiments to check the real case with calculations?

BUSBY: At Oak Ridge, I do not know of any such program yet.

CLOSING REMARKS OF SESSION CHAIRMAN:

I'd like to thank our four speakers. In summary, just a short one, there always will be requirements for ventilation systems to survive fire, explosion and natural disasters. I think we've had four good papers that will assist us in analyzing and designing facilities. Thank you.